



MODELLING AND DATA VALIDATION FOR THE ENERGY ANALYSIS OF ABSORPTION REFRIGERATION SYSTEMS

David Estefano Martinez Maradiaga

Dipòsit Legal: T.69-2014

ADVERTIMENT. L'accés als continguts d'aquesta tesi doctoral i la seva utilització ha de respectar els drets de la persona autora. Pot ser utilitzada per a consulta o estudi personal, així com en activitats o materials d'investigació i docència en els termes establerts a l'art. 32 del Text Refós de la Llei de Propietat Intel·lectual (RDL 1/1996). Per altres utilitzacions es requereix l'autorització prèvia i expressa de la persona autora. En qualsevol cas, en la utilització dels seus continguts caldrà indicar de forma clara el nom i cognoms de la persona autora i el títol de la tesi doctoral. No s'autoritza la seva reproducció o altres formes d'explotació efectuades amb finalitats de lucre ni la seva comunicació pública des d'un lloc aliè al servei TDX. Tampoc s'autoritza la presentació del seu contingut en una finestra o marc aliè a TDX (framing). Aquesta reserva de drets afecta tant als continguts de la tesi com als seus resums i índexs.

ADVERTENCIA. El acceso a los contenidos de esta tesis doctoral y su utilización debe respetar los derechos de la persona autora. Puede ser utilizada para consulta o estudio personal, así como en actividades o materiales de investigación y docencia en los términos establecidos en el art. 32 del Texto Refundido de la Ley de Propiedad Intelectual (RDL 1/1996). Para otros usos se requiere la autorización previa y expresa de la persona autora. En cualquier caso, en la utilización de sus contenidos se deberá indicar de forma clara el nombre y apellidos de la persona autora y el título de la tesis doctoral. No se autoriza su reproducción u otras formas de explotación efectuadas con fines lucrativos ni su comunicación pública desde un sitio ajeno al servicio TDR. Tampoco se autoriza la presentación de su contenido en una ventana o marco ajeno a TDR (framing). Esta reserva de derechos afecta tanto al contenido de la tesis como a sus resúmenes e índices.

WARNING. Access to the contents of this doctoral thesis and its use must respect the rights of the author. It can be used for reference or private study, as well as research and learning activities or materials in the terms established by the 32nd article of the Spanish Consolidated Copyright Act (RDL 1/1996). Express and previous authorization of the author is required for any other uses. In any case, when using its content, full name of the author and title of the thesis must be clearly indicated. Reproduction or other forms of for profit use or public communication from outside TDX service is not allowed. Presentation of its content in a window or frame external to TDX (framing) is not authorized either. These rights affect both the content of the thesis and its abstracts and indexes.

David Estéfano Martínez Maradiaga

**Modelling and Data Validation for
the Energy Analysis of Absorption
Refrigeration Systems**

Doctoral Thesis

Directed by:

Dr. Alberto Coronas Salcedo

Dr. Joan Carles Bruno Argilaguet

Department of Mechanical Engineering



UNIVERSITAT ROVIRA I VIRGILI

Tarragona, September 2013



**UNIVERSITAT
ROVIRA I VIRGILI
DEPARTAMENT D'ENGINYERIA MECÀNICA**

Escola Tècnica Superior d'Enginyeria Química (ETSEQ).
Av. Països Catalans 26. 43007 Tarragona (Spain)

Los abajo firmantes Dr. Alberto Coronas, Catedrático de Universidad y Dr. Joan Carles Bruno, Profesor Agregado, del Departament d'Enginyeria Mecànica de la Universitat Rovira i Virgili de Tarragona

HACEN CONSTAR:

Que el trabajo titulado: “Modelling and Data Validation for the Energy Analysis of Absorption Refrigeration Systems” presentado por el Sr. David Estéfano Martínez Maradiaga para optar al grado de Doctor de la Universitat Rovira i Virgili, ha sido realizado bajo su dirección inmediata en el CREVER - Grup de Recerca d'Enginyeria Tèrmica Aplicada del Departament d'Enginyeria Mecànica de la Universitat Rovira i Virgili.

Que todos los resultados han sido obtenidos en las experiencias y trabajos realizados por dicho doctorando.

Que la tesis se ha realizado dentro del proyecto de investigación - Modelización e integración eficiente de enfriadoras y bombas de calor por absorción en sistemas de poligeneración mediante procesado y reconciliación de datos – DATABS - del Plan Nacional de I+D+i con referencia ENE 2009-14182.

Que el doctorando cumple con los requisitos para poder optar a la Mención Europea.

Y para que así conste a los efectos oportunos, firmamos este documento.

Tarragona, 30 de Julio 2013

Acknowledgments

In the first place, I would like to thank my supervisors Prof. Alberto Coronas and Dr. Joan Carles Bruno for giving me the chance to be part of the CREVER research group, as well as for their support and guidance through this journey.

I want to thank the Universitat Rovira i Virgili for supporting financially my Ph.D. through a scholarship. I also acknowledge the financial support of the Spanish Ministry of Science and Innovation through project ref. ENE 2009-14182.

Thanks to Prof. Günter Wozny, Dr. Tilman Barz, Dr. Harvey Arellano-Garcia, and all the people in their research group at TU Berlin for their help during my research stay. This stay was also possible thanks to the mobility grant funded by Spanish Ministry of Education.

I also acknowledge my colleagues from the CREVER research group who have been supporting me by sharing ideas, discussing our doubts, and keeping a nice working environment.

Special thanks to Maria and her family for their kindness and care during these years in Tarragona.

Finally, I want to express my gratitude to my parents, my sisters, and my brother for all the support, care, and love that I've received from them during all the stages of my life.

Abstract

Data validation and reconciliation techniques have been extensively used in the process industry to improve the accuracy of data. These techniques exploit the redundancy in the measurements in order to obtain a set of adjusted measurements that satisfy the plant model. Nevertheless, not many applications deal with closed cycles with complex connectivity and recycle loops, as in absorption refrigeration cycles. This thesis proposes a methodology for the steady-state data validation of absorption refrigeration systems.

Data validation refers to the complete process for treating the raw measurements in order to obtain their most likely estimates. This includes the identification of steady-state, resolution of the data reconciliation and parameter estimation problems and the detection and elimination of gross errors. The methodology developed through this thesis will be useful for generating a set of coherent measurements and operation parameters of an absorption chiller for downstream applications: performance calculation, development of empirical models, optimisation, etc.

Firstly, the modelling approaches used to predict the performance of absorption refrigeration systems are reviewed since data reconciliation must rely on adequate models. Commonly used assumptions, degrees of freedom, and other aspects of modelling and simulation of absorption chillers are considered.

Secondly, we propose to combine two steady-state detection methods: the modified F-test to the data time series and a Student t-test to the mean difference of two data windows using an extended period strategy. Absorption chillers data may present a very slow drift that is difficult to track by conventional steady-state detection methods. The approach proposed in this thesis makes it possible to handle processes which present quasi-steady state behaviour (fast changes) and slow drifting as well.

The core of the data validation methodology is data reconciliation. Data reconciliation is the procedure used to optimally adjust measurements so that the calculated values obey conservation laws and other constraints. Depending on the amount of internal measurements of the absorption refrigeration system, two data reconciliation cases arise. In Case 1, the amount of measurements (internal and external) is enough to obtain the redundancy necessary for the resolution of the data reconciliation problem. On the other hand, in Case 2, the amount of internal measurements is not enough so there is the need to

estimate all of some of the absorption chiller main parameters. In this case the problem becomes a joint data reconciliation and parameter estimation procedure.

Systematic or gross errors occur because of malfunctioning instruments or process leaks. Their presence invalidates the data reconciliation results. They have to be identified and eliminated or corrected before or during the data reconciliation procedure. In this thesis, the Modified Iterative Measurement Test is used to detect gross errors.

Finally, the methodology is demonstrated using experimental data of different types of absorption refrigeration systems with different levels of redundancy.

Resumen

Los procedimientos de validación y reconciliación de datos se han utilizado extensamente en la industria de procesos con el fin de mejorar la precisión de los datos. Estos procedimientos explotan la redundancia que puede haber en las mediciones para obtener un conjunto de mediciones ajustadas que satisfacen el modelo de la planta. Sin embargo, no hay muchas aplicaciones que traten con ciclos cerrados, con configuraciones complejas y circuitos de recirculación, como en el caso de los ciclos de refrigeración por absorción. Esta tesis propone una metodología para la validación de datos en estado estacionario de enfriadoras de absorción.

Validación de datos se refiere al proceso completo de tratamiento de los datos de planta con el fin de obtener sus valores estimados más probables. Este proceso incluye la identificación del estado estacionario, la resolución de los problemas de reconciliación de datos y estimación de parámetros, además de la detección y eliminación de los errores sistemáticos. La metodología desarrollada mediante esta tesis será útil para generar un conjunto de medidas coherentes, así como parámetros de operación, de una enfriadora de absorción para aplicaciones como: cálculo de prestaciones, desarrollo de modelos empíricos, optimización, etc.

En primer lugar, se revisan los diferentes enfoques que se utilizan para modelar y calcular las prestaciones de las enfriadoras de absorción porque la reconciliación de datos debe basarse en modelos adecuados. Las suposiciones comúnmente usadas, grados de libertad, inicialización de variables, así como otros aspectos del modelado y simulación de las enfriadoras de absorción son considerados.

En segundo lugar, esta tesis propone la combinación de dos métodos para la detección del estado estacionario: evaluación de la desviación estándar dentro de una ventana de datos definida, y la prueba t de Student aplicada a la diferencia de las medias de dos ventanas de datos usando una estrategia de período extendido. Los datos de funcionamiento de las enfriadoras de absorción pueden presentar una deriva muy lenta que es difícil de seguir por los métodos convencionales de detección del estado estacionario. El método propuesto en esta tesis se puede aplicar a procesos que presentan tanto un comportamiento cuasi-estacionario (con cambios rápidos) así como derivas lentas.

El núcleo de la metodología de validación de datos es la reconciliación de datos. La reconciliación de datos es el procedimiento usado para ajustar óptimamente las medidas

para que los cálculos obtenidos obedezcan las leyes de conservación y otras restricciones. Dependiendo del número de mediciones internas disponibles en la enfriadora de absorción, surgen dos casos de reconciliación de datos. En el Caso 1, la cantidad de mediciones (internas y externas) son suficientes para obtener la redundancia necesaria para la resolución del problema de reconciliación de datos. Por otro lado, en el Caso 2, la cantidad de mediciones internas no es suficiente por lo que es necesario estimar todos, o algunos de los parámetros principales de la enfriadora de absorción. En este caso el problema se convierte en un procedimiento conjunto de reconciliación de datos y estimación de parámetros.

Los errores sistemáticos ocurren debido a eventos tales como instrumentación defectuosa o pérdidas en las corrientes de proceso. La presencia de errores sistemáticos invalidan los resultados de la reconciliación de datos. Es por ello que estos errores deben ser identificados y eliminados o corregidos antes o durante la resolución del problema de reconciliación de datos. En esta tesis se ha utilizado la Prueba de Mediciones Iterativa Modificada para detectar los errores sistemáticos.

Finalmente, la metodología es demostrada utilizando datos experimentales de diferentes enfriadoras de absorción, con diferentes niveles de redundancia.

Contributions in Journals

Martínez-Maradiaga, D.; Bruno, J.C.; Coronas, A. (2013) Steady-state data reconciliation for absorption refrigeration systems. *Applied Thermal Engineering*, 51:1170-1180.

Martínez-Maradiaga, D.; Bruno, J.C.; Coronas, A. (2013) Modelling of absorption refrigeration systems through data reconciliation and parameter estimation (in preparation).

Martínez-Maradiaga, D.; Bruno, J.C.; Coronas, A. (2013) Characterization of absorption refrigeration systems using data validation (in preparation).

Contributions in Congresses, Conferences and Symposia

Martínez, D.E.; Bruno, J.C.; Bagajewicz, M.J.; Coronas, A. (2010) Performance Analysis of Absorption Chillers Using Data Reconciliation. ASME 10th Biennial Conference on Engineering Systems Design (ESDA2010), 12-14 July, Istanbul, Turkey. (Oral presentation).

Martínez-Maradiaga, D.; Sendeku, D.; Bruno, J.C.; Coronas, A. (2011) Integrated approach for the treatment of steady-state operational data of absorption chillers and heat pumps. International Sorption Heat Pump Conference (ISHPC11), 28-29 April, Padua, Italy. (Oral presentation).

Martínez-Maradiaga, D.; Sendeku, D.; Ortiga, J.; Bruno, J.C.; Coronas, A. (2011) A new methodology for operational data treatment, monitoring and performance analysis of absorption chillers. 4th International Conference Solar Air- Conditioning, 12-14 October, Larnaca, Cyprus (Poster - Best Poster Award).

Martínez-Maradiaga, D.; Sendeku, D.; Ortiga, J.; Bruno, J.C.; Coronas, A. (2012) Reconciliación de Datos y Detección de Errores Sistemáticos en Sistemas de Refrigeración por Absorción. VI Congreso Ibérico y IV Congreso Iberoamericano de Ciencias y Técnicas del Frío (CYTEF-2012), 22-24 February, Madrid, Spain (Oral presentation).

Figueredo, G. R.; Martínez-Maradiaga, D.; Bruno, J. C.; Coronas, A. (2012) Application of the data reconciliation methodology in a double-stage absorption chiller driven at two input temperatures. Heat Powered Cycles Conference (HPC2012), 10-12 September, Alkmaar, Netherlands (Oral presentation).

Martínez-Maradiaga, D.; Bruno, J.C.; Coronas, A. (2013) Steady-State Modelling of Absorption Chillers through Parameter Estimation and Data Reconciliation. 5th International Conference Solar Air- Conditioning, 25-27 September, Black Forest, Bad Krozingen, Germany (Oral presentation).

Participation in projects

DATABS - Modelización e integración eficiente de enfriadoras y bombas de calor por absorción en sistemas de poligeneración mediante procesado y reconciliación de datos. Entidad: Ministerio de Ciencia e Innovación - Plan Nacional de I+D+i. Código de concesión: ENE 2009-14182. Período: 2010-2012. Investigador principal: Joan Carles Bruno.

Table of Contents

Chapter 1	Introduction and Objectives	1-1
1.1	Energy Efficiency and Refrigeration.....	1-1
1.2	Absorption Refrigeration Systems	1-3
1.2.1	Working fluids in absorption refrigeration cycles.....	1-4
1.2.2	Absorption refrigeration cycle configurations.....	1-5
1.2.3	Applications of absorption refrigeration systems.....	1-7
1.2.4	Shortcomings in absorption refrigeration technology	1-9
1.3	Data Validation and Reconciliation	1-10
1.3.1	Mathematical formulation of the Data Reconciliation problem.....	1-12
1.3.2	Variable classification	1-13
1.3.3	Gross error detection	1-14
1.4	Objectives.....	1-15
1.5	Thesis structure	1-16
Chapter 2	Steady-State Modelling and Simulation of Absorption Refrigeration Systems: A Review	2-1
	Abstract.....	2-1
2.1	Introduction	2-2
2.2	Thermodynamic Modelling.....	2-2
2.2.1	Modelling based on finite-time thermodynamics.....	2-3
2.2.2	Modelling based on mass and energy balances	2-9
2.2.3	Correlations for calculating the thermodynamic properties of working fluids.....	2-12
2.2.4	Typical Assumptions and Degrees of Freedom Analysis.....	2-14
2.2.5	Simulation of absorption refrigeration systems in steady-state.....	2-15
2.3	Data Driven Modelling.....	2-16
2.3.1	Artificial Neural Networks	2-17
2.3.2	Multivariable Polynomial Regression	2-18
2.4	Semi-Empirical Modelling	2-20

2.4.1	A semi-empirical thermodynamic model from finite-time thermodynamics	2-20
2.4.2	The Characteristic Equation Method	2-21
2.4.3	Other semi-empirical approaches	2-22
2.5	Applications	2-23
2.5.1	Performance Analysis of Absorption Cycles	2-23
2.5.2	Evaluation of advanced cycle configurations	2-24
2.5.3	Integration into other systems	2-25
2.5.4	Evaluation of alternative working fluids	2-25
2.5.5	Optimisation	2-27
2.6	Modelling Issues and Data Reconciliation in Absorption Refrigeration Systems	2-27
2.7	Conclusions	2-29
Chapter 3	A Combined Steady-State Detection Method for Absorption Refrigeration Systems	3-1
3.1	Introduction	3-2
3.2	Steady-State Detection Methods	3-2
3.2.1	Parametric methods	3-2
3.2.2	Nonparametric methods	3-3
3.2.3	Slow drifting processes	3-4
3.3	A Combined Steady-State Detection Method	3-4
3.3.1	Test 1: Calculation of the standard deviation in a moving window ..	3-4
3.3.2	Test 2: t-test to difference between two means	3-6
3.3.3	Combining the two methods	3-6
3.4	Application to real absorption chiller data	3-8
3.5	Conclusions	3-13
Chapter 4	A Framework for the Data Validation of Absorption Refrigeration Systems	4-1
4.1	Introduction	4-2
4.2	Data Reconciliation	4-3

4.3	Data Validation for Absorption Refrigeration Systems	4-4
4.3.1	Steady-State Detection	4-5
4.3.2	Variable Classification and Degrees of Freedom Analysis	4-6
4.3.3	Modelling Aspects.....	4-6
4.3.4	Resolution of the DR problem.....	4-12
4.3.5	Gross Error Detection.....	4-18
4.4	Case Studies	4-19
4.4.1	Data reconciliation of a single-effect NH ₃ /H ₂ O absorption chiller (Case 1)	4-19
4.4.2	Simultaneous Data Reconciliation and Parameter Estimation of a single-effect H ₂ O/LiBr absorption chiller (Case 2).....	4-28
4.5	Conclusions	4-35
Chapter 5 Characterisation of Absorption Refrigeration Systems through Data Validation.....		5-1
5.1	Introduction	5-2
5.2	The Characteristic Equation Method.....	5-2
5.3	Case study	5-4
5.3.1	Data Validation.....	5-4
5.3.2	Adapted Characteristic Equation	5-7
5.4	Conclusion.....	5-9
Chapter 6 Conclusions and further work.....		6-1
6.1	Conclusions	6-1
6.2	Further work.....	6-3
Appendix A Uncertainty Calculation		A-1
Appendix B Degrees of freedom catalogue.....		B-1
References.....		R-1

List of Figures

Figure 1-1: World primary energy consumption [1].	1-1
Figure 1-2: CO ₂ emissions related to consumption of oil, gas and coal [1].	1-2
Figure 1-3: Schematics and comparison of a vapour compression system and an absorption system.	1-3
Figure 1-4: Single-effect absorption refrigeration cycle.	1-6
Figure 1-5: Double-effect absorption refrigeration cycle.	1-7
Figure 1-6: Rated energy performance for each engine in the ST4 polygeneration plant [12].	1-8
Figure 1-7: General schematic of a solar absorption refrigeration system.	1-9
Figure 1-8: Comparison between random and systematic errors.	1-11
Figure 1-9: General data validation scheme.	1-12
Figure 2-1: Reversible representation of an absorption refrigeration machine.	2-3
Figure 2-2: Three and Four Heat Reservoir schemes.	2-6
Figure 2-3: Schematic of a single-effect absorption cycle including external streams.	2-9
Figure 2-4: Counter-flow heat exchanger.	2-12
Figure 2-5: Artificial Neural Network multi-layer feed-forward architecture	2-18
Figure 3-1: Moving window.	3-5
Figure 3-2: Example of Slow Drifting with SSD by a single test.	3-5
Figure 3-3: Combined test for steady-state detection.	3-7
Figure 3-4: Example of Slow Drifting with SSD by the combined test.	3-7
Figure 3-5: Single-effect absorption chiller external circuit measurements.	3-8
Figure 3-6: Absorption chiller heat loads, temperature trends and steady-state indicator during one day of operation.	3-9
Figure 4-1: General scheme of the data validation framework.	4-5
Figure 4-2: Schematic of a Single-Effect H ₂ O/LiBr Absorption Cycle.	4-7

Figure 4-3: Heat exchanger diagrams with temperature pinch assumptions for (a) generator, (b) evaporator, (c) condenser, and (d) absorber.	4-10
Figure 4-4: Guessed and final state values in a T-P diagram.	4-11
Figure 4-5: Schematic of the two-stage approach for DR.	4-13
Figure 4-6: Heat exchanger system with bypass.	4-15
Figure 4-7: Flow diagram for nonlinear example.	4-16
Figure 4-8: Simplified schematic of the single-effect ammonia-water absorption cycle.	4-20
Figure 4-9: Steady-state detector and temperature trends during one day of operation. .	4-21
Figure 4-10: Number of tests with measurements containing gross errors after the 1 st DR (a) and the 2 nd DR (b).	4-23
Figure 4-11: Value of the objective function before and after DR	4-24
Figure 4-12: Q_e and COP calculation using raw and reconciled measurements (filled markers correspond to raw data and blank markers correspond to reconciled data).	4-25
Figure 4-13: Energy balances before and after DR for hot-water inlet temperature (T_{11}) at 85 °C and cooling-water inlet temperature (T_{13}) at 27°.	4-26
Figure 4-14: Absorption chiller heat loads, temperature trends and steady-state indicator during one day of operation.	4-29
Figure 4-15: Experimental and predicted cooling capacity and COP using the thermodynamic model with three different sets of parameters and raw measurements. .	4-33
Figure 4-16: Experimental and predicted cooling capacity and COP using the thermodynamic model with three different sets of parameters and reconciled measurements.	4-34
Figure 4-17: Coefficient of variation for the predicted cooling capacity and COP using the thermodynamic model with three different sets of parameters and raw and reconciled measurements.	4-35
Figure 5-1: Schematic of the single-effect $NH_3/LiNO_3$ absorption chiller.	5-4
Figure 5-2: Experimental cooling capacity (Q_e) and COP vs simulated predicted by the thermodynamic model with the estimated parameters.	5-6
Figure 5-3: Comparison of the predicted cooling capacity and COP using the Characteristic Equation from raw data (circular markers) and reconciled data (triangular markers).	5-8

Figure 5-4: Coefficient of variation for the predicted cooling capacity and COP using the Characteristic Equation from raw data (green bars) and the Characteristic Equation from reconciled data (yellow bars).....5-9

List of Tables

Table 1-1: Absorption working fluid properties [3].	1-5
Table 2-1: Property correlations for the H ₂ O/LiBr mixture available in the literature. ...	2-13
Table 2-2: Property correlations for the NH ₃ /H ₂ O mixture available in the literature [76].	2-14
Table 3-1: SSD parameters for case study.	3-8
Table 3-2: Average cooling capacity and COP and their corresponding uncertainties calculated using the two SSD methods.	3-10
Table 3-3: Reconciled values and residuals of the average measurements from steady-state period 1 using the single SSD test.	3-12
Table 3-4: Reconciled values and residuals of the average measurements from steady-state periods 1 and 2 using the combined SSD test.	3-12
Table 4-1: Temperatures selected for the logarithmic mean temperature definitions.	4-8
Table 4-2: Flow reconciliation for the linear example.	4-15
Table 4-3: Measured and reconciled values for the nonlinear example.	4-16
Table 4-4: Process variables measured for the NH ₃ /H ₂ O absorption chiller.	4-20
Table 4-5: Calculation of degrees of freedom for single-effect absorption systems.	4-22
Table 4-6: Raw and reconciled measurements for hot-water inlet temperature (t_{11}) at 85 °C, cooling-water inlet temperature (t_{13}) at 27, and chilled -water outlet temperature (t_{17}) at 7 °C.	4-27
Table 4-7: Parameters calculated during the three DR steps (in the same conditions as Table 4-6).	4-27
Table 4-8: Operating conditions for the single effect H ₂ O/LiBr Absorption Chiller.	4-28
Table 4-9: Summary of the operating steady state points during 5 days of operation	4-30
Table 4-10: Calculation of degrees of freedom for single-effect absorption systems.	4-31
Table 4-11: Absorption chiller parameters	4-32
Table 4-12: Nominal conditions for calculating the initial value of the chiller parameters	4-32

Table 4-13: Reconciled measurements values	4-34
Table 5-1: Summary of the operating conditions.....	5-5
Table 5-2: Estimated parameters using Parameter Estimation (PE) and Data Reconciliation and Parameter Estimation (DR+PE).	5-5
Table 5-3: Coefficient of variation (CV) for the thermodynamic model with estimated parameters.	5-7
Table 5-4: Fitted parameters of the adapted characteristic equation for this case study....	5-7
Table A-1: Uncertainty budget for Q_e	A-3
Table A-2: Uncertainty budget for COP	A-4
Table B-1: Elements catalogue of vapour absorption cycles	B-1
Table B-2: Component catalogue of vapour absorption cycles	B-2
Table B-2: Stream legend for Tables B-1 and B2.....	B-3

Chapter 1

Introduction and Objectives

1.1 Energy Efficiency and Refrigeration

Figure 1-1 shows the world primary energy consumption by fuel type. In 2009 world energy consumption decreased for the first time since 1982 because of the financial and economic crisis. After this year, global energy consumption started to grow again but at a slower pace. During 2011 this growth was about 2.5% while in 2012 was about 1.8%. Part of this slowdown is explained by the economic slowdown, but it also corresponds to a more efficient use of energy in industry as well as in the residential sector [1].

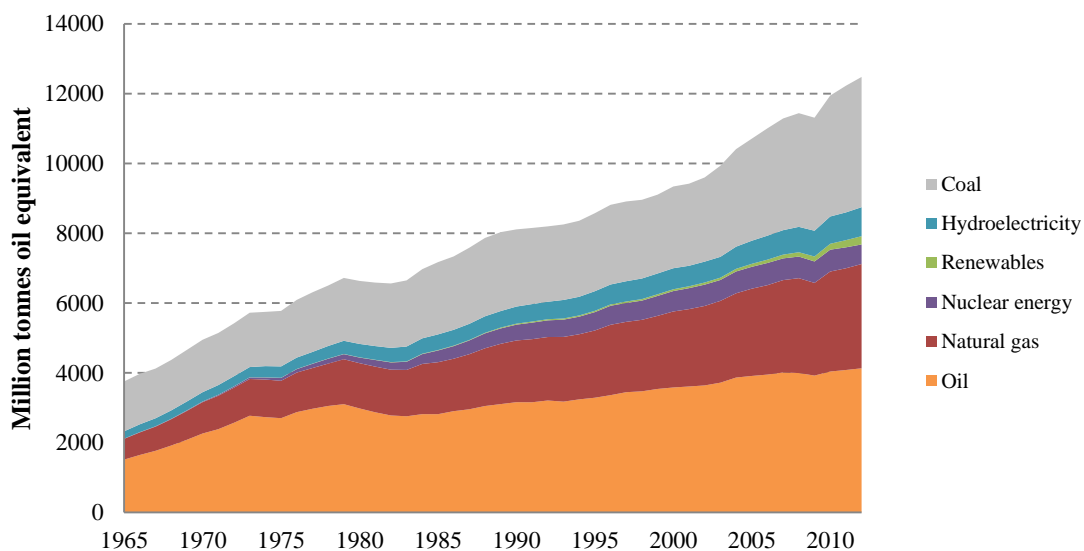


Figure 1-1: World primary energy consumption [1].

Chapter 1. Introduction and Objectives

Energy efficiency is not only important because of the economic benefits related to a better use of energy, but is also important from an environmental point of view. Fossil fuels are still the main source of energy and therefore they are one of the main contributors to global warming. The CO₂ emissions related to the consumption of oil, gas and coal is still growing (Figure 1-2).

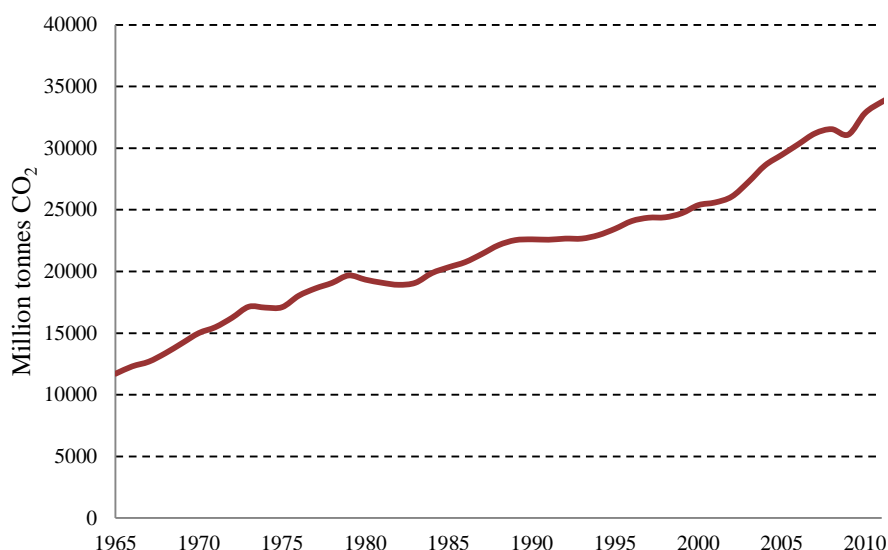


Figure 1-2: CO₂ emissions related to consumption of oil, gas and coal [1].

In 2007 the European Union set the “20-20-20” targets in order to convert Europe in a highly energy efficient and low carbon economy by 2020 (“The EU climate and energy package”). These targets are:

- A 20% reduction in EU greenhouse gas emissions from 1990 levels;
- Raising the share of EU energy consumption produced from renewable resources to 20%;
- A 20% improvement in the EU's energy efficiency.

In order to reinforce the feasibility of reaching the 20% improvement in energy efficiency, the European Commission is adopting additional measurements and directives such as the “Energy Efficiency Plan 2011” and the “Energy Efficiency Directive” (Directive 2012/27/EU). Therefore, it's important to continue researching and developing energy efficient technologies. Refrigeration technology is an important field with strong potential for energy efficiency improvements.

Refrigeration is essential for today's living. It's present in the residential sector (air-conditioning in buildings, data centres, etc.), transportation sector (cold chains), and in the

industrial sector. Refrigeration represents a 15% of the world energy consumption, and this figure is expected to increase [2]. All improvements related to energy efficiency within the refrigeration sector are of significant impact under a global energy scheme.

Absorption refrigeration systems play an important role in energy efficiency and in reducing the emission of greenhouse gases since they can make use of different renewable thermal energy sources (solar thermal, biomass, geothermal, etc.), they can recover waste heat from industrial processes, or they can be integrated into energy polygeneration systems. Although the principle of operation of these systems has been known for a long time, absorption refrigeration systems have gained increasing interest in recent years.

1.2 Absorption Refrigeration Systems

Absorption refrigeration systems use thermal energy as the driving energy, instead of electrical or mechanical power as in more conventional vapour compression devices. The compressor is the main component of vapour compression systems. In absorption systems this compressor is substituted by three components: an absorber where the vapour refrigerant is absorbed into another fluid, a pump that pressurizes the mixture, and a generator that separates the refrigerant from the absorbent (see Figure 1-3). It's important to highlight that the energy required for pressurising a liquid is much less than the energy required for pressurising a gas. The condenser and evaporator have the same functions in vapour compression and in absorption systems; in the condenser the high pressure vapour refrigerant rejects heat changing to liquid phase, and in the evaporator the low pressure liquid refrigerant absorbs heat producing the cooling effect, and changing to vapour phase again.

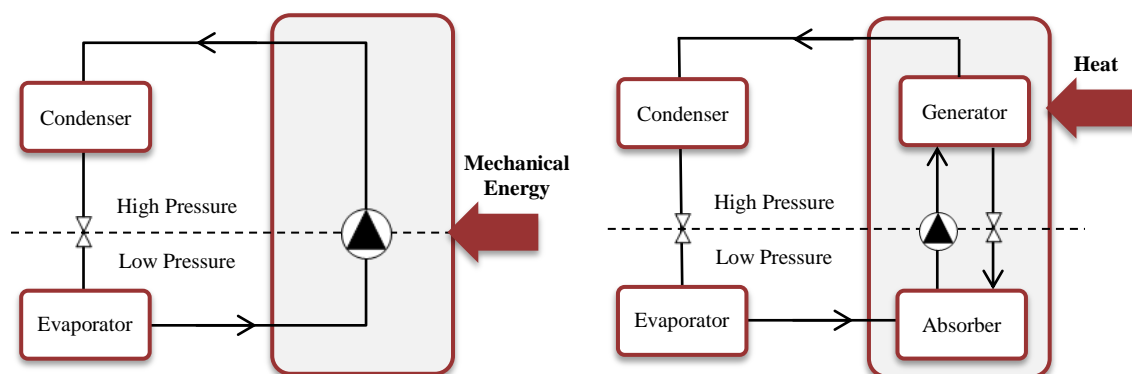


Figure 1-3: Schematics and comparison of a vapour compression system and an absorption system.

Chapter 1. Introduction and Objectives

The Coefficient of Performance (COP) is a common measure of the performance of a refrigeration cycle. It's defined as the ratio of cooling power produced to the energy input in the system. In the case of absorption refrigeration systems COP is the cooling power divided by the heat input in the generator. Since the work input for the solution pump is very small compared with the heat input in the generator, this value is sometimes neglected for the calculation of the COP.

1.2.1 Working fluids in absorption refrigeration cycles

The working fluid in an absorption refrigeration system is a solution consisting of refrigerant and absorbent. In liquid phase both substances must be miscible within the temperature range at which the cycle operates. Refrigerant is separated from absorbent because of their difference in boiling point, therefore it is desired that this difference should be as large as possible. Refrigerant produces the cooling effect when it vaporizes in the evaporator taking heat from the water that is being chilled. It is therefore desired that refrigerant have high heat of vaporisation in order to minimize its flow rate.

The most common working fluids mixtures are $\text{NH}_3/\text{H}_2\text{O}$ (NH_3 is the refrigerant and H_2O is the absorbent) and $\text{H}_2\text{O}/\text{LiBr}$ (in this case H_2O is the refrigerant and LiBr is the absorbent). Both refrigerants have a high latent heat, but neither have ideal vapour pressure characteristics. Ammonia vapour pressures are much higher than those of water. The freezing point of water restricts the use of $\text{H}_2\text{O}/\text{LiBr}$ systems to temperatures above $0\text{ }^\circ\text{C}$, while the very low freezing point of ammonia, $-77\text{ }^\circ\text{C}$, allows operating $\text{NH}_3/\text{H}_2\text{O}$ systems at below zero temperatures. LiBr is excellent as absorbent because its non-volatility. Water is advantageous as absorbent because it does not crystallize [3]. Table 1-1 summarizes the main characteristics of these working fluids.

The rejection of heat in the absorber and condenser of $\text{H}_2\text{O}/\text{LiBr}$ chillers requires the use of cooling towers to avoid crystallisation problems because cooling water has better heat transfer properties than air to maintain the absorber and condenser temperatures at a safe distance from the crystallisation curve at the system working concentrations. Therefore, in $\text{H}_2\text{O}/\text{LiBr}$ systems continuous maintenance of cooling towers is needed to keep the system clean and free of legionellosis problems [4], with the corresponding increment in operation costs. $\text{NH}_3/\text{H}_2\text{O}$ systems have the advantage that the heat can be rejected directly into ambient air.

1.2 Absorption Refrigeration Systems

Table 1-1: Absorption working fluid properties [3].

Desired Property	<i>Ammonia/Water</i>	<i>Water/LiBr</i>
Refrigerant		
High latent heat	Good	Excellent
Moderate vapour pressure	Too high	Too low
Low freezing temperature	Excellent	Limited application
Low viscosity	Good	Good
Absorbent		
Low vapour pressure	Poor	Excellent
Low viscosity	Good	Good
Mixture		
No solid phase	Excellent	Limited application
Low toxicity	Poor	Good
High affinity between refrigerant and absorbent	Good	Good

Research has been carried out to investigate new working fluids, but still $\text{NH}_3/\text{H}_2\text{O}$ and $\text{H}_2\text{O}/\text{LiBr}$ are the most common in commercial devices. One example of this research is the addition of salts to the working fluids. Balamuru et al. [5] and Steiu et al. [6, 7] showed that adding NaOH to the $\text{NH}_3/\text{H}_2\text{O}$ mixture lowers the operating temperature in the generator and therefore improving its performance. However, the NaOH has a negative effect in the absorber because the electrolyte reduces the solubility of the ammonia in water. Thus for high concentrations of hydroxide a hydroxide separation system would be required [7]. A complete review of working fluids of absorption cycles was presented by Sun et al. [8].

1.2.2 Absorption refrigeration cycle configurations

A single-effect absorption refrigeration system is the simplest and most commonly used design. Figure 1-4 shows a schematic of such cycle. Heat is provided to the generator where the refrigerant is evaporated out from the mixture. The high pressure vapour of refrigerant is liquefied in the condenser, rejecting heat to a thermal reservoir that is usually cooling water in the case of $\text{H}_2\text{O}/\text{LiBr}$, and cooling water or air in the case of $\text{NH}_3/\text{H}_2\text{O}$ systems. A throttling device expands the refrigerant to the low pressure level and at the

Chapter 1. Introduction and Objectives

same time reduces its temperature. In the evaporator the refrigerant removes heat from the chilling fluid and evaporates producing the cooling effect. The low pressure vapour refrigerant flows to the absorber where it is absorbed by the poor solution (low concentration of refrigerant) that comes from the generator. A solution pump delivers the rich solution (high concentration of refrigerant) to the generator where the cycle starts again.

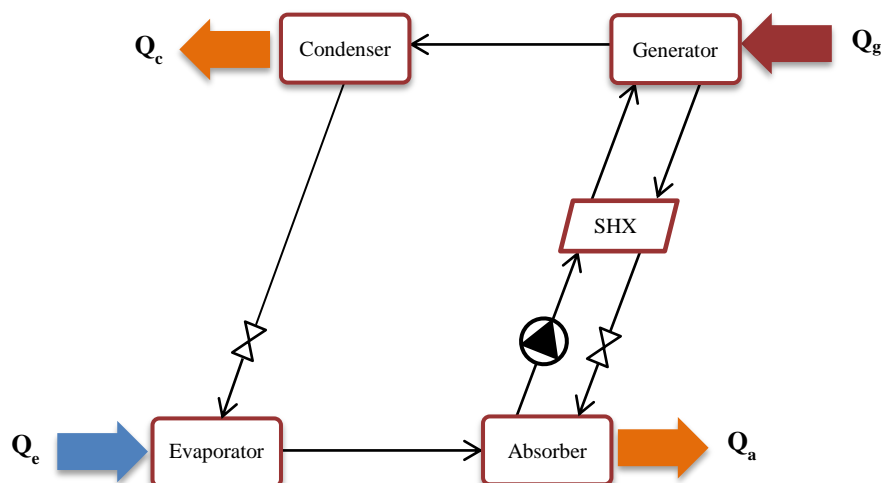


Figure 1-4: Single-effect absorption refrigeration cycle.

When high temperature heat source is available multi-effect cycles can be used to increase the system performance. Each cycle has to be designed in a way that heat rejected from a high temperature stage is used as heat input in a lower temperature stage. Double-effect absorption systems are commercially available. Figure 1-5 shows a schematic of a double-effect absorption cycle. In this cycle, vapour produced in the high temperature generator flows to the high temperature condenser where changes phase by rejecting heat to the low temperature generator, driving vapour out of the solution. With the same heat source vapour is produced in two generators augmenting the flow of refrigerant per unit of energy introduced in the cycle, which results in an increase of the COP.

Triple or more effect devices are not commercially available, they are still under development [9] and most existing units are in experimental phase. They have the inconvenient of needing very high temperature heat sources, compromising the thermal stability of the working fluid, and also complexity of the cycle is increased. Other advanced configurations have been proposed in order to improve the efficiency of absorption refrigeration systems such as the introduction of ejectors, osmotic membranes,

1.2 Absorption Refrigeration Systems

combined absorption-compression cycles, etc. [10]. More details about absorption technology can be found in the book by Herold et al. [3] or the paper by Srihirin et al. [10].

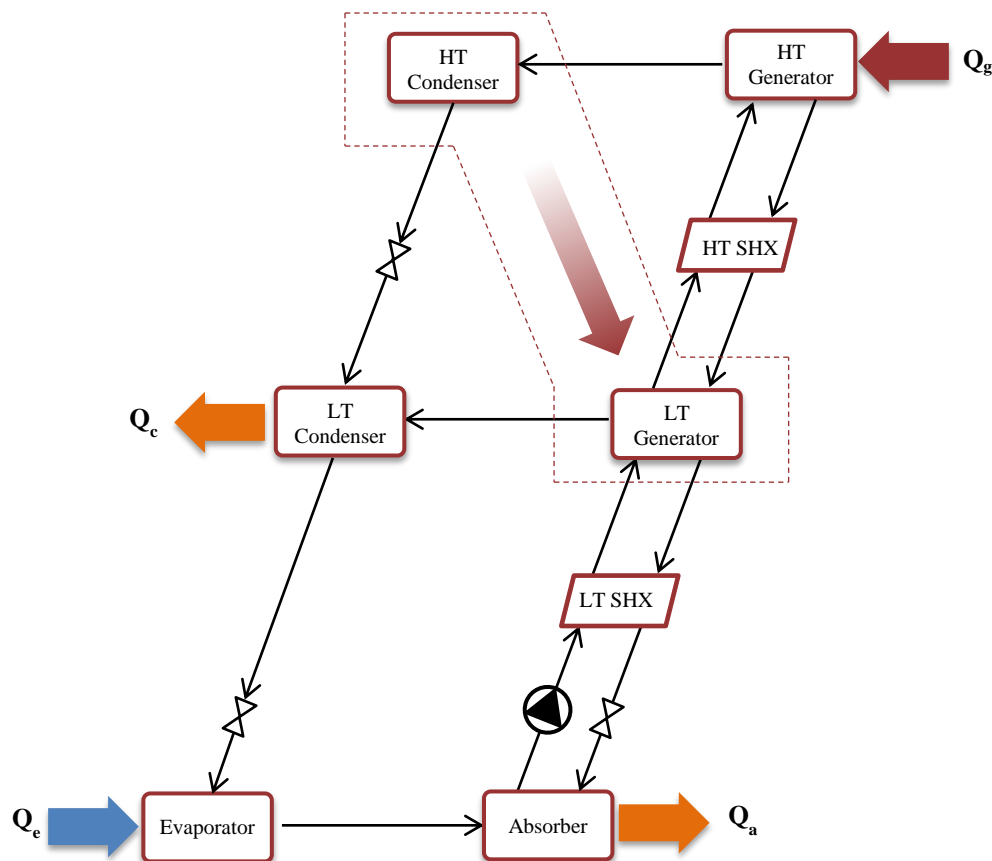


Figure 1-5: Double-effect absorption refrigeration cycle.

1.2.3 Applications of absorption refrigeration systems

Absorption refrigeration systems are particularly attractive in applications where there is a cooling demand, and at the same time there is a source of heat, that if not used it would be rejected to the environment. For instance, absorption systems are being used in the ST4 polygeneration plant that has been installed in Cerdanyola del Valles (Spain) in the framework of the PolyCity project [11]. Currently the main energy consumer of the polygeneration plant is a Synchrotron Light Facility (ALBA) connected to the plant by means of a district heating and cooling network of four tubes. The main units of the plant are 3 cogeneration engines with an electrical nominal capacity of 3,354 kW each. The plant has two absorption chillers with $\text{H}_2\text{O}/\text{LiBr}$ as working fluid. The rated COP and chilled water capacity of the chillers is 0.75/3 MW and 1.3/5MW for the single and the double effect, respectively. The double-effect absorption chiller is fired directly with the exhausts

Chapter 1. Introduction and Objectives

gases of the cogeneration engines while the single-effect absorption chiller is fired with the water from the engine cooling jacket. Figure 1-6 depicts the rated energy generation for each of the engines. The heat recovered from the engines is used to produce cooling power, enhancing the overall energy efficiency of the plant.

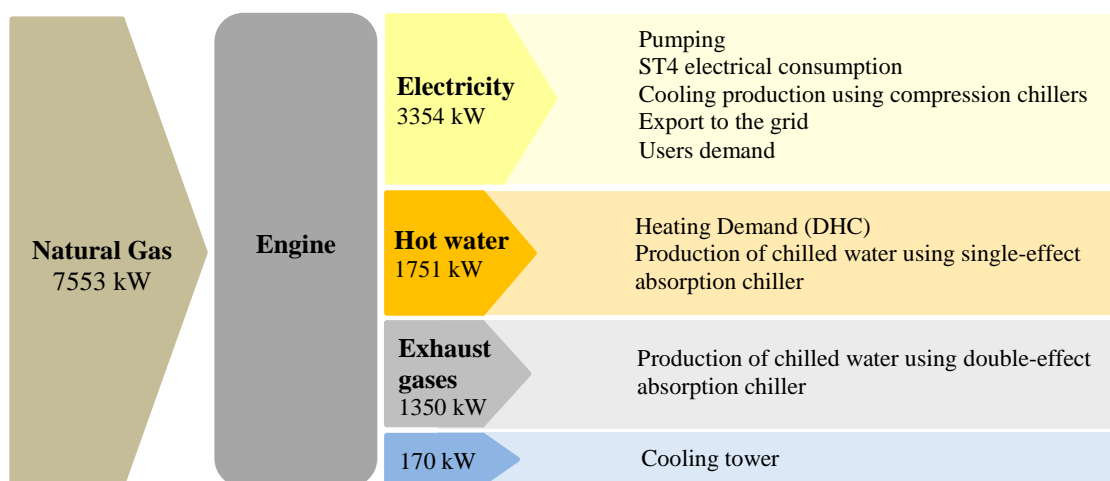


Figure 1-6: Rated energy performance for each engine in the ST4 polygeneration plant [12].

The fishery industry is a potential field of application for absorption refrigeration systems. Studies have been done to assess the improvements in energy savings and efficiency by recovering waste heat from the vessel engines [13]. The typical energy demand services in fishing vessels include cooling power for refrigeration and/or freezing. Part of this cooling power could be supplied by an absorption refrigeration system driven by the heat rejected from the vessel engines.

Solar thermal cooling is an interesting application because usually maximum cooling loads take place when most solar radiation is available. Solar thermal systems are especially interesting in remote areas or islands where conventional cooling is difficult and solar energy is always available [14]. Figure 1-7 shows a general schematic of a solar absorption refrigeration system. Solar radiation from the sun increases the temperature of the heat transfer fluid circulating through the solar collector. Usually a thermal storage tank is used as a buffer between the solar collector and the absorption chiller for a more steadily operation of the system [15]. The absorption refrigeration system may be driven directly by the heat transfer fluid in the refrigerant tank, or indirectly by another heat transfer fluid using a heat exchanger between the tank and the chiller. Solar cooling systems consisting of double-effect absorption cycles and concentrating trough collectors is one of the most promising systems in terms of investment cost [16].

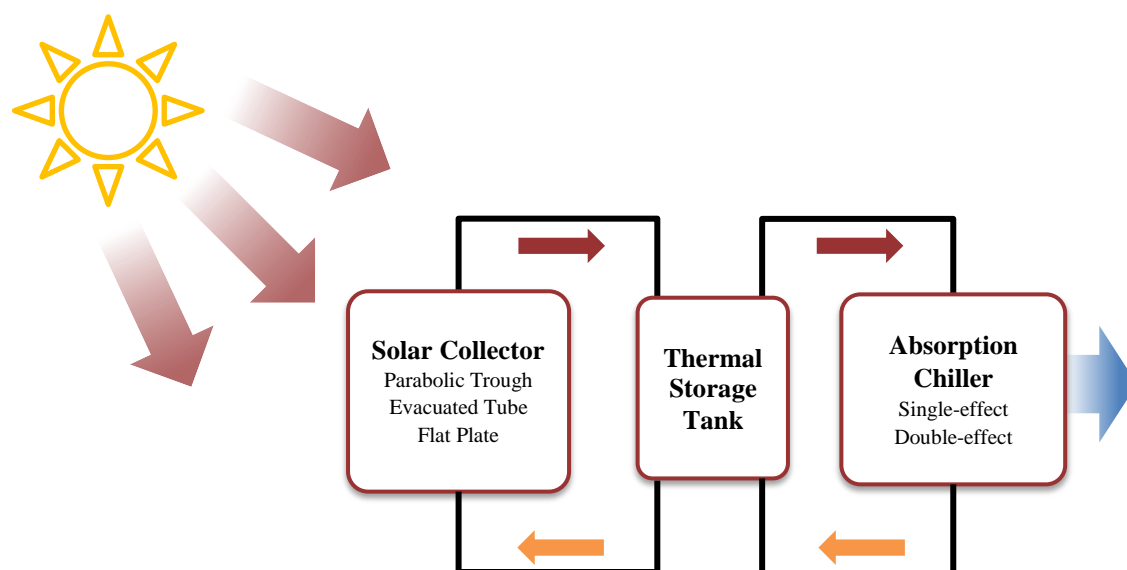


Figure 1-7: General schematic of a solar absorption refrigeration system.

Absorption cycles are also important for the industrial sector. In the oil and gas industry the processing of natural gas requires low temperature cooling. The process overall energy efficiency can be improved when using absorption chillers recovering waste heat from a power generating gas turbine instead of supplying the cooling power with vapour compression systems [17]. Costa et al. [18] studied three configurations integrating absorption heat pumps to a Kraft pulping process. The authors show that, depending on the energy cost, absorption heat pumps can be attractive options for improving savings related to the plant energy consumption.

It is clear that for a particular application, absorption refrigeration systems are valid alternative to vapour compression systems. Nevertheless, there are still barriers, and at the same time improvement margins, for a wider implementation of these systems.

1.2.4 Shortcomings in absorption refrigeration technology

Despite the fact that absorption cooling is a well-known and mature technology, there are still shortcomings for a wider implementation and commercialisation of absorption refrigeration systems. One barrier is a higher capital cost than traditional vapour compression systems. Nevertheless, depending on the situation, absorption chillers can be less costly than vapour compression chillers in terms of overall cost (capital and operation). Another barrier is the weight and size of absorption chillers, since they are heavier and larger than equivalent capacity vapour compression chillers. Research towards cheaper and more compact designs is therefore important.

However, apart from the necessary cost reduction and continuous improvement of this technology, it is necessary to increase confidence in the equipment by the user by providing methodologies and tools to verify that the equipment conforms to the optimum operating conditions in each of the different scenarios of actual operation. In practice, it is very difficult to operate absorption refrigeration systems at nominal conditions during most of the time because of the varying nature of the heat sources (process waste heat, solar heat, etc.) and heat sinks (cooling water from towers, ambient air, etc.). In order to reduce this barrier is fundamental being able to characterize absorption refrigeration systems accurately at conditions other than the nominal. For this purpose, the development of methodologies for obtaining reliable operational data is necessary.

Nowadays data acquisition systems can record multiple variables in short sampling times. As a result, the volume of information available is very large and can be difficult to manage when calculating mass and energy balances. These balances may be violated for various reasons: random and gross errors in the measurements, deviations from steady-state, redundancy in the measurements, etc. Therefore, the methodologies used for data treatment must generate a coherent set of measurements so that the performance of the absorption systems can be reliably estimated. This methodology should be based on the data validation framework.

1.3 Data Validation and Reconciliation

Adequate estimation of the state of the process is fundamental for its correct monitoring. Reliable process measurements are necessary in order to obtain adequate performance indicators required for process control and optimisation. However, process measurements often contain errors. Because of these errors, the mass and energy balances that describe the process are not satisfied when calculated from raw and untreated measurements.

Errors in measurements can be random or systematic. Random errors are the ones due to noise in the signals or natural variability of the process. They are considered to have zero mean. Systematic errors are mainly due to malfunctioning sensors and process leaks. In this case their mean value is expected to be different from zero. Measurement error is the sum of systematic and random errors. Figure 1-8 shows a graphical comparison of random and systematic errors.

1.3 Data Validation and Reconciliation

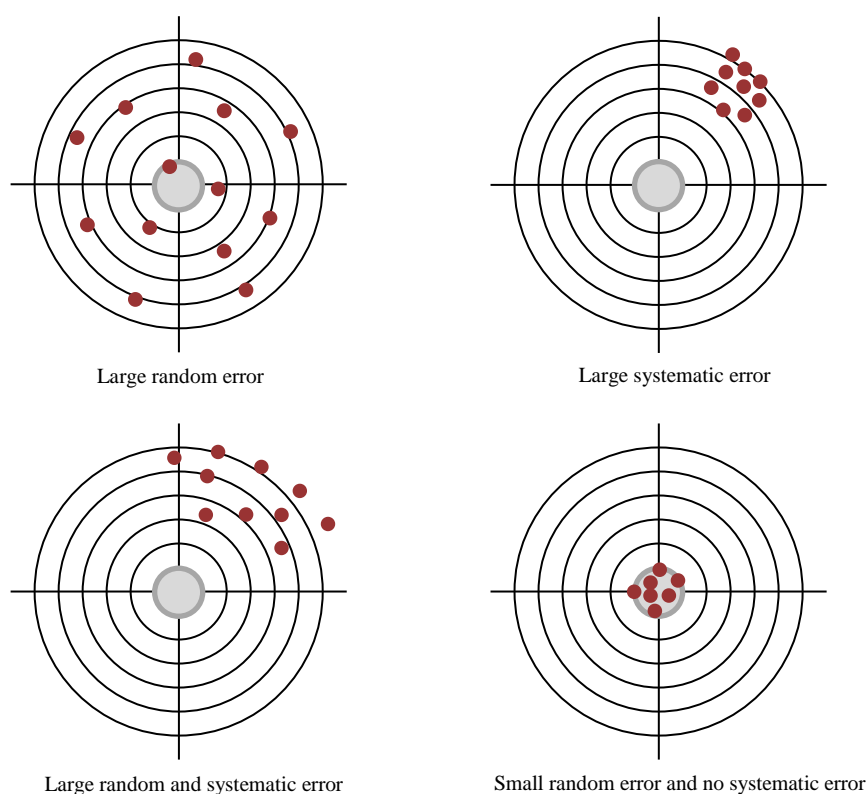


Figure 1-8: Comparison between random and systematic errors.

In this thesis the term “Data Validation” refers to the procedure that aims to improve the reliability of measured data. Data reconciliation (DR) is the core of the data validation procedure. DR is the procedure used to optimally adjust measurements so that the calculated values obey conservation laws and other constraints [19]. A general data validation procedure is represented in Figure 1-9. A set of collected measurements is first pre-processed (steady-state detection, averaging, calculation of covariance, etc.). DR can be performed when the set of measurements has redundancy. Model constraints such as mass and energy balances establish relationships between the process variables. Redundancy exists when there are more measurements than the minimum necessary to reduce the degrees of freedom of the model to zero. If redundant measurements are available, DR procedures are applied. During DR step gross or systematic errors must be identified and eliminated. DR makes use of models which might have unknown parameters. Those parameters can be estimated during the DR procedure. Finally, the set of validated data can be used for other applications like performance estimation, optimisation, control, fault detection, etc.

In summary, the objective of the data validation procedure is to estimate the most likely values of the measurements. During this procedure random error is reduced, systematic

Chapter 1. Introduction and Objectives

errors are detected, and unmeasured variables are calculated; while the contradictions between the data and the process model are reconciled. Complete reviews about DR can be found in the paper by Crowe [19] and the books by Romagnoli and Sánchez [20], and Narasimhan and Jordache [21].

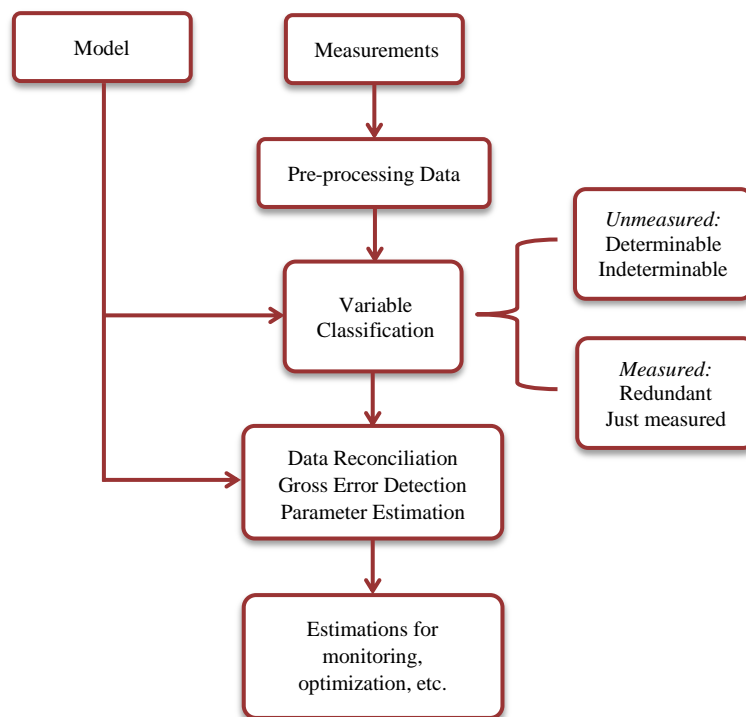


Figure 1-9: General data validation scheme.

1.3.1 Mathematical formulation of the Data Reconciliation problem

Depending on the nature of the model constraints the DR problem can be linear or nonlinear. Linear DR basically deals with flow rate measurements only. Mass balance equations are linear in the flow variable. However, most processes in the industry are nonlinear. Besides flow rate measurements, composition, pressure or temperature measurements are required for the calculation the process variables. Mass balances, component balances, energy balances and other constraints compose a nonlinear model. In this case the DR problem is nonlinear.

Depending if we are interested on a process at steady-state or at transient conditions, the DR problem can be Steady-State DR or Dynamic DR. The approach to treat such problems is totally different. The scope of this thesis is within the steady-state DR problem.

The DR problem is mathematically expressed as a constrained minimisation problem in which the estimate of each variable is as close as possible to the measured value weighted

by its standard deviation. The typical formulation of steady-state DR is the weighted least-squares problem:

$$J = \min \left(\frac{\chi - \chi^*}{\sigma} \right)^2$$

subjected to,

1-1

$$f(\chi, v) = 0$$

$$\chi_{\min} \leq \chi \leq \chi_{\max}$$

$$v_{\min} \leq v \leq v_{\max}$$

where J is the scalar value of the objective function, χ^* is a vector of measurements, χ is a vector of reconciled values of the measurements, v is a vector of estimated non-measured variables, σ is a vector of the standard deviations of the measurements, and $f(\chi, v)$ is the set of equations that describes the system.

1.3.2 Variable classification

As stated above, process variables need to be classified since DR can only be performed when there are redundant measurements. A measured variable is redundant if it can also be estimated from the available measurements using the balance equations.

Classifying the variables enables the DR problem to be formulated correctly: redundant measurements will be adjusted; non-redundant measurements will remain untouched, determinable variables will be calculated, and undeterminable variables will remain unknown [22].

There are two main approaches to classify the process variables using algorithms: the topological approach and the equation-oriented approach. The former is based on graph theory and uses the graphs associated to the process topology. The latter is based on the matrixes associated to the equation system that represents the process.

Regarding the topological approaches, Stanley and Mah [23, 24] developed variable classification algorithms which are only valid for single-component networks. The case of multi-component flow networks is addressed by Kretsovalis and Mah [25]. Later, these authors generalize the variable classification problem including multi-component networks

Chapter 1. Introduction and Objectives

with energy flows, chemical reactions and splitters [26, 27]. The drawback of these algorithms is that they consider enthalpy as function of temperature only, while in many processes it is necessary to take into account the influence on enthalpy of the concentration (if there are two or more components involved), as well as the pressure in vapour streams. Topological approaches have proved to be efficient for linear and bilinear systems; however, they lose rigor when used with highly nonlinear systems [28].

Equation-oriented approaches seem to be more robust when used with nonlinear systems. Some authors proposed classification methods based on the linear algebraic properties of the matrices involved. These methods include the Crowe's matrix projection [29], LU factorisation [30], and recursive matrix inversion by partition and Cholesky factorisation [31]. These algorithms differ in numerical efficiency and complexity. Other authors proposed classification methods based on the rearrangement of the occurrence matrix. The occurrence matrix is a binary array that indicates all the variables that are present in each model equation. Sanchez et al. [32] developed a computer package, called PLADAT, able to classify the variables of large scale processes occurrence matrix. The occurrence matrix rearrangement is accomplished by an output set assignment which consist in assign to any unmeasured variable one equation, or two or more variables the same number of equations. More robust and computationally efficient algorithms have developed by Ponzoni et al. [33, 34] using graph theory to rearrange the occurrence matrix.

1.3.3 Gross error detection

The presence of gross errors invalidates the DR results. They have to be identified and eliminated or corrected before or during the DR procedure. Methods of gross error detection (GED) can be divided into two categories: statistical tests and robust estimators. The former apply a statistical test to the objective function value after DR (global test), to the residuals of the measurements (measurement test), or to the residuals of the balance equations (nodal test). Heenan and Serth [35] and Serth and Heenan [36] explain and compare several methods based on measurement and nodal tests.

The other category of GED methods is based on robust estimators. Martínez-Prata [37] define them as estimators that are not sensitive to the presence of gross errors in the data set. Robust estimators can solve the DR problem and at the same time eliminate gross errors. It has to be mentioned that robust estimators have to be tuned if they are to perform adequately. Several authors have discussed about these methods proposing different robust functions such as the Welsch estimator [37], Contaminated Gaussian distribution [38],

Generalized T distribution [39], or the Quasi-Weighted Least Squares estimator [40]. Ozyurt and Pike [41] compare six different robust estimators along with the weighted least squares estimation. The authors highlight the methods based on the Cauchy distribution and the Hampel's M-estimator because they require less computational effort.

1.4 Objectives

So far, data validation and reconciliation has been extensively used to treat data from open chemical processes. Nevertheless, not many applications deal with closed cycles with complex connectivity and recycle loops, as in absorption refrigeration cycles. Difficulties arise because the reliable thermodynamic property models used to predict temperature-pressure-concentration and enthalpy in several aggregation states introduce additional complexity and convergence problems. These issues have not been treated extensively in the literature. A previous attempt of DR including rigorous calculation of thermodynamic properties in complex absorption refrigeration cycles using the Aspen Plus process simulator revealed that the use of the reconciliation features in that process simulator for this application requires a lot of expertise in their use and the tracking of convergence errors was not easy [42].

This thesis is focused in the development of a methodology for the steady-state data validation and reconciliation of absorption refrigeration systems. This methodology includes the detection of the steady-state, degrees of freedom and redundancy analysis, data reconciliation, parameter estimation, and gross error detection. The methodology is demonstrated by means of cases study of different absorption refrigeration systems configurations with different degrees of redundancy. The methodology presented in this thesis will be useful for generating a set of coherent measurements and operation parameters of an absorption chiller for downstream applications: performance calculation, development of empirical models, optimisation, etc.

The specific objectives of this thesis are listed below:

- Review and compare the current modelling approaches available to describe the steady-state behaviour of absorption refrigeration systems.
- Propose a composite of a steady-state detection algorithm able to track sudden changes as well as slow drifts during absorption refrigeration systems operation.
- Development of a procedure for applying data reconciliation and gross error detection to absorption refrigeration systems.

- Development of methodologies for adequate parameter estimation of absorption refrigeration systems.
- Application of the data validation methodology to various real absorption chillers with different working fluids, configurations and capacities.

1.5 Thesis structure

This thesis is divided into six Chapters. Chapter 1 has shown the importance of energy efficiency inside the current world energy and environmental context. Absorption refrigeration systems play a key role under this scheme, but they lack of more robust methodologies for adequate performance estimation and characterisation. Chapter 1 also presents basic concepts regarding absorption refrigeration technologies and data validation. Finally, this chapter presents the justification and objectives of the thesis.

Chapter 2 presents a comprehensive review of the steady-state modelling and simulation of absorption refrigeration systems. A model is fundamental for data validation. Here the main contributions for modelling and understanding the behaviour of these systems are presented.

Steady-state is one of the main assumptions done when analysing a process. It is very important to establish a robust criterion to determine when the process is at steady-state. Many times in absorption systems there are slow drifts in some of the operating conditions. These slow drifts are not well tracked with traditional steady-state detectors. In Chapter 3 proposes a combined steady-state detector that is able to track sudden changes and slow drifting as well.

Chapter 4 describes a general framework for the simultaneous steady-state modelling, data validation and parameter estimation of absorption refrigeration systems. By means of typical assumptions and the external circuits' measurements we are able to characterize any absorption refrigeration system. The reliability of the measurements is guaranteed by the data validation process.

In order to highlight the benefits of the data validation, applications and case studies are addressed in Chapter 5. Data validation is used for the characterisation of an absorption chiller by means of the Characteristic Equation Method. The benefit of using data validation becomes clear when the parameters of the characteristic equation are estimated with validated data since the prediction of the model is improved.

Finally, in Chapter 6 the main conclusions of the thesis are presented as well as the possibilities of future work.

Chapter 2

Steady-State Modelling and Simulation of Absorption Refrigeration Systems: A Review

Abstract

Data reconciliation makes use of a model for adjusting the measurements to satisfy the process constraints. Therefore, it's fundamental that the model can represent the behaviour of the process accurately. Furthermore, since the resolution of a nonlinear DR problem involves iterative procedures, it is also important that the model is formulated in a way that convergence is not difficult to achieve because absorption refrigeration systems models are highly nonlinear.

In this chapter different aspects about the modelling and simulation of absorption refrigeration systems are reviewed. These aspects include different modelling approaches, simulation strategies, typical assumptions and degrees of freedom analysis, correlations for calculating the thermodynamic properties of the working fluids, as well as different applications where modelling and simulation has been used.

2.1 Introduction

There's a vast literature about theoretical studies where modelling and simulation are used to analyse the performance of absorption refrigeration systems under different scenarios. Different modelling approaches with different levels of complexity have been proposed. Modelling is necessary for optimisation, process control, fault detection, data reconciliation, etc. Not all models are useful for all tasks. Some are too complex to be used for control where rapid convergence is needed, and others are too simple to derive accurate conclusions about thermodynamic issues.

Most of the information about the modelling and simulation of absorption refrigeration systems is usually scattered and seldom put together. There are studies reviewing specifically finite-time thermodynamics approaches in absorption cycles [43, 44], simulation of various types of refrigeration cycles [45], or the use of artificial neural networks in the field of refrigeration, air-conditioning and heat pump systems [46]. This study aims to gather relevant literature related to the steady-state modelling and simulation of absorption cycles taking into account several important aspects that are not usually included together: modelling approaches, simulation strategies, typical assumptions and degrees of freedom analysis, correlations for calculating the thermodynamic properties of the working fluids, and the different fields of application.

In this study we have classified the modelling approaches in three categories: thermodynamic, data driven, and semi empirical. Thermodynamic models are based on the mass and energy conservation principles, vapour-liquid equilibrium, as well as other physical constraints. Data driven models are based on data only and their equations have no physical meaning. Semi empirical models are a middle point between the former two. In semi empirical models some unknown parameters are estimated from experimental or manufacturer data; or some parts of a thermodynamic model are replaced by empirical correlations.

2.2 Thermodynamic Modelling

Absorption refrigeration systems are thermodynamic cycles that mainly exchange heat with the surroundings while heat and mass transfer process occur inside the system. In a thermodynamic model we establish relationships between the operating conditions and the internal states of the cycle in order to describe its behaviour. These relationships must be based on physical principles. The level of complexity of a thermodynamic model depends

on various factors (e.g. available information regarding the absorption cycle, assumptions taken into account, scope of the application, etc.).

2.2.1 Modelling based on finite-time thermodynamics

Finite-time thermodynamics can be used to study thermodynamic cycles based on the temperature differences between the internal cycle and the heat sources or sinks [47]. Depending on the sources of irreversibilities taken into account, the finite-time thermodynamic models can be: reversible, when no irreversibilities are considered; endoreversible, when only irreversibilities due to external heat transfer losses are considered; and irreversible, when internal and external heat and mass transfer losses are considered.

An ideal reversible absorption refrigeration cycle can be represented by means of two combined Carnot cycles in an entropy-temperature diagram (Figure 2-1). In the process line $a-b$ heat Q_{high} is added to the cycle at temperature T_{high} . Line $b-c$ represents the isentropic work production (W). In line $c-d$ heat $Q_{i,2}$ is rejected at temperature T_i . Line $d-a$ represents the isentropic work input. This first cycle ($a-b-c-d$) works as a heat engine.

The cycle $e-f-g-h$ works in the opposite direction and works as a refrigerator or heat pump. The line $e-f$ represents the isentropic compression of working fluid. In the process line $f-g$ heat $Q_{i,1}$ is rejected from the cycle at temperature T_i . Afterwards, in line $g-h$ the working fluid is expanded isentropically. Finally, line $h-g$ represents the heat input Q_{low} at temperature T_{low} .

We assume that the work produced in the first cycle is the same required by the second. The combination of the two Carnot cycles represents a reversible heat driven refrigerator.

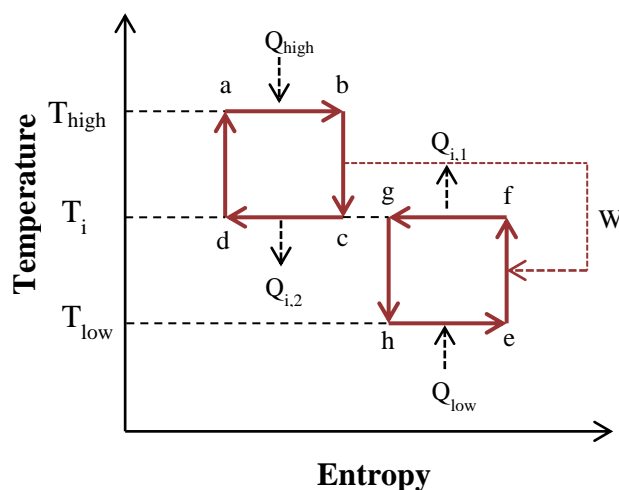


Figure 2-1: Reversible representation of an absorption refrigeration machine.

The efficiency of the power generation η cycle is defined as

$$\eta = \frac{W}{Q_{high}} \quad 2-1$$

The first law analysis of this cycle leads to

$$Q_{high} = W + Q_{i,2} \quad 2-2$$

For a reversible cycle the net entropy production is zero

$$\frac{Q_{high}}{T_{high}} - \frac{Q_{i,2}}{T_{i,2}} = 0 \quad 2-3$$

Combining previous equations we arrive to an expression of the Carnot efficiency that only depends on the two temperature levels.

$$\eta^C = \frac{T_{high} - T_i}{T_{high}} \quad 2-4$$

A similar analysis can be made for the refrigeration cycle. In this case the performance of a refrigerator is defined as

$$COP = \frac{Q_{low}}{W} \quad 2-5$$

where COP stands for coefficient of performance. This term is used because its value can be greater than 1. In this case the benefit obtained from the cycle is Q_{low} , which is the heat absorbed (cooling effect) at the low temperature level T_{low} . Applying a similar analysis as in Equation 2-4 we can express the COP of the refrigeration cycle in terms of the temperature levels:

$$COP^C = \frac{T_{low}}{T_i - T_{low}} \quad 2-6$$

Now, for the combined cycle representing an absorption refrigeration machine the COP is defined as

$$COP_{abs} = \frac{Q_{low}}{Q_{high}} \quad 2-7$$

Now applying the first and second law, equation 2-7 can be expressed as:

$$COP_{abs}^C = \frac{T_{high} - T_i}{T_{high}} \cdot \frac{T_{low}}{T_i - T_{low}} \quad 2-8$$

It can be seen that the Carnot efficiency of an absorption refrigeration cycle depends only on the three temperature levels.

Reversible processes are idealized representations of the real cycles. Therefore COP^C represents a performance limit. All refrigeration machines will perform with a COP lower than COP^C due to the irreversibilities that occur in real thermodynamic processes. In absorption refrigeration systems the main irreversible effects occur because of viscous friction, thermal mixing, mass mixing, heat transfer, and unrestrained expansion [3].

Endoreversible processes are the ones that consider only finite-rate heat transfer losses or simply external losses [48]. The simplest thermodynamic representation of an endoreversible absorption machine is the so called Three-Heat-Reservoir model (Figure 2-2a). The high temperature reservoir corresponds to the generator where the heat input, Q_g , is supplied to the absorption chiller at the temperature T_g . The heat sink reservoir corresponds to the absorber and condenser where the rejected heat, Q_{ac} , is delivered to the surroundings at the temperature T_{ac} . The low temperature reservoir corresponds to the evaporator where the cooling load, Q_e , is supplied to the absorption chiller at the temperature T_e . Nevertheless, in absorption refrigeration systems, absorber and condenser normally reject heat at different temperature levels. In this case a more adequate representation is the Four-Heat-Reservoir (Figure 2-2b). Heat flows Q_a and Q_c are rejected at temperature levels T_a and T_c , respectively.

Chapter 2. Steady-State Modelling of Absorption Refrigeration Systems: A Review

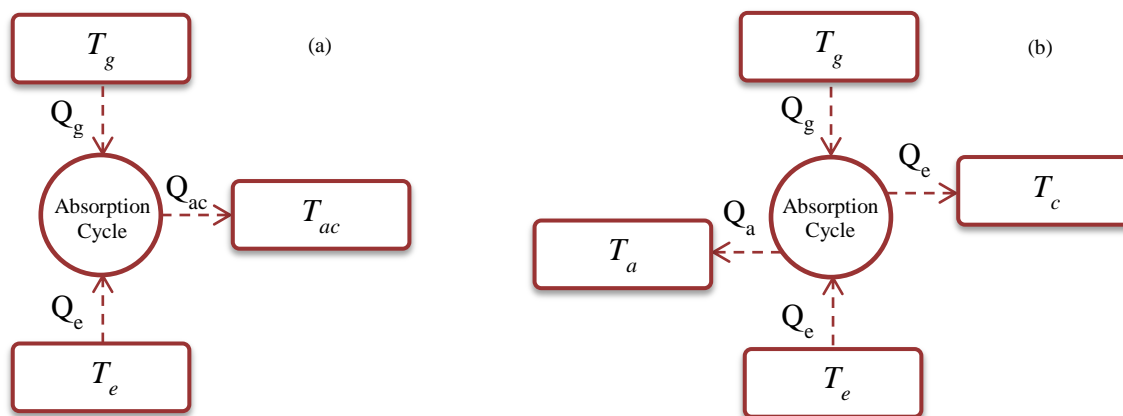


Figure 2-2: Three and Four Heat Reservoir schemes.

Several theoretical studies based on endoreversible models have been published. An optimisation study based on a Three-Heat-Reservoir model demonstrated that optimal endoreversible COP is lower than Carnot [49]. Wijesundera [50] obtained expressions for the maximum cooling load and for the COP at the maximum cooling load in terms of the operating temperatures and heat conductances irreversibilities. In order to compare the performance prediction he estimated the value of the conductances by fitting manufacturer data of an absorption chiller. The prediction resulted satisfactory in terms of trends only since the actual values were significantly different. The same author published a similar study [51], but in this case the comparison was done with detailed simulation data using the same conductances values from the simulation. The agreement was good trendwise.

Hellmann [52] derived the COP for a heat driven refrigerator based on the Four-Heat-Reservoir model:

$$COP_{4t}^C = \frac{T_g - \bar{T}_{ac}}{T_g} \cdot \frac{T_e}{\bar{T}_{ac} - T_e} \quad 2-9$$

where \bar{T}_{ac} is the entropic mean temperature of the total heat rejection according to:

$$\bar{T}_{ac} = \frac{1 + \frac{Q_a}{Q_c}}{\frac{1}{T_c} + \frac{Q_a}{Q_c} \cdot \frac{1}{T_a}} \quad 2-10$$

Chen et al. [53] presented a theoretical optimisation study based on a Four-Heat-Reservoir model. They obtained the fundamental optimal relation between the COP and the cooling load, as well as the maximum cooling load and the corresponding COP of the cycle. A linear heat transfer law was adopted to model the irreversibilities related to heat transfer between the cycle and the heat reservoirs. Zheng et al. [54] did the same study but taking into account heat leaks additionally to the linear heat transfer law irreversibilities. A similar work is the one of Qin et al. [55] but they used a generalized heat transfer law for describing the irreversibilities related to the heat conductances. In another study, Qin et al. [56] obtained the optimal performance of an absorption refrigeration system based on a thermo-economic optimisation and a four heat reservoir model. The authors derived an expression for the optimal fundamental relation between cooling load and COP taking into account the investment and energy consumption costs.

Endoreversible models are not accurate when predicting the performance of real absorption systems because they don't take into account the internal irreversibilities of the cycle. However, they may be useful in providing maximum performance limits which are lower than Carnot limits [57].

Irreversible models take into account the internal irreversibilities besides the external heat transfer irreversibilities. An irreversible Four-Heat-Reservoir model was used by Zheng et al. [58] and Chen et al. [59] for a performance optimisation study. They obtained expressions for the maximum COP and the corresponding cooling load, the maximum cooling load and the corresponding COP, and the fundamental optimal relation between the cooling load and COP. In order to take into account the internal generation of entropy the authors introduced the irreversibility factor I (Equation 2-11). The cycle is endoreversible when $I=1$, and irreversible when $I \geq 1$.

$$I = \frac{\frac{Q_g}{T_g} + \frac{Q_e}{T_e}}{\frac{Q_a}{T_a} + \frac{Q_c}{T_c}} \geq 1 \quad 2-11$$

Huang et al. [60] used a Four-Heat-Reservoir model to optimise the performance of an absorption heat pump. This optimisation was done in two steps. First, the optimal relation among the heating load, the COP and total heat-transfer area is obtained. Afterwards, an

ecological criterion, which takes into account entropy generation, is used for determining optimal COP with its corresponding heating load.

Previously exposed studies are not focused in predicting the performance of a real absorption machine but focused in theoretical performance optimisation. In order to reproduce the behaviour of a real absorption chiller by means of an irreversible model it is necessary to account for the internal entropy generation of the cycle. Nevertheless, it is difficult to obtain such information when there aren't internal measurements or when design parameters are unknown. Some proposed irreversible models use experimental or manufacturer data to fit parameters that account for internal irreversibilities. Wijesundera [61] presented an irreversible Three-Heat-Reservoir model where semi-empirical expressions with different functional forms were used to model the internal entropy generation of the cycle. The functional forms considered were: constant entropy, linear variation of entropy, and logarithmic variation of entropy. Each of the functional forms has parameters that were fitted using a set of simulated data. The linear and logarithmic entropy functions were found to give the better performance prediction. This approach falls in the category of semi-empirical modelling which will be explained with more detail in section 2.4.

When modelling heat transfer processes occurring in absorption cycles, it is practical to consider that they take place at constant temperature. Nevertheless, in practice these processes are not isothermal. The working fluid experiment temperature glides in the main components of the absorption cycle because of mass fraction variations, superheating, subcooling, etc. The entropic average temperature (T_{sa}) is an appropriate representation of a non-isothermal heat transfer process [3]. Equation 2-12 presents a general definition of T_{sa}

$$T_{sa} = \frac{Q}{S} = \frac{Q}{\int \frac{dQ}{T}} \quad 2-12$$

The process average temperature relates the internal irreversibilities to the operating conditions. Ng et al. [62] derived T_{sa} expressions for the non-isothermal processes occurring in each of the main heat exchangers of absorption chillers. They have showed that correct formulation of T_{sa} is essential for accurate model predictions. The work of Chua et al. [63] is focused in the thermodynamic modelling of the absorber and generator

of a H₂O/LiBr chiller. Besides taking into account T_{sa} , they introduced extra physical constraints in the form local thermodynamic balances. As a result, more realistic upper performance limit can be obtained and the losses due to mass transfer can be calculated. As a continuation of this work they performed a simulation of an NH₃/H₂O chiller taking into account heat and mass transfer processes in the absorber, generator, and rectifier as well [64].

Complete and comprehensive reviews about finite-time thermodynamic modelling can be found in the papers by Ngouateu Wouagfack et al. [44] and Feidt [43].

2.2.2 Modelling based on mass and energy balances

In order to estimate all the internal states of an absorption refrigeration system we need a model based on mass and energy balances applied on each component of the absorption cycle. Figure 2-3 shows a schematic of a single-effect absorption chiller. From this configuration the governing equations are detailed below.

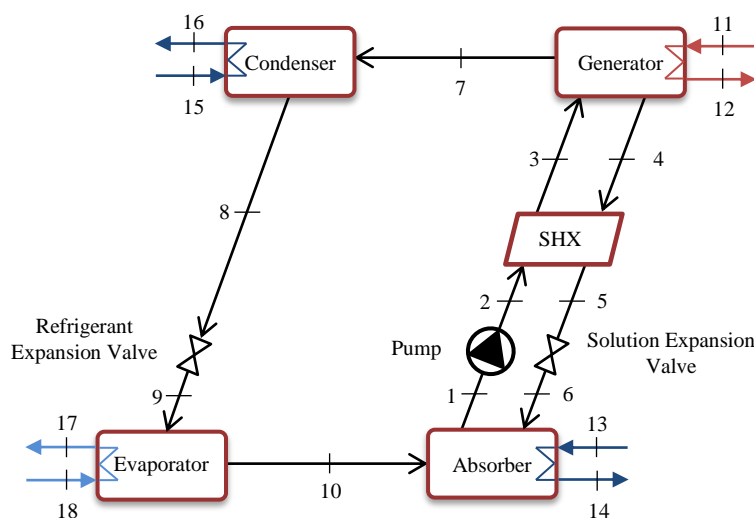


Figure 2-3: Schematic of a single-effect absorption cycle including external streams.

Absorber:

$$m_1 = m_6 + m_{10} \quad 2-13$$

$$m_1 \cdot x_1 = m_6 \cdot x_6 + m_{10} \cdot x_{10} \quad 2-14$$

$$Q_a + m_1 \cdot h_1 = m_6 \cdot h_6 + m_{10} \cdot h_{10} \quad 2-15$$

Chapter 2. Steady-State Modelling of Absorption Refrigeration Systems: A Review

Pump:

$$m_2 = m_1 \quad 2-16$$

$$x_2 = x_1 \quad 2-17$$

$$m_2 \cdot h_2 = m_1 \cdot h_1 + W \quad 2-18$$

Solution heat exchanger:

$$m_3 = m_2 \quad 2-19$$

$$x_3 = x_2 \quad 2-20$$

$$m_5 = m_4 \quad 2-21$$

$$x_5 = x_4 \quad 2-22$$

$$m_3 \cdot h_3 + m_5 \cdot h_5 = m_2 \cdot h_2 + m_4 \cdot h_4 \quad 2-23$$

Generator:

$$m_3 = m_4 + m_7 \quad 2-24$$

$$m_3 \cdot x_3 = m_4 \cdot x_4 + m_7 \cdot x_7 \quad 2-25$$

$$Q_g + m_3 \cdot h_3 = m_4 \cdot h_4 + m_7 \cdot h_7 \quad 2-26$$

Solution expansion valve:

$$m_6 = m_5 \quad 2-27$$

$$x_6 = x_5 \quad 2-28$$

$$h_6 = h_5 \quad 2-29$$

Condenser:

$$m_8 = m_7 \quad 2-30$$

$$x_8 = x_7 \quad 2-31$$

$$Q_c + m_8 \cdot x_8 = m_7 \cdot x_7 \quad 2-32$$

Refrigerant expansion valve:

$$m_9 = m_8 \quad 2-33$$

$$x_9 = x_8 \quad 2-34$$

$$h_9 = h_8 \quad 2-35$$

Evaporator:

$$m_{10} = m_9 \quad 2-36$$

$$x_{10} = x_9 \quad 2-37$$

$$Q_e + m_9 \cdot h_9 = m_{10} \cdot h_{10} \quad 2-38$$

Note that the global and component mass balances in absorber (Equations 2-13 and 2-14) and generator (Equations 2-24 and 2-25) are equivalent. For binary working fluids like NH₃/H₂O and H₂O/LiBr only one overall mass balance and one species mass balances are required.

Simplified heat exchanger models allow relating the internal cycle variables with the external operating conditions. The most common approach is the use of the product of the overall heat transfer coefficient, U , and the heat exchanger area, A , as a single parameter, UA .

$$Q = UA \cdot \Delta t_{lm} \quad 2-39$$

Δt_{lm} is the logarithmic mean temperature difference, defined as:

$$\Delta t_{lm} = \frac{(t_{hot,1} - t_{cold,1}) - (t_{hot,2} - t_{cold,2})}{\ln\left(\frac{t_{hot,1} - t_{cold,1}}{t_{hot,2} - t_{cold,2}}\right)} \quad 2-40$$

where *hot* and *cold* refer to the hot and cold sides of the heat exchanger, respectively. The subscripts *1* and *2* refer to either end of the heat exchanger (see Figure 2-4).

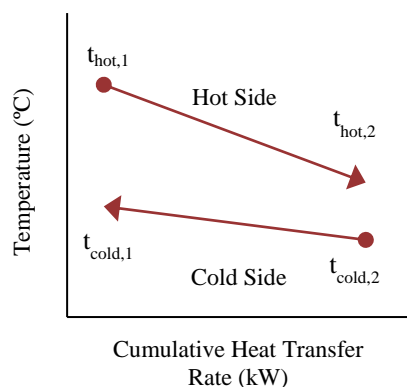


Figure 2-4: Counter-flow heat exchanger

In order to solve the mass and energy balances we need to calculate the thermodynamic states (pressure, temperature, concentration, enthalpy, etc.) within the absorption cycle. Therefore, correlations for calculating the thermodynamic properties of the working fluid are necessary.

2.2.3 Correlations for calculating the thermodynamic properties of working fluids

In this section we review some thermodynamic properties formulations proposed in the literature for the two most common working fluids in absorption refrigeration systems: LiBr/H₂O and NH₃/H₂O.

Table 2-1 shows some of the formulations available for calculating the thermodynamic properties of the H₂O/LiBr mixture. The formulation proposed by McNeely [65] has been one of the most used since its proved to be accurate in the operation ranges of conventional absorption machines. Herold and Moran [66] presented a thermodynamically consistent formulation based on the Gibbs free energy. Chua et al. [67] proposed functions for calculating the specific enthalpy, entropy, and heat capacity for temperatures from 0 to 190 °C, and concentrations from 0 to 75 wt%. Kaita [68] extended the temperature range up to 210 °C proposing another formulation. This formulation is intended to be used for the

modelling of triple-effect absorption cycles. Kim and Infante-Ferreira [69] proposed a Gibbs energy equation to cover a wide range of operation: solution concentration from 0 to 70 wt%, temperature from 0 to 210 °C, with the equilibrium vapour pressures ranging from 74 to 1 MPa. Patek and Klomfar [70] presented a formulation as a set of separate empirical equations describing pressure, molar density, isobaric heat capacity, enthalpy, and entropy. These equations are interesting from a numerical point of view since they are explicit functions of temperature and composition.

Table 2-1: Property correlations for the H₂O/LiBr mixture available in the literature.

Reference	Correlation Basis	Application Range	
		LiBr Mass Fraction	Temperature (°C)
McNeely [60]	Dühring equation	0 to 0.70	0 to 180
Herold and Moran [66]	Gibbs free energy	0.45 to 0.70	15 to 166
Chua et al. [64]	Dühring equation	0 to 0.75	0 to 190
Kaita [65]	2 nd degree T _{dew} equation	0.40 to 0.65	40 - 210
Kim and Infante-Ferreira [66]	Gibbs free energy	0 to 0.70	0 -210
Patek and Klomfar [67]	Empirical polynomial correlations	0 to 0.75	0-227

Besides being used for absorption refrigeration cycles, the mixture NH₃/H₂O is also used for power cycles. Therefore many formulations covering a wide working range have been proposed. Table 2-2 summarises some of the most used formulations.

The formulation by Ziegler and Trepp [71] based on Gibbs free energy expressions have been used for the simulation absorption refrigeration systems. Afterwards, other formulations have been proposed for increasing the working range such as the formulation by Stecco and Desideri [72]. Patek and Klomfar [73] presented a formulation which is relatively simple in comparison other correlations. These correlations were obtained fitting critically assessed experimental data to polynomial functional forms. The formulation proposed by Tillner-Roth and Friend [74] uses a Helmholtz free energy model where the most reliable thermodynamic properties to the time were used for obtaining the model Tillner-Roth and Friend [75]. This formulation has been adopted by the IAPWS.

Chapter 2. Steady-State Modelling of Absorption Refrigeration Systems: A Review

Table 2-2: Property correlations for the NH₃/H₂O mixture available in the literature [76].

Reference	Correlation Basis	Application Range	
		Pressure (bar)	Temperature (°C)
Ziegler and Trepp [71]	Gibbs free energy	up to 50	up to 227
El-Sayed and Tribus [77]	Gibbs free energy	0.1 to 110	27 to 499
Stecco and Desideri [72]	Gibbs free energy	up to 115	N.A.
Smolen et al. [78]	Cubic EoS	up to 34	20 to 140
Moshfeghian et al. [79]	Cubic EoS and Group contribution theory	up to 35	up to 121
Ibrahim and Klein [80]	Extension of Ziegler and Trepp	0.2 to 110	-43 to 327
Patek and Klomfar [73]	Empirical polynomial correlations	up to 20	up to 200
Tillner-Roth and Friend [74]	Helmholtz free energy	up to 400	N.A.
Xu and Goswami, [81]	Gibbs free energy and empirical T _{bubble} and T _{dew} equations	0.2 to 110	-43 to 327

Thorin [82] compared the influence of different NH₃/H₂O properties correlations on simulations of absorption cycles. The properties used were the formulations by Stecco and Desideri [72], Ibrahim and Klein [80] and Tillner-Roth and Friend [74]. The author showed that the differences in the result are small but they tend to increase with increasing maximum pressure in the cycle.

2.2.4 Typical Assumptions and Degrees of Freedom Analysis

When modelling complex non-linear systems like absorption chillers, there is always some information (internal temperature measurements, concentrations, pressure drops, geometry of the components, etc.) that is not available. Without this information the model cannot be solved, and therefore the modeller must either include extra restrictions (increasing the complexity of the model) or make some assumptions. When modelling absorption refrigeration systems, the assumptions that systematically appear in the literature are the following:

- No pressure drops through the components, except through expansion valves
- Heat losses are neglected
- Kinetic and potential energy effects are neglected
- Saturated liquid conditions at the absorber, condenser and generator outlets
- Saturated vapour conditions at the evaporator outlet
- If heat transfer between the internal and external circuits is considered then constant heat transfer coefficients (UA values) are assumed to be constant

The numbers of assumptions taken, as well as the available information, determine the degrees of freedom of the model. A systematic methodology developed exclusively for absorption cycles has been proposed by Ayou et al. [83]. The authors developed a catalogue that reports the degrees of freedom for the typical components of absorption chillers. As soon as the model represents the absorption system and the set of measurements obtained from the monitoring devices we can account for the degrees of freedom of the absorption system by adding the degrees of freedom of each of the components. This methodology requires only the schematics of the cycle and the number of components in the working fluid mixture. One advantage of this methodology is that it analyses the degrees of freedom of the whole absorption cycle, as well as for of each component of the cycle reducing the chances of developing ill-conditioned models.

2.2.5 Simulation of absorption refrigeration systems in steady-state

Once we have the set of equations, considered the relevant assumptions, defined the set of model inputs, and selected the adequate properties correlations, we can proceed to simulate the absorption cycle. In the literature different strategies have been used for this task. Applications using programming languages like C [84] and Fortran [85] use iterative methods to solve the model in a sequential modular way. Bakhtiari et al. [86] characterized and modelled a single-stage H_2O – LiBr absorption chiller of 14 kW. The entire set of non-linear equations is solved with the Gauss–Newton method. In Ahmed and Gilani [87] an iterative solving procedure was used for the simulation of a double-effect absorption chiller driven by steam. Wang et al. [88] used the bisection method with an iterative procedure for the simulation of a gas-fired air-cooled $\text{H}_2\text{O}/\text{LiBr}$ adiabatic absorption refrigeration system.

The Engineering Equation Solver (EES) [89] is very popular software for the modelling and simulation of thermodynamic cycles. It has the advantage of having a large database with the thermodynamic properties of many substances, including the working fluids used in absorption refrigeration systems. Several EES simulation studies of absorption cycles

have been published including second law analysis of single and two-stage $\text{NH}_3/\text{H}_2\text{O}$ chillers [90], modelling of a double-effect chiller adjusted with experimental data [91], parametric investigation of single single-effect and series flow double-effect $\text{LiBr}/\text{H}_2\text{O}$ chillers [92], comparison of double-effect chiller configurations [93], estimation of the conductances of a double-effect chiller [94], etc.

A convenient option for the modelling and simulation of absorption refrigeration systems is the use of flowsheet simulation software. In this case the model is built by connecting modules or blocks that correspond to the components of the absorption cycle. Underlying those block are the mass and energy balances and equilibrium relationships involved in each cycle component. This approach have the advantage of avoiding the introduction of the equations, nevertheless some parameters have to be set. The software ABSIM (Absorption SIMulation), which has been developed since the 1980s [95], has been developed for simulation of absorption systems in a flexible and modular form. The set of governing equations is generated as the user draws the cycle diagram on the computer screen. Park et al. [96] used ABSIM to study the partial load operation of a double-effect absorption chiller. There are other general flowsheet simulators such as ASPEN Plus and Hysys that have been used in absorption refrigeration applications. In Balamuru et al. [5] ASPEN is used to study an $\text{NH}_3/\text{H}_2\text{O}+\text{NaOH}$ absorption chiller. They study the effect of the salt in the cycle performance through simulation. Darwish et al. [97] used ASPEN to study an air-cooled $\text{NH}_3/\text{H}_2\text{O}$ chiller looking for strategies to improve the performance. In Somers et al. [98] ASPEN is used to model single and double-effect $\text{H}_2\text{O}/\text{LiBr}$ chillers. Comparison is made with EES and some experimental data with good agreement. Brunet et al. [99] used ASPEN to simulate an $\text{NH}_3/\text{H}_2\text{O}$ chiller as part of an optimisation framework. Martins et al. [100] used HYSYS for the performance analysis of a trigeneration system including an $\text{NH}_3/\text{H}_2\text{O}$ chiller.

2.3 Data Driven Modelling

Data driven models, also called black-box models, have the advantage over thermodynamic models that they converge very fast. These types of models are based on adjustable parameters that are tuned in order to reproduce selected data. Their drawback is that their predictions are limited to the region of operating data used, in other words, they don't have good extrapolation properties.

In absorption refrigeration systems modelling, data driven models are mainly used when there are no measurements of the internal variables, or when there is no information regarding design parameters of the chiller.

Most common examples of data driven modelling are artificial neural networks (ANN) and multivariable polynomial regression models.

2.3.1 Artificial Neural Networks

Artificial neural networks are able to learn the relationship between inputs and outputs, independently of the physical complexity of the system. They can be found in a wide variety of applications such as patten recognition, data mining, stock market prediction, etc. During last two decades, they have been also used to solve complex problems in the refrigeration and air conditioning field [46].

An ANN is trained to reproduce a particular behaviour based just on input and output information. The connections or weights (w) between the nodes are adjusted by means of training algorithms in order to model complex relationships between inputs and outputs.

The architecture of an ANN refers to the way in which nodes are connected and how the information flows through the network. The most common architecture is the multi-layer feed-forward network (Figure 2-5). An input layer is followed by one or more hidden layers and an output layer. The input layer contains the set of parameters that affects the system behaviour (X); the hidden layers contain the transfer functions; and the output layer contains the output parameters to be predicted by the network. The product of the weights and the bias (b) of each node are summed and transformed by the transfer function (F) to generate a final output (Y).

In the field of modelling and simulation of absorption cycles there are many works that have used ANN at different stage of the modelling process. Manohar et al. [101] presented a neural network model for steady-state modelling of a double effect absorption chiller using steam as heat input. The ANN predicts the COP within a $\pm 1.2\%$ of error. Şencan [102] used ANN to predict the COP and circulation ratio of an $\text{NH}_3/\text{H}_2\text{O}$ chiller from the temperatures of the main heat exchangers and the solution concentrations. The correlation coefficients obtained for circulation ratio and COP were 0.9996 and 0.9873, respectively. In Rosiek and Batlles [103] an ANN is used to predict the performance of a solar-assisted air-conditioning system. This system includes a flat-plate collector field, single-effect $\text{H}_2\text{O}/\text{LiBr}$ absorption chiller and a cooling tower. The ANN model is able to predict the

COP of the absorption chiller as well as the global system efficiency with a root mean square error less than 1.9%.

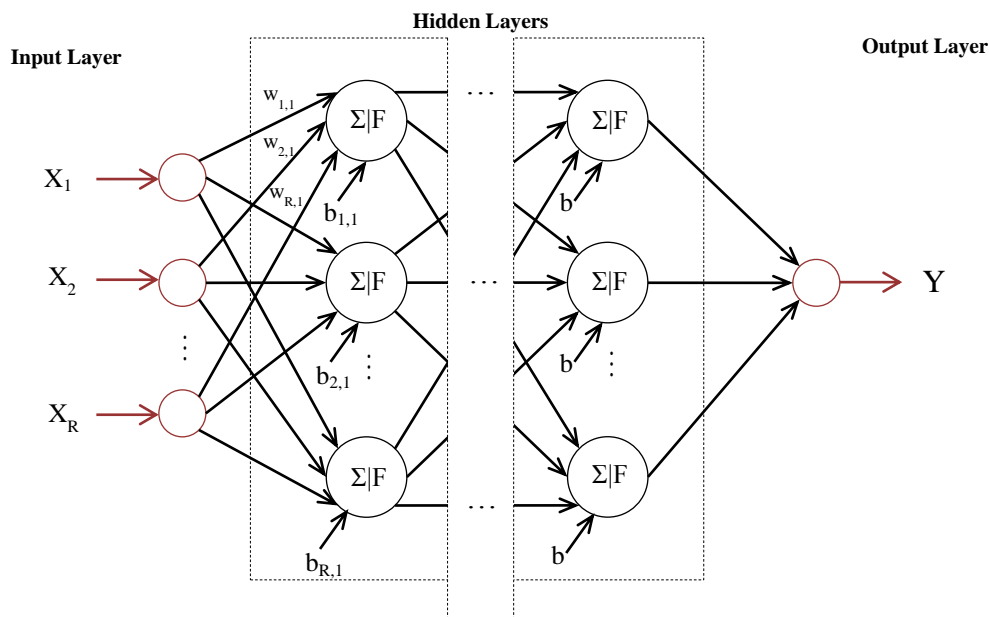


Figure 2-5: Artificial Neural Network multi-layer feed-forward architecture

ANNs have been also used for second law analysis of absorption cycles. Sözen and Arcaklioglu [104] used ANN to calculate the non-dimensional exergy losses of the main components (evaporator, generator, absorber and condenser) of an ejector-absorption heat transformer. The correlation coefficient was reported to be above 0.99 for all variables.

Chow et al. [105] used an ANN model of a direct-fired double-effect H₂O/LiBr absorption chiller. By means of genetic algorithms and the ANN model, optimal chiller operation, in terms of minimum consumption of fuel and electricity, is achieved. Labus et al. [106] used an ANN model for model based control strategy for a small-scale absorption chiller with a nominal cooling capacity of 4.5 kW. They propose using an “inverse ANN” coupled with an optimisation algorithm in order to find optimal operating parameters for a required cooling load. The term inverse indicates that the direction of the ANN/optimisation algorithm combination is opposite: from required output to the optimized parameters.

2.3.2 Multivariable Polynomial Regression

A linear regression model aims to represent the relationship between one or more independent variables (vector a) and one dependent variable (z) by fitting some parameters (β) (Equation 2-41). The term ε is called error term. It captures the influences on the dependent variable that are not related to the independent variables.

$$z = a \cdot \beta + \varepsilon \quad 2-41$$

Multivariable Polynomial Regression Models (MPRMs) contain squared and higher order terms. Take for instance the model represented by Equation 2-42

$$z = \varepsilon + a_1 \cdot \beta_1 + a_2 \cdot \beta_2 + a_1 \cdot a_2 \cdot \beta_3 + a_1^2 \cdot \beta_4 + a_2^2 \cdot \beta_5 \quad 2-42$$

Note that the model contains squared terms in a_1 and a_2 . This model is a second order model because the maximum power of the terms in the model is two. Also this model contains a cross-product term, $a_1 a_2$, representing an interaction between independent variables a_1 and a_2 . Higher order models offer better accuracy of prediction; however, excessive polynomial order for a relatively small database may worsen data interpolation [107].

Regression models have been used to study the influence of some variables in the performance of absorption chillers using statistical tools. In order to improve the initial design of an absorption chiller, Martínez and Pinazo [108] used regression models for COP and cooling capacity. Analysis of variance was used to study effects and interactions of the five heat exchanger areas on the chiller performance. Their study show an improved design with a 10% better COP at the same nominal cooling capacity.

Martínez and Pinazo [109] developed regression models for estimating the performance of absorption chillers in terms of the operating conditions. The authors used experimental design and analysis of variance techniques in order to determine appropriate model order as well as the significant parameters. Their study was based on simulated data using thermodynamic model developed in TRNSYS. A first order model was reported to be adequate for the cooling capacity (squared correlation of about 99.89 %). In the case of the COP a second order model was necessary (squared correlation of about 98.99 %) but the effect of the hot water mass flow rate is not significant.

There are a couple of studies comparing different data driven modelling approaches applied to absorption refrigeration systems. Şencan [110] compared ANN, Linear Regression and M5'Rules. The author concluded that ANN model is the best. In Şencan et al. [111] the authors compare Linear Regression, Pace Regression, Sequential Minimal

Optimisation, M5 Model Tree Algorithm, M5'Rules, Decision Table and ANN. The inputs of all models are the temperatures at each of the main components of the absorption chiller (absorber, generator, condenser and evaporator) while the performance indicators are the COP and the circulation ratio. ANN is reported to be the most accurate.

2.4 Semi-Empirical Modelling

Semi-empirical models, also called grey-box models are based on thermodynamic principles, but they have also adjustable parameters from data that may or may not have physical interpretation. These models are usually simpler than thermodynamic models, easier to build, present fast convergence, and usually have good extrapolation properties.

2.4.1 A semi-empirical thermodynamic model from finite-time thermodynamics

Gordon and Ng [112] derived a general thermodynamic model which takes into account irreversibilities such as finite-rate mass transfer processes in generator and absorber as well as heat leaks. From energy and entropy balances applied to each component of the cycle an expression for the COP in terms of the operating conditions and cooling rate is obtained:

$$\frac{I}{COP} = \left[\frac{T_{ac}^{in} - T_e^{out}}{T_e^{out}} \right] \left[\frac{T_g^{in}}{T_g^{in} - T_{ac}^{in}} \right] + \frac{I}{Q_e} \left[\frac{T_g^{in}}{T_g^{in} - T_{ac}^{in}} \right] \left[q_{ac}^l - q_e^l \frac{T_{ac}^{in}}{T_e^{out}} - q_g^l \frac{T_{ac}^{in}}{T_g^{in}} \right] \quad 2-43$$

where the superscripts *in* and *out* refer to the inlet and outlet streams of the corresponding external circuits and q^l refers to the losses from all sources other than finite-rate heat transfer. Considering that the dominant irreversibility is finite-rate mass transfer and that it is roughly temperature-independent, then the term q_e^l is treated as negligible and the terms q_{ac}^l and q_g^l are considered as constants characteristic of a particular absorption chiller. The final approximate formula for COP is then:

$$\frac{I}{COP} = \left[\frac{T_{ac}^{in} - T_e^{out}}{T_e^{out}} \right] \left[\frac{T_g^{in}}{T_g^{in} - T_{ac}^{in}} \right] + \frac{I}{Q_e} \left[\frac{T_g^{in}}{T_g^{in} - T_{ac}^{in}} \right] \left[A_1 - A_2 \frac{T_{ac}^{in}}{T_e^{out}} \right] \quad 2-44$$

On the right hand of Equation 2-44 the first term represents the COP or an endoreversible chiller while the second term represents the internal irreversibilities. The

two parameters (A_1 and A_2) that characterize the irreversibilities of the chiller are found by data fitting. Afterwards, the authors extended this idea to other types of chillers [113].

2.4.2 The Characteristic Equation Method

The Characteristic Equation Method developed by Hellmann et al. [114] and Ziegler et al. [115] allows calculating the cooling capacity and the COP of a single-effect H₂O/LiBr absorption chiller by means of simple algebraic equations. This method implicitly gathers the mass and heat transfer processes occurring in the four main components of the absorption cycle. By combining the Duhring's rule with the driving temperature differences in the heat exchangers the authors found that the total heat transfer between the absorption chiller and the ambient is proportional to a characteristic temperature difference $\Delta\Delta t$

$$\Delta\Delta t = \bar{t}_g - \bar{t}_{ac} - B(\bar{t}_{ac} - \bar{t}_e) \quad 2-45$$

where \bar{t} is the arithmetic mean temperature of the external circuits, and B is an average solution concentration in the absorber and generator. The value of B is considered to be 1.1 for single-effect H₂O/LiBr absorption chillers

Kühn and Ziegler [116] proposed an adaptation of the Characteristic Equation where catalogue or experimental data to fit the parameters of an adapted characteristic temperature function:

$$\Delta\Delta t' = T_g - A \cdot T_{ac} + E \cdot T_e \quad 2-46$$

and the linear characteristic equation for the cooling load

$$Q_e = s' \cdot \Delta\Delta t' + r \quad 2-47$$

Combining Equations 2-46 and 2-47 we obtain

$$Q_e = s' \cdot T_g - s' \cdot A \cdot T_{ac} + s' \cdot E \cdot T_e + r \quad 2-48$$

The four parameters (s' , A , E and r) are obtained through data fitting.

The characteristic equation approaches have been used in many studies. In Lecuona et al. [117] authors used the characteristic equation to find optimum hot water temperature in solar cooling installations for single-effect LiBr–water absorption machine that maximizes the whole solar installation efficiency. Puig-Arnavat et al. [118] compared the two previously exposed approaches of the characteristic equation ([114, 116]). According to this study the Kühn and Ziegler [116] approach is simpler and equal or more accurate than the one of Hellman et al. [114]. Gutiérrez-Urueta et al. [119] extended the characteristic equation method to deal with absorption chillers with adiabatic absorbers. New parameters are added to the original characteristic equation because of the effects of both overflow and thermal losses in the absorber and generator, respectively. Jakob et al. [120] reported the use of another extended characteristic equation method for a diffusion $\text{NH}_3/\text{H}_2\text{O}$ absorption chiller.

2.4.3 Other semi-empirical approaches

Other semi-empirical approaches have been found in the literature. Kim and Infante-Ferreira [121] presented a reduced model consisting of cubic and quadratic equations based on the heat exchanger effectiveness of the main heat exchangers and on the Dühring equation. This model is valid for absorption cycles with and without refrigerant circulation. It can be used when there is no much information about the working fluid properties, so it is useful for quick evaluation of new working fluids.

Marc et al. [122] used parameter estimation procedures in order to obtain the optimal values of the main parameters of a single-effect $\text{H}_2\text{O}/\text{LiBr}$ chiller using a reduced set of steady-state data. This approach relies in the fact that the performance of an absorption chiller can be estimated from a detailed mass and energy balance model if the operating conditions as well as the main parameters of the chiller are known. These parameters are usually unknown, but by means of parameter estimation techniques they can be adequately estimated from experimental or manufactured data.

Semi-empirical models are also the result of substituting some physical relationships with empirical relationships. For instance, the thermodynamic properties of working fluids have been formulated using ANN and then used together with mass and energy balances. Sözen et al. [123, 124] used ANN to calculate the thermodynamic properties alternative working fluids (methanol/LiBr and methanol/LiCl) in ejector–absorption cycles. In both cases ANN are able to predict the working pair's properties with high accuracy and with

better calculation speed and less complexity than using analytic equations. In Sözen et al. [125, 126] a comparison of the properties calculations through ANN for these working fluid is given. They report that the ANN approach has better prediction than the analytic equation approach (correlation coefficient of 0.999 for ANN versus 0.992 for analytic equations). Sencan et al. [127] used ANN for the calculation of the enthalpy of LiBr–water and LiCl–water working fluids for the modelling and simulation of absorption systems. In both cases the correlation coefficient is around 0.999. Singh and Maheshwari [128] used ANN to calculate the enthalpy of H₂O/LiBr working fluid.

A comparison of different empirical and semi-empirical modelling approaches applied to a small scale absorption chiller is presented in Labus et al. [129]. The authors compared an adapted formulation of the Gordon and Ng [112] model, the adapted characteristic equation, a multivariate polynomial regression, and an artificial neural network model. Their results show that, with exception of the adapted formulation of the adapted Gordon and Ng model, all approaches are suitable for chiller control and monitoring applications, since they predicted the chiller performance accurately.

2.5 Applications

In this section we present some of the most common applications of modelling and simulation of absorption cycles.

2.5.1 Performance Analysis of Absorption Cycles

The most common application found in the literature is the performance analysis of absorption systems at different operating conditions. Quick and affordable evaluation of absorption systems under different scenarios can be achieved through simulation.

Lazzarin et al. [130] presented a thermodynamic model of an air-cooled NH₃/H₂O chiller. This model was solved iteratively assuming parameters such as the effectiveness and temperature differences in the main heat exchangers. They obtained good agreement with experimental results and based on this model they proposed some modifications to increase the range of application of the chiller. Xu et al. [131] developed an iterative computer code to simulate a double-effect absorption chiller with series flow. The authors studied the effect of the design parameters (heat recovery ratios in heat exchangers, solution concentration, and circulation ratio) on the COP and the total heat transfer area. Kaynakli and Kilic [132] presented a parametric study of a H₂O/LiBr chiller. They used the model to analyse the performance of the chiller at different operating temperatures, and

also to analyse the impact of the solution heat exchanger and the refrigerant heat exchanger. They conclude that the refrigerant heat exchanger does not improve significantly the performance. Fernández-Seara and Sieres [133] studied the performance of $\text{NH}_3/\text{H}_2\text{O}$ chillers from the rectification point of view. They concluded that the use of the stripping section has more impact on the COP rather than the rectifying section. Gomri [134] compared single and double-effect absorption chillers in terms of thermal COP and exergetic efficiency. This study concluded that while the COP of double-effect systems is about twice the COP of single-effect system, the exergetic efficiency of double-effect system is just slightly higher than the exergetic efficiency of single-effect system. Other studies dealing with exergy analysis include [135-139].

2.5.2 Evaluation of advanced cycle configurations

Research on new configurations is aimed to obtain absorption cycle designs with enhanced performance. Modelling and simulation is a valuable tool in order to estimate the performance of new or modified cycle configurations. It is also useful to evaluate the impact of a determined component within the cycle.

Sözen [140] presented a thermodynamic analysis including irreversibilities of an $\text{NH}_3/\text{H}_2\text{O}$ chiller for three cases: solution heat exchanger and refrigerant heat exchanger (SHX + RHX), solution heat exchanger only (SHX), and refrigerant heat exchanger only (RHX). According to his results, the RHX does not improve significantly the performance of the cycle. Ezzine et al. [141] used FORTRAN for the modelling and simulation of an $\text{NH}_3/\text{H}_2\text{O}$ double-effect double-generation absorption chiller. They calculated the irreversibility of each cycle component finding that the absorber, solution heat exchangers, and condensers have the most potential for enhancing the efficiency of the chiller. Lin et al. [142] investigated the feasibility of a two-stage air-cooled $\text{NH}_3/\text{H}_2\text{O}$ system in order to improve the electrical COP. Their simulation results showed that while thermal COP was 0.34 the electrical COP was 26 for the following operating conditions: hot water temperature at 85 °C, air temperature at 35 °C and chilled water temperature at 10 °C. Garousi-Farshi et al. [143] used EES in order to study the crystallisation risk in three types of double-effect $\text{H}_2\text{O}/\text{LiBr}$ chillers (series, parallel and reverse parallel) of the same cooling capacity. They conclude that the range of operating conditions without crystallisation risks is wider in the parallel and the reverse parallel configurations than those of the series flow system. Mehr et al. [144] proposed two ejector GAX (generator absorber heat exchanger) cycles. These are compared with standard and hybrid GAX

cycles at different operating conditions and looking into COP and second law efficiency. Figueredo et al. [145] presented an EES simulation of a two-stage absorption chiller driven a two temperature levels. They optimised the distribution of the total area between the various components. Rameshkumar et al. [146] studied a GAXAC (generator-absorber-exchange absorption compression) system using EES to evaluate the impact of the UAs and operating conditions on the system. Ventas et al. [147] used EES to study an $\text{NH}_3/\text{LiNO}_3$ absorption chiller with an integrated low-pressure compression booster. They concluded that this cycle can achieve a higher electrical COP than that in an ammonia vapour compression cycle. Vereda et al. [148] investigated the performance of an ejector-absorption refrigeration cycle using $\text{NH}_3/\text{LiNO}_3$ as working pair. Their simulation results in EES show that the use of an ejector allows decreasing the activation temperature in about 9 °C with respect to the conventional single-effect absorption cycle. Yari et al. [149] used EES to compare the GAX and GAX hybrid absorption refrigeration cycles performance (1st and 2nd law) at different generator temperatures.

2.5.3 Integration into other systems

Modelling and simulation is useful in order to study how absorption refrigeration units interact with other units as part larger systems. For example, Bruno et al. [150] evaluated the integration of $\text{NH}_3/\text{H}_2\text{O}$ chillers combined heat and power plants. The authors developed a computer program that allows selecting the optimal refrigeration cycle or combination of them according to an economic criterion.

Solar cooling systems including absorption refrigeration systems have also been studied using modelling and simulation. In these systems it is also necessary to model the solar collectors or storage tanks in order to evaluate the performance of the whole system. Examples can be found in Mazloumi et al. [15], Gomri [151] and Atmaca and Yigit [152]. The effects of the solar collector type and storage tank can be investigated.

2.5.4 Evaluation of alternative working fluids

Modelling and simulation is also useful for quick evaluation of the performance of absorption refrigeration system using alternative working fluids. Karn and Ajib presented a simulation of an absorption refrigeration cycle with acetone-zinc bromide as working fluid [153]. According to simulations and experiments, this system is able to operate with generation temperatures of 50 °C. The reported COP was 0.6 by simulation and 0.4 by experimental measurements.

Steiu et al. presented a set of correlations for calculating the equilibrium properties and solution enthalpies for $\text{NH}_3/\text{H}_2\text{O}$ /alkaline hydroxide mixtures [6]. Using these correlations simulations of an absorption cycle with $\text{NH}_3/\text{H}_2\text{O}+\text{NaOH}$ as working fluid have been carried out. According to their results, with a NaOH concentration of 12%, the temperature at the generator decreases by about 17 °C, the COP increases by 28% and the rectifier can be up to 46% smaller than that required using $\text{NH}_3/\text{H}_2\text{O}$ as working fluid.

During the last years, ionic liquids are gaining attention in many fields because of their properties. In the case of absorption refrigeration systems, ionic liquids can be suitable absorbents since they have a negligible vapour pressure. By means of simulation, Zhang and Hu studied the performance of an absorption chiller using H_2O and ionic liquid 1-ethyl-3-methylimidazolium dimethylphosphate ([EMIM][DMP]) as working pair [154]. Their results showed that, while the COP of the system using [EMIM][DMP] as absorbent is lower than the COP of the system using LiBr as absorbent, the generation temperature is lower using [EMIM][DMP]. This would make this system suitable for low driving temperature applications. Dong et al. presented correlations for the thermophysical properties of the working pair H_2O and 1,3-dimethylimidazolium dimethylphosphate ([DMIM]DMP) [155]. Using these correlations they simulated the performance of an absorption cycle. Their results showed that the performance of the cycle with $\text{H}_2\text{O}/[\text{DMIM}]\text{DMP}$ is close to that of conventional working pair $\text{H}_2\text{O}/\text{LiBr}$. However, for the cycle using $\text{H}_2\text{O}/[\text{DMIM}]\text{DMP}$ the operating temperature range has been extended avoiding crystallization and corrosion issues which occur in $\text{H}_2\text{O}/\text{LiBr}$ systems.

Chekir and Bellagi presented a simulation of an absorption chiller working with the n-butane as refrigerant and the octane as absorbent [156]. The simulated cycle has a COP of 0.36 and a Second Law efficiency of 0.24. It was found that the solution heat exchanger is responsible on the highest entropy generation with 44%. Other components also present high entropy generation: the distillation column 24% and the rectifier 16%. In order to improve the performance of this system, the authors propose a modification consisting on recovering a fraction of the energy discharged out of the rectifier by means of preheating the strong solution in the rectifier before getting into the generator. The initial configuration is then enhanced. The COP is increased up to 0.59 and the second law efficiency up to 0.39.

2.6 Modelling Issues and Data Reconciliation in Absorption Refrigeration Systems

2.5.5 Optimisation

Modelling and simulation are essential part of optimisation procedures. In this sense, there are many papers with optimisation studies of all sorts. Bulgan [157] presented a first law based optimisation of an ammonia water chiller using QBasic. The optimisation variables are the generator temperature and ammonia concentration of the rich solution looking to maximize COP. Fernandez-Seara and Vazquez [158] used Fotran in order to obtain the optimal generation temperature (for which the COP is maximum) at different operating conditions and design parameters. Chávez-Islas and Heard [159] used GAMS for the modelling and simulation of an ammonia water chiller considering the heat rejection using either cooling water or air. Afterwards, the same authors used the above model for the optimisation of the design considering operating and annual capital cost [160]. Le Lostec et al. [47] presented a theoretical optimisation study based on finite time thermodynamics. This study finds optimal COP values that reduce the overall conductance, overall irreversibility, and overall exergetic efficiency. Studies about the optimal design of absorption cooling systems taking into account the total annualized cost and the environmental impact of the cycle have been treated by Gebreslassie et al. [161-163]. Marcos et al. [164] used EES in order to optimise the performance of single and double-effect absorption chillers in terms of the condensation temperatures and the solution concentration variation. This allows defining the crystallisation limit for different scenarios. Rubio-Maya et al. [165] used GAMS for optimizing a single effect absorption chiller using the exergy concept and defining the annual operating cost as the objective function to be minimized.

2.6 Modelling Issues and Data Reconciliation in Absorption Refrigeration Systems

Data reconciliation makes use of a model and a redundant set of measurements in order to obtain reliable estimate of process variables. It is necessary that the model used is as accurate as possible. Generally speaking, this model can be physical, empirical, or semi-empirical, as long as it is reliable.

The Three and Four-Heat Reservoirs models are not suitable since they don't make use of internal parameters. As a consequence, if measurements of internal variables are available, they wouldn't be exploited. Furthermore, they are too simplified and not accurate for the estimation of real absorption systems performance.

Using a detailed thermodynamic model allows exploiting the information regarding any measured variable, internal or external. Nevertheless, complications may arise due the nonlinear nature of the process. These nonlinearities may cause convergence problems during the iterative procedures for the simulation and for the data reconciliation problem, especially if nonlinear programming approaches are used. However, these difficulties may be overcome or minimised by taking into account modelling aspects such as:

- Setting adequate limits to the variables. This could avoid divergence if the optimisation algorithm searches values out of the range of the properties correlations.
- Obtaining initial values of the variables as close as possible to the final solution. This could improve the convergence time for the simulation and for data reconciliation
- Performing an adequate degrees of freedom analysis. This is important for identifying the inputs and outputs of the model, as well as for accounting for redundant variables.
- Replacing the logarithmic mean temperature difference from a close approximation in order to avoid the evaluation of a division by zero when temperature differences in each end of the heat exchanger are equally valued [166]. A good approximation is the one presented by Chen [167]:

$$\Delta t_{lm} = \left[\frac{1}{2} (t_{hot,1} - t_{cold,1})^{0.3275} + \frac{1}{2} (t_{hot,2} - t_{cold,2})^{0.3275} \right]^{\frac{1}{0.3275}} \quad 2-49$$

The nature of the formulations for calculating the properties of the working fluids play a key role for the simulation and data reconciliation of the absorption cycle. They must be accurate, and yet implemented efficiently in order to avoid convergence issues. Using EES allows efficient implementation of the thermodynamic properties formulation because of its powerful solving capabilities. Another option is the use of numerically consistent and computationally effective formulations such as the ones proposed by Pátek and Klomfar [70, 73].

The use of data driven models may be not adequate for steady-state data reconciliation of absorption systems since they would be based in non-reconciled data. Also, the lack of extrapolation reliability would compromise the data reconciliation if the optimisation

algorithm evaluates variables outside the region where the data has been used for obtaining the data driven model.

The use of semi-empirical approaches could be suitable for data reconciliation if simultaneous parameter estimation and data reconciliation is used. In this way, the estimated parameters would be obtained at the same time when measurements are adjusted and model constraints are satisfied. The parameter identification approach proposed by Marc et al. [122] would need to be extended to other absorption chillers such as double-effect configurations, $\text{NH}_3/\text{H}_2\text{O}$ chillers etc.

2.7 Conclusions

This chapter presents an overview about the existing approaches for the steady-state modelling and simulation of absorption chillers. Not all works have been included but relevant papers in a wide range of related areas in order to give an integral and complete overview of modelling and simulation of absorption refrigeration systems in steady state.

Despite the fact that many simulation studies have been published during the last years, there are still new challenges to overcome due to the complex nature of absorption refrigeration systems. One of these challenges is the application of data reconciliation methodologies to the operational data of these systems.

In order to use thermodynamic models for data reconciliation it is necessary to take into account important modelling aspects that are usually overlooked: setting adequate variables limits and guess values, performing adequate degrees of freedom analysis, selecting adequate properties correlations, etc.

The use of simultaneous data reconciliation and parameter estimation techniques seems promising for its application with semi-empirical modelling of absorption refrigeration systems.

Nomenclature

COP ,	Coefficient of performance
I ,	Irreversibility factor
Q ,	Heat flow (kW)
S ,	Entropy (kJ/K)
T ,	Absolute temperature (K)
\bar{T} ,	Entropic mean temperature according to equation 2-10
UA ,	Overall heat transfer coefficient times the heat exchanger area (kW/K)
W ,	Work (kW)
X ,	Input ANN
Y ,	Output ANN
Δt_{lm}	Logarithmic mean temperature difference
h ,	Specific enthalpy (kJ/kg)
m ,	Mass flow rate (kg/s)
x ,	Mass fraction
Greek letters	
η ,	Efficiency
Subscripts	
$4t$	Four-Heat-Reservoir
a ,	Absorber
abs ,	Absorption cycle
ac ,	Absorber-Condenser
c ,	Condenser
$cold$,	Cold side of a counter-current heat exchanger
e ,	Evaporator
g ,	Generator
$high$	High temperature level
hot ,	Hot side of a counter-current heat exchanger

i, Intermediate temperature level
low, Low temperature level
sa, Entropic average

Superscripts

C Carnot

Chapter 3

A Combined Steady-State Detection Method for Absorption Refrigeration Systems

Abstract

Steady-state is one of the main hypotheses made about a process. Steady-state DR can have strong negative effects in situations in which the steady-state hypothesis is incorrect. Therefore it is important to use adequate criteria for deciding when the process is at steady-state.

In this chapter a combined steady-state detection method is proposed. The method combines a moving window based test which has been proved to work adequately for quasi steady-state processes and a mean test using a period extending strategy.

It can be seen that the uncertainty of the measurements is reduced using the combined test because the standard deviation is also reduced. Furthermore, adequate determination of steady-state periods influences the direct calculation of the covariance, which is an important factor for the data reconciliation problem.

3.1 Introduction

Steady-State Detection (SSD) is an important step within any data treatment framework. Some applications like optimisation, fault detection and diagnosis, and data reconciliation (DR) are based on either steady-state models or dynamic models. If the process is not at steady-state, the mathematical model and calculations required would be totally different. According to Poulin et al. [168] steady-state DR can have strong negative effects in situations in which the steady-state hypothesis is incorrect.

Adequate identification of the steady-state is also important when averaging. In order to obtain information about a process, it is common practice to condensate the time series of data through the calculation of the mean value at steady-state. If the time series under consideration contains transient data the results of averaging would be strongly biased.

In the DR problem, the weighted least-squares estimator makes use of the standard deviations of the measurements as the weighting factor. These standard deviations are considered as the direct estimation of the covariance matrix of measurement errors. If the variations of the true values are significant over time (no steady-state), estimation of the variances of process measurements could give incorrect estimates [169].

Therefore, it is important to have an adequate criterion to distinguish between steady-state periods and transient periods.

3.2 Steady-State Detection Methods

In the literature there are many approaches proposed to determine if a process is in steady-state or not. SSD methods can be broadly classified into two categories: parametric methods and nonparametric methods.

3.2.1 Parametric methods

Parametric methods rely on the assumption of a known shape of the data probability distribution. For example, the composite statistical test by Narasimhan et al. [170] is a combination of multivariate statistical tests applied to a set of measurements sampled over a moving time window. The test is performed in two stages: first the covariance of two consecutive data windows is test to be equal. Afterwards, depending on the result of this test, the means of the two consecutive data windows is test to be equal assuming a Hotelling T^2 distribution. Narasimhan et al. [171] proposed a method based on the mathematical theory of evidence. A statistic based on the mean and the variance for each variable in two consecutive data window is calculated. This statistic obeys a Hotelling T^2

distribution. Depending on the value of the statistic three quantities called beliefs (corresponding to the propositions of steady state, no steady state, and uncertainty) are calculated and then combined for all the variables under study. The process is at steady-state if the overall belief corresponding to steady state is greater than the overall belief corresponding to no steady-state. Cao and Rhinehart [172] presented a method based on an F-like test applied to the ratio of two different estimated variances. This method does not require a moving data window since the variances are calculated through an exponential moving-average filter. Siyi et al. [173] apply the same test as Narasimhan et al. [171] but using a period extending strategy. In this case, if the test applied to two consecutive data windows is successful, then the test is applied again to the first and the third data windows. If the test is successful again, then the process is at steady-state. In Önöz and Bayazit [174] the power of statistical tests are compared for two probability distributions: t-test to the slope of a linear regression and the Mann-Kendall. The authors conclude that both have similar performance.

3.2.2 Nonparametric methods

On the other hand, nonparametric methods make no assumption about the shape of the data probability distribution. This is why nonparametric methods are also known as distribution-free tests [175]. Jiang et al. [176] presented a method based on wavelet transform. A steady-state index is obtained from the wavelet transform modulus. The advantage of this method is that does not depend on a time window size. Kim et al. [177] designed a steady-state detector for a vapour compression system based on a moving window. If the standard deviation of any of the monitored process variables is below a threshold the process remains in steady-state. This method has been used in the monitoring of a residential heat pump performance in order to characterize vapour compression systems faults [178]. Han et al. [179] use steady-state detection in order to pre-process data for the development of a chiller fault detection model. They use a method based on computing geometrically weighted variances. The chiller is in steady-state if the weighted deviations of the variables under study fall below a pre-determined threshold.

Le Roux et al. [180] compare four different approaches for steady-state detection: Modified F-test [172], Reverse Arrangement Tests, Rank von Neumann Test, and Polynomial Interpolation Test. Except for the modified F-test, all techniques are non-parametric methods. The authors conclude that the Polynomial Interpolation Test is the method that performs better.

3.2.3 Slow drifting processes

According to Narasimhan et al. [170] most process in industry present a quasi-steady state behaviour. Quasi-steady state processes have the tendency to remain steady for long intervals of time. If change from one steady-state to another happens, this change takes place in the shortest time possible. Most of the steady-state detectors discussed above are designed to deal with quasi-steady state processes. However, there are some processes where the variables show a very slow drift. Previous SSD approaches cannot detect these slow drifts. In order to deal with slow drifts [170] suggested applying their test to periods 1 and 2, 1 and 3, etc., until the test detects that the system is no longer at steady-state.

In this chapter we propose to combine two SSD methods: the algorithm proposed by Kim et al. [177] and a Student t-test to the mean difference of two data windows using an extended period strategy. This combined approach makes it possible to handle processes which present quasi-steady state behaviour and slow drifting as well.

The performance of this approach will be tested and compared to other approaches. Also an example of a real absorption chiller operation will be showed and the importance of detecting steady-state when there are slow and fast changes will be demonstrated.

This makes possible to obtain data in steady state, as well as their averages and standard deviations which will be suitable for using the steady-state data reconciliation procedures, or other applications.

3.3 A Combined Steady-State Detection Method

3.3.1 Test 1: Calculation of the standard deviation in a moving window

Figure 3-1 illustrates a moving or sliding data window. The window size is a predefined time interval, n , over which important parameters are sampled at regular intervals, k . This first test is based on the steady-state detector for a vapour compression system developed by Kim et al. [177]. This algorithm calculates the standard deviation (σ) of the data contained in a data window. The standard deviation can be considered as a representation of the random variation of the measured variable. The standard deviation is calculated on each data window as follows:

$$\sigma_k = \sqrt{\frac{1}{n-1} \sum_{i=1}^n (X_i - \bar{X}_n)^2} \quad 3-1$$

3.3 A Combined Steady-State Detection Method

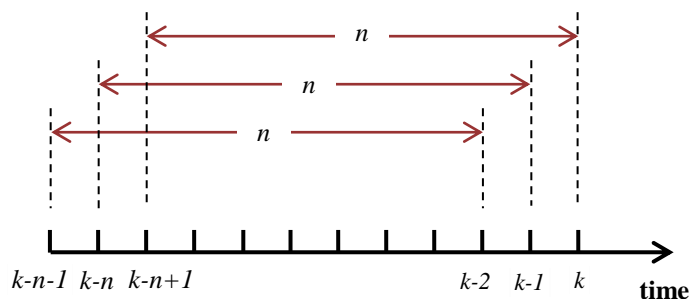


Figure 3-1: Moving window.

The algorithm identifies steady-state operation if the standard deviation is below a defined threshold. In this study the selected threshold is set to $\pm 3\sigma$. This requires an a priori knowledge about the standard deviation at steady-state of the variable under study. This information can be retrieved from historical data and can be updated if necessary. According to Kim et al. [177], considering that the measurements are random and normally distributed, the $\pm 3\sigma$ threshold will filter out less than 1% of data. Smaller thresholds would delay the steady-state identification, or may cause that steady-state is never detected. Large thresholds would include transient data.

The advantage of this test is that is simple and can be easily applied to any kind of process. However, this test is not suitable for dealing with slow drifting processes. This test is based on the idea that the variance or standard deviation within a data window will be large when process is in transient state. This is true; however, it is also true that if a process presents a very slow drift, the variance won't be necessarily large and the SSD will always indicate steady operation. Take for instance the slow drifting example in Figure 3-2. The value of the measured output starts at a value of 25 in time $t = 0$ and finishes at a value of 30 in $t = 500$. Steady operation is indicated through the whole period, but the operating condition is shifted from 25 to 35.

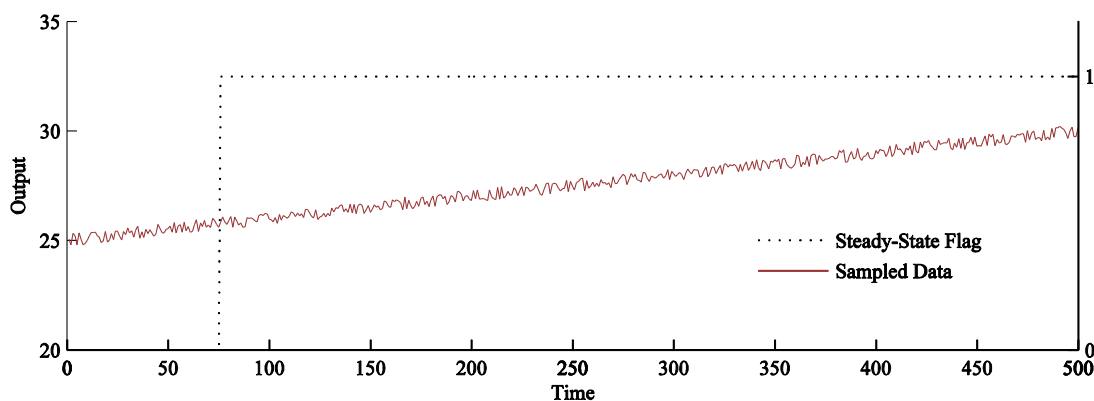


Figure 3-2: Example of Slow Drifting with SSD by a single test.

3.3.2 Test 2: t-test to difference between two means

In order to determine if there has been a significant change in the operating conditions a t-test to the difference of the means can be used. This test is applied, as suggested by Narasimhan et al. [170], to periods k and $k+1$, and $k+2$, etc., until the test detects that the means are significantly different.

The t statistic is calculated using the following expression:

$$t = \frac{\bar{X}_1 - \bar{X}_2}{S_{1,2} \sqrt{\frac{2}{n}}} \quad 3-2$$

where $S_{1,2}$ is the pooled standard deviation:

$$S_{1,2} = \sqrt{\frac{1}{2}(\sigma_1^2 + \sigma_2^2)} \quad 3-3$$

The value of t is compared with the critical value, t_c , for $2n-2$ degrees of freedom. If the value of statistic t is greater than t_c , then the two compared means are significantly different, otherwise, the means are equal.

3.3.3 Combining the two methods

Figure 3-3 shows a schematic of the combined test for steady-state detection. First, Test 1 is applied. If Test 1 detects that operation is steady (the standard deviation σ of the data window is below the threshold 3σ) Test 2 is then applied. If Test 2 detects a significant change in the mean (statistic t is greater than critical value t_c), then the process is still at steady-state but at slightly different operating conditions. The window size used for both tests may be different. The result is an approach that can deal with quasi steady-state processes and process with slow drifting.

3.3 A Combined Steady-State Detection Method

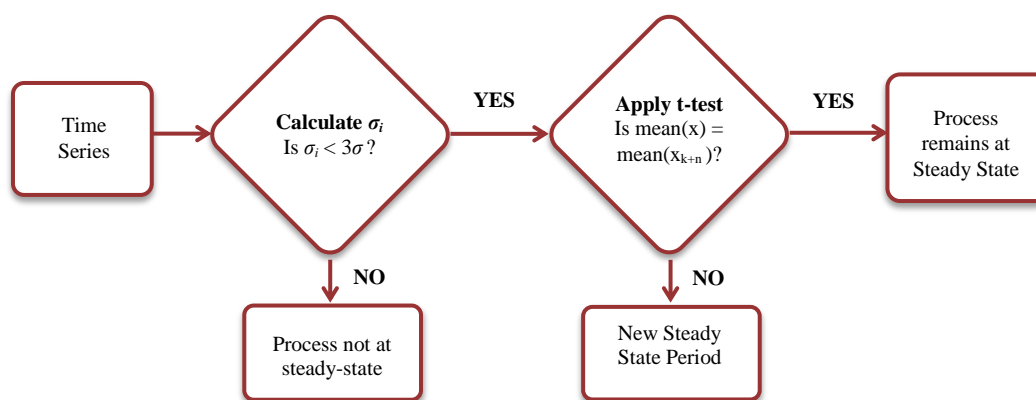


Figure 3-3: Combined test for steady-state detection.

Figure 3-4 shows the same drifting operation and SSD as in Figure 3-2, but in this case the proposed combined SSD method is used. It can be seen that now the significant changes in the mean of the sample data can be tracked. The steady-state period of Figure 3-2 includes all the data from time $k = 75$ up to time $k = 500$, while in Figure 3-4 there are 14 smaller steady-states in the same time frame. In Figure 3-2 we obtain one average value with a standard deviation value of 1.3, while in Figure 3-4 we obtain 14 different averages with their corresponding standard deviations values of about 0.4 for each steady-state period. The impact of the combined test in the data reconciliation procedure is that we would reconcile 14 data points instead of one, and also the adjustment magnitude for this particular variable would be smaller since the standard deviation (weight in equation 1-1) is smaller. Furthermore, as a consequence of smaller standard deviations, the uncertainties of the measurements and calculations obtained from these measurements would be smaller. The following example of real operational data of an absorption chiller will illustrate these points.

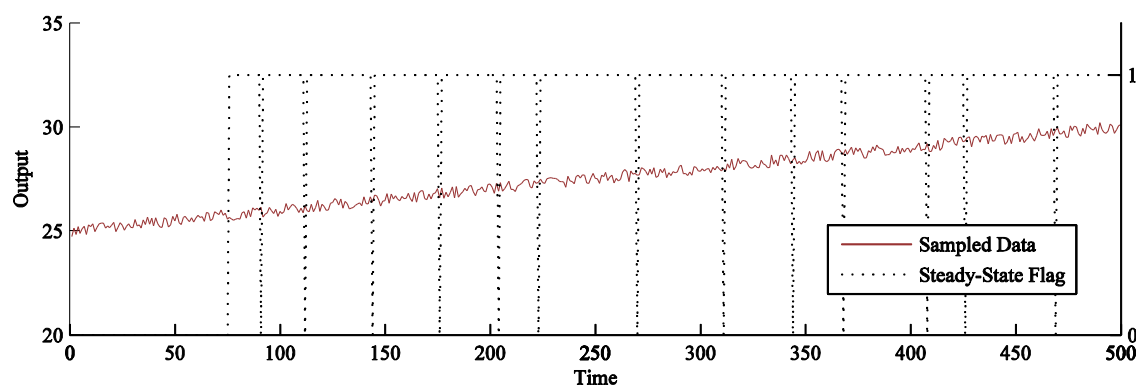


Figure 3-4: Example of Slow Drifting with SSD by the combined test.

3.4 Application to real absorption chiller data

In order to demonstrate the usefulness of adequate SSD, we apply the proposed test to the operational data of a single-effect H₂O/LiBr absorption chiller working in the polygeneration plant ST4 in Cerdanyola del Vallès (Spain) [11]. The rated COP and chilled water capacity of the single effect chillers is 0.75 and 3 MW, respectively, and is fired directly with the cooling water of internal combustion cogeneration engines.

The available measurements for this case are the inlet and outlet temperatures for each of the external circuits, as well as their corresponding volumetric flow rates. A simplified diagram is shown in Figure 3-5. Measurements are sampled each minute.

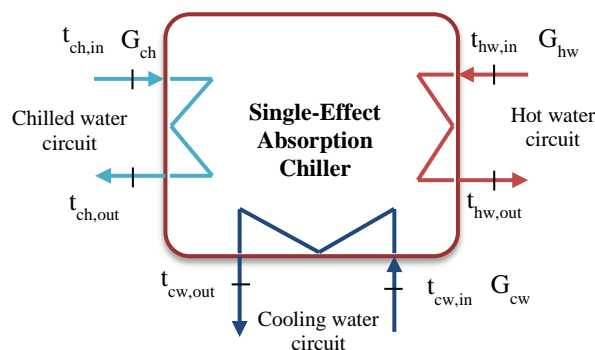


Figure 3-5: Single-effect absorption chiller external circuit measurements.

In real processes several variables are monitored. For practical issues, not all variables are considered for the indication of steady operation. In this study we selected two features as indicators of steady-state: estimated cooling capacity (Q_e) and the cooling water flow rate (G_{cw}). Q_e is an indirectly measured variable estimated through the measured chilled water inlet temperature ($t_{ch,in}$), chilled water outlet temperature ($t_{ch,out}$) chilled water flow rate (G_{ch}). If both Q_e and G_{cw} are at steady-state, we consider that the whole absorption refrigeration system is at steady-state. Table 3-1 summarises the parameter values used for SSD in this case study.

Table 3-1: SSD parameters for case study.

Parameter	Value
σ_{Q_e}	36 kW
$\sigma_{G_{cw}}$	2 m ³ /h
n_1	60
n_2	30

3.4 Application to real absorption chiller data

Figure 3-6 shows data of a single-effect absorption chiller during one day of operation. The heat loads are plotted as well as the external circuits' inlet and outlet temperatures, and volumetric flow rates. Two steady state detectors have been applied: the combined test proposed in this chapter (black dotted line) and the first part of the test only, as in Kim et al. [177] (blue dotted line). Both SSD have been applied off-line.

In absorption refrigeration systems, there are variables that may show slow drifting. For instance, Figure 3-6 shows that the hot water outlet temperature ($t_{hw,out}$), cooling water outlet temperature ($t_{cw,out}$) and chilled water inlet temperature ($t_{ch,in}$) drift slowly during the day. The operating conditions are, therefore, slightly changing during operation. The combined test is able to distinguish when the operating conditions have changed. It can be seen in Figure 3-6 that when the chiller is operating from 14:00 to 20:00 the cooling loads are decreasing very slowly. While the single test detects steady operation at the same operating conditions during this whole period, the combined test detects six steady-state periods with different operating conditions.

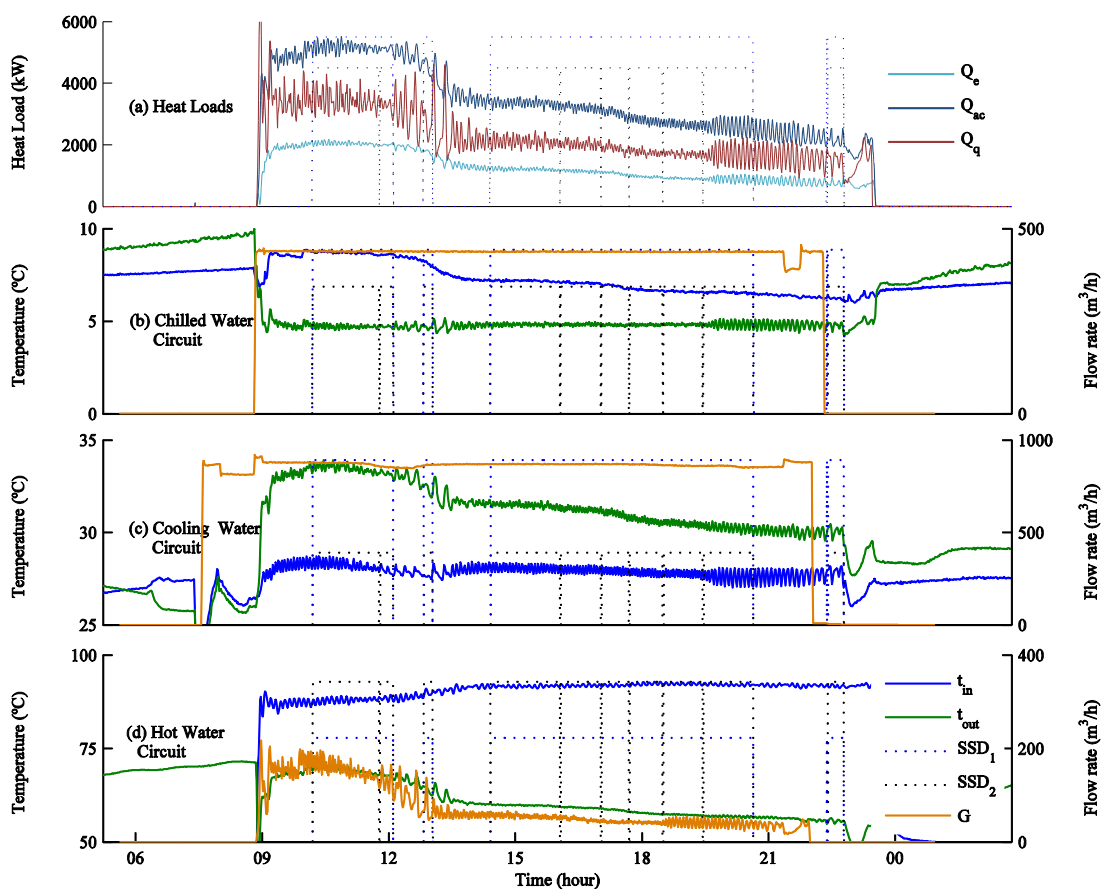


Figure 3-6: Absorption chiller heat loads, temperature trends and steady-state indicator during one day of operation.

Chapter 3. A Combined Steady State Detection Method for Absorption Systems

The benefits of detecting such slow drifts are reflected in the variability of the calculated performance parameters. If we take a look at the Table 3-2 we can see that the uncertainties (U) of the cooling capacities and COP are much smaller using the combined test than using a traditional SSD method.

The reduction of the uncertainty is consequence of a smaller variability, in other words, a smaller standard deviation.

Table 3-2: Average cooling capacity and COP and their corresponding uncertainties calculated using the two SSD methods.

Combined Test					Single Test				
SS Size*	Q_e (kW)	COP	U_{Q_e} (kW)	U_{COP}	SS Size	Q_e (kW)	COP	U_{Q_e} (kW)	U_{COP}
95	2041	0.60	150	0.15	115	2034	0.60	148	0.16
19	2000	0.62	107	0.10					
13	1763	0.68	168	0.22					
99	1208	0.58	129	0.12					
57	1146	0.57	120	0.10					
39	1073	0.57	136	0.11	374	1045	0.56	304	0.25
47	966	0.55	115	0.10					
56	907	0.54	112	0.09					
71	885	0.56	217	0.24					
23	753	0.54	214	0.24	23	753	0.54	214	0.24

* Number of consecutive data samples. Measurements are sampled at a rate of one sample per minute.

Uncertainties were calculated following the United Kingdom Accreditation Service guidelines [181]. Type B evaluation of standard uncertainty was evaluated by judgement based on available information on the possible variability of input quantities. The following input quantities were taken into account in order to calculate the uncertainty for Q_e and COP : inlet and outlet temperatures of chilled and hot water circuits, volumetric flow rate of chilled and hot water circuits, density, and specific heat capacity. Uncertainty contribution for temperature and volumetric flow rate was calculated as a combination of different sources of uncertainty: repeatability, accuracy of the instrument and resolution of the instrument. Repeatability was estimated as the standard deviation of the measured input quantity. Values for the accuracy and resolution were taken from the equipment catalogue. To calculate uncertainty contribution for density and specific heat, uncertainties were assigned to reference data taken from NIST homepage.

When all uncertainty sources for each input quantity were determined, they were multiplied by their probability distribution and summed to calculate the uncertainty

3.4 Application to real absorption chiller data

contribution u . Sensitivity coefficient (c) was calculated as the partial derivative of the function (Q_e or COP) with respect to input quantity. Afterwards, using the law of propagation of uncertainty the combined standard uncertainty was calculated using equation 3-4:

$$U = \sqrt{\sum_{i=1}^n c_i^2 \cdot u_i^2} \quad 3-4$$

The last step was to calculate expanded uncertainty by multiplying the standard uncertainty by a coverage factor of 2, which corresponds to a coverage probability of approximately 95% for a normal distribution. More details can be found in Appendix A.

The adequate estimation of the standard deviation is fundamental for the DR problem, because the objective function makes use of the standard deviations as the covariance matrix of measurement errors. This allows the measurements being adjusted in the right proportion during the DR procedure.

For this example, we have reconciled the following problem:

$$J = \min \sum \left(\frac{X_i - X_i^*}{\sigma_i} \right)^2 \quad 3-5$$

subjected to,

$$Q_e + Q_g + Q_{ac} = 0$$

where X_i^* is the vector of the external circuits measurements ($t_{ch,in}$, $t_{ch,out}$, $t_{cw,in}$, $t_{cw,out}$, $t_{hw,in}$, $t_{hw,out}$, G_{ch} , G_{cw} , G_{hw}), X_i is the vector of the reconciled values, and σ is the corresponding standard deviation. The constraint of the minimisation problem is the global energy balance around the absorption chiller unit.

Table 3-3 shows the raw values, standard deviations, reconciled values and residuals obtained from the resolution of the DR problem using the steady-state data from the first period found by the single SSD test. Table 3-4 shows the same information as Table 3-3 but for the steady-state periods 1 and 2 found by the combined SSD test. It can be seen that, in general, the standard deviations computed from the steady-state periods using the

Chapter 3. A Combined Steady State Detection Method for Absorption Systems

combined test are smaller than the ones computed from the single SSD test. The residuals (the difference between the raw and reconciled measurement), as well as the final value of the objective function (J), are also smaller for the combined test. This is because the slow drifting transient behaviour is eliminated through the combined SSD test.

Table 3-3: Reconciled values and residuals of the average measurements from steady-state period 1 using the single SSD test.

Measurement	Raw Value	σ	Rec Value	Residual
$t_{ch,in}$ (°C)	8.7	0.07	8.7	1.5E-02
$t_{ch,out}$ (°C)	4.7	0.10	4.7	6.4E-03
$t_{cw,in}$ (°C)	28.2	0.25	28.2	1.8E-02
$t_{cw,out}$ (°C)	33.4	0.21	33.4	1.4E-02
$t_{hw,in}$ (°C)	88.0	0.63	88.0	6.2E-02
$t_{hw,out}$ (°C)	69.0	0.86	69.1	6.3E-02
G_{ch} (m ³ /h)	438.5	0.59	438.5	3.2E-02
G_{cw} (m ³ /h)	873.8	5.22	873.9	1.3E-01
G_{hw} (m ³ /h)	155.2	17.89	150.9	4.3E+00
J			0.11	

Table 3-4: Reconciled values and residuals of the average measurements from steady-state periods 1 and 2 using the combined SSD test.

Measurement	Period 1				Period 2			
	Raw Value	σ	Rec Value	Residual	Raw Value	σ	Rec Value	Residual
$t_{ch,in}$ (°C)	8.7	0.06	8.7	8.5E-04	8.6	0.02	8.6	5.5E-03
$t_{ch,out}$ (°C)	4.7	0.10	4.7	8.9E-03	4.7	0.06	4.7	1.6E-03
$t_{cw,in}$ (°C)	28.2	0.23	28.2	4.9E-02	27.9	0.17	27.9	1.7E-02
$t_{cw,out}$ (°C)	33.5	0.20	33.5	5.2E-02	33.2	0.12	33.2	6.0E-03
$t_{hw,in}$ (°C)	87.9	0.62	87.9	6.2E-02	88.4	0.55	88.4	4.0E-02
$t_{hw,out}$ (°C)	69.3	0.71	69.3	6.0E-02	67.8	0.34	67.8	1.4E-02
G_{ch} (m ³ /h)	438.5	0.55	438.5	4.1E-02	438.9	0.66	438.9	2.1E-02
G_{cw} (m ³ /h)	875.8	2.05	875.8	7.2E-03	863.7	4.59	863.6	8.6E-02
G_{hw} (m ³ /h)	159.1	16.83	157.2	1.9E+00	136.6	9.58	137.8	1.2E+00
J			0.03				0.03	

3.5 Conclusions

Despite the fact that several SSD methods have been proposed in the literature, most of them aren't designed for tracking slow drifts. In this chapter a combined test for SSD in absorption systems is developed. This test takes into account the possible slow drifts that occur in this kind of systems as well as sudden changes in operating conditions.

This combined test consists in two different tests based on moving data windows. The tests are applied successively. The first test compares the standard deviation calculated in a data window with a predefined threshold [177]. If the first test indicates steady operation, the second test is applied. In the second test a Student t-test to the difference of the means is applied following an extended period strategy. If the second test detects a change in operating conditions, then a new steady-state period with different operating conditions is defined.

The effectiveness of this test is demonstrated using real absorption chiller operational data. It can be seen that the estimated uncertainties of the performance parameters (Q_e and COP) are much smaller using the combined test than using a traditional SSD method. This is very important for the Data Validation framework, since the measurements that will be treated in the DR step will carry a smaller standard deviation, needing smaller adjustments. This is demonstrated by analysing the residuals and the final value of the objective function obtained from the resolution of a DR problem using the global energy balance as constraint.

Nomenclature

C ,	Sensitivity coefficient for the uncertainty calculation
G ,	Volumetric mass flow rate (m^3/h)
Q ,	Heat load (kW)
S ,	Pooled standard deviation
U ,	Uncertainty
X ,	Measurement
\bar{X} ,	Average of the measurements in a data window

n ,	Data window size
t ,	t-statistic

Greek letters

σ ,	Standard deviation
------------	--------------------

Subscripts

a ,	Absorber
ac ,	Absorber and condenser
c ,	Critical value for the t-test
ch ,	Chilled water circuit
cw ,	Cooling water circuit
e ,	Evaporator
g ,	Generator
hw ,	Hot water circuit
in ,	Inlet
out ,	Outlet

Chapter 4

A Framework for the Data Validation of Absorption Refrigeration Systems

Abstract

In this chapter a data validation framework for the analysis of absorption refrigeration systems is proposed. The framework exposed in this chapter comprehends a steady state detection stage, formulation and resolution of the DR and Parameter Estimation problems and the detection of measurements with gross errors.

Depending on the amount of available measurements two different cases arise. In Case 1, the amount of measurements is enough to obtain the redundancy necessary for the resolution of the DR problem. The DR can be solved using a sequential or a direct approach. On the other hand, in Case 2, the amount of internal measurements is not enough so there is the need to estimate all or some of the absorption chiller main parameters. In this case a joint DR and parameter estimation procedure is developed.

The results show that this methodology can identify and remove the sources of gross errors. It also provided performance calculations such as Q_e and COP based on reconciled data. Because this reconciled data is consistent with the mass and energy balances these calculations are more reliable than calculations based on raw measurements.

4.1 Introduction

Nowadays data acquisition systems can record multiple variables in short sampling times. As a result, the volume of information available is very large and can be difficult to manage when calculating mass and energy balances. These balances may be violated for various reasons: random and gross errors in the measurements, deviations from steady-state, redundancy in the measurements, etc. Data validation and reconciliation techniques have been extensively used in the process industry to improve the accuracy of data. These techniques exploit the redundancy in the measurements in order to obtain a set of adjusted measurements that satisfy the plant model. The main step of the data validation process is the resolution of the DR problem.

So far, DR has been extensively used to treat data from such open chemical processes as mineral processes [182], distillation processes [183, 184], pyrolysis reactions [185], steam reforming [186], gas pipeline systems [187], naphtha reforming [188], etc. Nevertheless, not many applications deal with closed cycles with complex connectivity and recycle loops, as in absorption refrigeration cycles. Difficulties arise because the reliable thermodynamic property models used to predict temperature-pressure-concentration and enthalpy in several aggregation states introduce additional complexity and convergence problems. Bruno et al. [42] tried to apply DR in complex absorption refrigeration cycles using the Aspen Plus process simulator but they concluded that the use of the simulator's reconciliation features for this application requires considerable expertise and convergence errors were difficult to track.

DR requires a redundant set of measurements in order to be applied. In absorption refrigeration systems redundancy may not be available since in many applications only the external circuits are measured while internal variables are not monitored and/or some design parameters are unknown. Therefore, depending on the amount of available measurements two different cases arise. In Case 1, the amount of external and internal measurements is enough to obtain the redundancy necessary for the resolution of the DR problem. On the other hand, in Case 2, the amount of internal measurements is not enough so it becomes necessary to estimate all or some of the absorption chiller main parameters from experimental data. In this case a joint DR and parameter estimation procedure is required.

The data validation framework exposed in this chapter comprehends the steady state detection, formulation and resolution of the DR and Parameter Estimation problems, and

the detection of measurements with gross errors. Two approaches have been followed for the resolution of the DR problem: a sequential approach using Matlab [189] in combination with the Engineering Equation Solver [89], and a simultaneous approach using the General Algebraic Modeling System (GAMS) [190]. The methodology presented in this chapter will be useful for generating a set of coherent measurements and operation parameters of an absorption refrigeration system. These measurements can then be used for downstream applications: development of empirical models, optimisation, control, etc.

4.2 Data Reconciliation

The first published study on DR was the mass flow rate reconciliation presented by Kuehn and Davidson [191]. Subsequently more publications appeared dealing with linear DR [192-195] and nonlinear DR [22, 196-200]. The case of DR for transient processes has also been extensively studied, but this topic is beyond the scope of this thesis.

Handling linear constraints in the DR problem is not difficult. Methods such as matrix projection [195] or QR factorisation [197] can be easily implemented. However, most of the cases in the process industry are better described by nonlinear models. In the case of bilinear systems (like multicomponent flow networks), modifications of the above methods can solve the DR problem without difficulty.

When the system is more complex (multiple phases, enthalpy calculation of mixtures, etc.) the above techniques cannot be directly implemented and more general approaches are required. One option is to linearize the nonlinear constraints around a feasible point and then apply a linear DR procedure. This approach can be simple and fast, but it is an approximate solution. According to Kim et al. [201] DR is sensitive to linearization errors. Another option is to use nonlinear programming (NLP) techniques. NLP, however, requires more computation time and if the problem is ill-conditioned it may not converge. Therefore, the successful application of DR to a highly nonlinear problem depends on the problem itself.

Generally speaking, the steady-state DR problem is mathematically expressed as a constrained minimisation problem in which the estimate of each variable is as close as possible to the measured value weighted by its standard deviation. The typical formulation of DR is the weighted least-squares problem:

$$J = \min \left(\frac{\chi - \chi^*}{\sigma} \right)^2$$

Subjected to

$$f(\chi, v) = 0 \quad 4-1$$

$$\chi_{\min} \leq \chi \leq \chi_{\max}$$

$$v_{\min} \leq v \leq v_{\max}$$

where J is the scalar value of the objective function, χ^* is a vector of measurements, χ is a vector of reconciled values of the measurements, v is a vector of estimated non-measured variables, σ is a vector of the standard deviations of the measurements, and f is the set of equations (model) that describes the system in steady-state.

DR aims to estimate the most likely value of the system variables χ and v by minimising the difference between the set of raw measurements χ^* and the set of reconciled measurements χ while satisfying the system constraints f . Not all measured variables are adjusted in the same proportion. Measurements with high variability are prone to receive larger adjustments than measurements with low variability. The standard deviation of each measurement is used as an indicator of the variability of the process variable.

4.3 Data Validation for Absorption Refrigeration Systems

Data validation, in this framework, refers to the complete process for treating the raw measurements in order to obtain their most likely estimates. This includes the identification of steady-state, resolution of the data reconciliation and parameter estimation problems and the detection and elimination of gross errors.

Figure 4-1 shows the general scheme of the data validation framework. First, the steady-state detector is applied on the time series of collected data. In this step we remove the transient data, and then we obtain the average values of the measurements at steady-state. Next, using the thermodynamic model and the set of measurements, we perform a degrees of freedom analysis. In this step we determine the set of inputs required for simulating the absorption cycle. This analysis is also useful for classifying the variables and determining if there are redundant measurements so that DR can be performed, or if there is the need to

4.3 Data Validation for Absorption Refrigeration Systems

formulate a joint DR and parameter estimation problem. In the next step, we solve either the DR problem or the joint DR and parameter estimation problem by means of thermodynamic model and the set of measurements. Then we apply the GED step. If we suspect that one measurement contains a gross error we remove it and is now considered as a non-measured variable. Then we go back to the degrees of freedom analysis. If we suspect that there are no measurements containing gross errors then the procedure has finished. The final result is a series of calculations consistent with the laws of conservation.

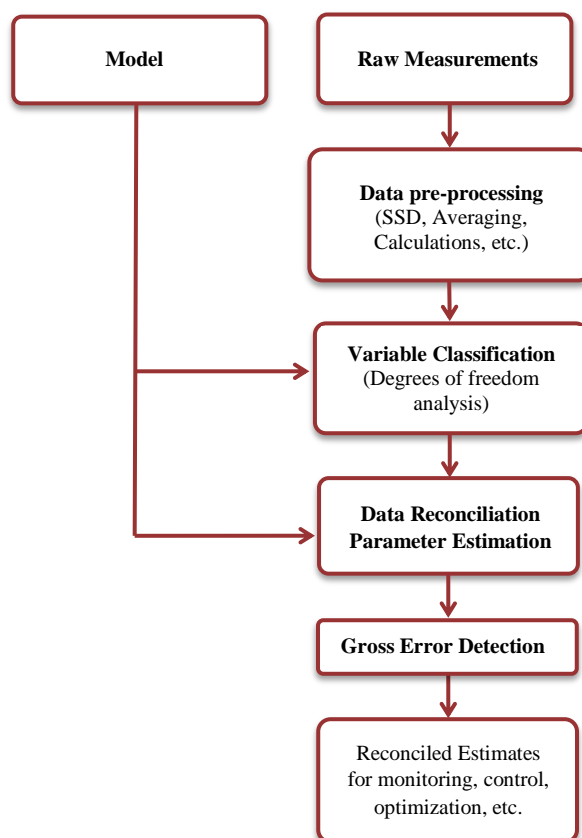


Figure 4-1: General scheme of the data validation framework.

4.3.1 Steady-State Detection

Although steady-state DR generates benefits, it can have strong negative effects in situations in which the steady-state hypothesis is violated [168]. Therefore, it is important to determine which measurements correspond to a steady-state period.

The combined steady-state detection method exposed in Chapter 3 is used to obtain the averages and standard deviations of the set of measurements used in the DR problem.

4.3.2 Variable Classification and Degrees of Freedom Analysis

The process variables need to be classified since DR can only be performed when some measurements are redundant. A measured variable is redundant if it can also be estimated from the available measurements using the model equations.

Since redundancy is equal to the statistical degrees of freedom [20] a redundancy analysis can be made by counting the degrees of freedom of the process model. Ayou et al. [83] developed a catalogue that reports the degrees of freedom for the typical components of absorption chillers. As soon as we get the model that represents the absorption system and a set of measurements obtained from the monitoring devices we can account for the degrees of freedom of the absorption system by adding the degrees of freedom of each component of the system.

The degrees of freedom determine the minimum number of process variables that have to be measured to reproduce the absorption chiller performance. Once a set of measured variables reduces the degrees of freedom to zero, additional measurements will provide the redundancy required for DR to be performed.

The result of this analysis leads to the definition of two sets of measurements: the inputs and outputs of the absorption system model. All the measurements that belong to the set of outputs are redundant because they can be estimated through the model and the measured inputs. For the measurements that belong to the input set, we check whether they are redundant by exchanging one or more with measurements that belong to the output set. If the exchanged measurements can also be calculated from the model and the modified inputs, then they are redundant. If not, they are just measured.

Appendix B presents the degrees of freedom catalogue developed by Ayou et al. [83] for the typical components in absorption refrigeration systems.

4.3.3 Modelling Aspects

Data reconciliation makes use of mathematical model constraints in order to adjust the measurements and estimate process variables which satisfy the constraints. Therefore, an adequate model formulation of the absorption refrigeration system is fundamental for a successful resolution of the DR problem.

The single-effect H₂O/LiBr cycle depicted in Figure 1-4 is used to illustrate the methodology proposed in this chapter. The points treated in this section can be extended to other configurations such as double-effect H₂O/LiBr and NH₃/H₂O cycles.

4.3 Data Validation for Absorption Refrigeration Systems

The following modelling aspects have been considered in order to obtain a numerically stable model:

4.3.3.1 Modelling Assumptions

In order to keep the model simple, the following assumptions are made:

- No heat losses.
- No pressure drops except through expansion valves.
- Saturated liquid state at the absorber, condenser and generator outlet.
- Saturated vapour at the evaporator outlet.
- Temperature of vapour leaving the generator is the saturation temperature of the solution at the conditions of the generator inlet stream.

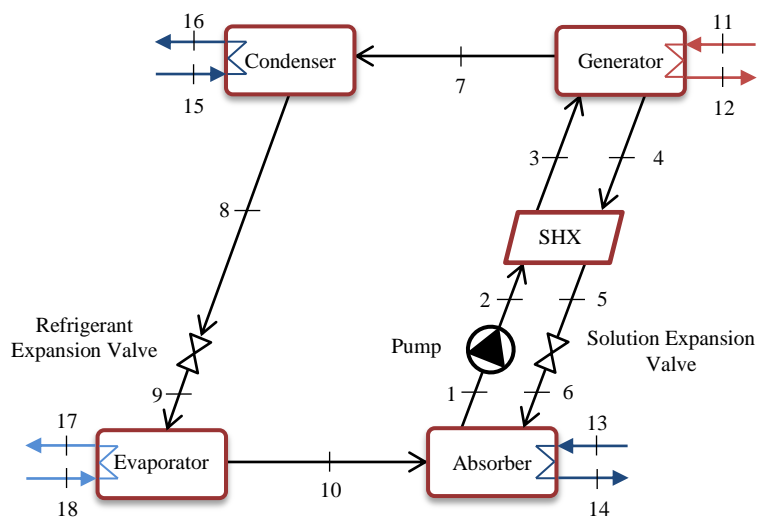


Figure 4-2: Schematic of a Single-Effect H₂O/LiBr Absorption Cycle.

4.3.3.2 Heat Transfer Models

As discussed in Chapter 2, the internal circuits are related to the external circuits by means of Equation 4-2

$$Q = UA \cdot \Delta t_{lm} \quad 4-2$$

where Q is the heat load transferred in the main heat exchangers and Δt_{lm} is the corresponding logarithmic mean temperature as defined in Equation 4-3:

Chapter 4. A framework for the Data Validation of Absorption Refrigeration Systems

$$\Delta t_{lm} = \frac{(t_{hot,1} - t_{cold,1}) - (t_{hot,2} - t_{cold,2})}{\ln\left(\frac{t_{hot,1} - t_{cold,1}}{t_{hot,2} - t_{cold,2}}\right)} \quad 4-3$$

where the subscript *hot* stands for the hot stream, the subscript *cold* stands for the cold stream, and the subscripts *1* and *2* stand for each of the sides of the heat exchanger. The logarithmic mean temperature has the drawback that convergence issues occur when the temperature differences in each side of the heat exchanger are equally valued. There are replacements of the logarithmic mean equation that overcome this situation. As stated by Pettersson [166] a good approximation to the logarithmic mean temperature is the one of Chen:

$$\Delta t_{chen} = \left[\frac{1}{2} (t_{hot,1} - t_{cold,1})^{0.3275} + \frac{1}{2} (t_{hot,2} - t_{cold,2})^{0.3275} \right]^{1/0.3275} \quad 4-4$$

Another important issue is the criteria to select the temperatures that take part in the temperature difference definitions. Table 4-1 shows the temperatures selected in this study. The temperatures are based on the streams of Figure 1-4. The temperatures have been selected following the criteria exposed in section 2 of section 6.2 of the book by Herold et al. [3].

Table 4-1: Temperatures selected for the logarithmic mean temperature definitions.

Component	$t_{hot,1}$	$t_{cold,1}$	$t_{hot,2}$	$t_{cold,2}$
Absorber	t_6	t_{14}	t_1	t_{13}
Generator	t_{11}	t_4	t_{12}	t_7
Condenser	t_8	t_{15}	t_8	t_{14}
Evaporator	t_{16}	t_{10}	t_{17}	t_{10}

4.3.3.3 Guess Value Generation

Absorption cycles models are composed by nonlinear equations which are solved by iterative procedures. In iterative solvers, the selection of guess values that are close to the final solution is useful to avoid divergence. In this study we draw up a procedure to estimate guess values of the model variables using the external circuits' measurements:

4.3 Data Validation for Absorption Refrigeration Systems

1. Calculate the heat loads in each of the main heat exchangers based on the external measurements

$$Q_x = m_x C_{p_x} \Delta t_x \quad 4-5$$

where Q is the heat load at the heat exchanger, m is the mass flow rate of the heat transfer fluid, C_p is the heat capacity of the heat transfer fluid, Δt is the temperature difference between the inlet and outlet streams, and the subscript x stands for the different external circuits: absorber-condenser, evaporator, or generator.

2. If the absorber and condenser are connected in series the outlet temperature of the heat transfer fluid at the absorber outlet is the same at the condenser inlet. In order to estimate this temperature we assume that heat duty in the absorber (Q_a) is 55% of the total heat rejected ($Q_a + Q_c$). Q_a is usually larger than Q_c because of the mixing heat released in the absorber. If the absorber and condenser are connected in parallel, the cooling water inlet temperature is the same, and the outlet temperature for each of the components is obtained by means of an energy balance assuming also that Q_a is 55% of the total heat rejected.
3. Temperature in the generator, t_4 , is equal to the outlet temperature of the external circuit minus 5 degrees (5 degrees pinch). Temperature in the evaporator, t_{10} , is equal to the outlet temperature of the external circuit minus 2 degrees (2 degrees pinch). Temperature in the condenser, t_8 is equal to the outlet temperature of the external circuit plus 5 degrees (5 degrees pinch). Temperature in the absorber, t_1 , is equal to the outlet temperature of the external circuit plus 1 degree (1 degree pinch). These assumptions are illustrated in Figure 4-3.
4. The initial guess for the remaining temperatures in each stream are calculated as follows:
 - t_2 is equal to t_1 .
 - t_3 is the mean temperature of the absorber and generator temperatures.
 - t_5 is equal to t_3 .
 - t_6 is the mean temperature of the absorber and t_5 .

Chapter 4. A framework for the Data Validation of Absorption Refrigeration Systems

- t_7 is equal to t_4 .
- t_9 is equal to t_{10} .

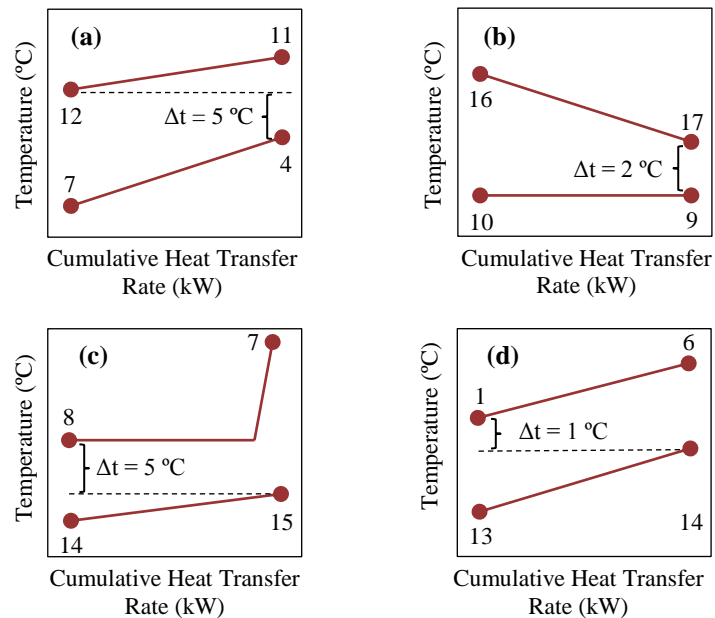


Figure 4-3: Heat exchanger diagrams with temperature pinch assumptions for (a) generator, (b) evaporator, (c) condenser, and (d) absorber.

5. We calculate the pressure levels from the estimated temperatures in the evaporator (t_{10}) and condenser (t_8) at saturation conditions.
6. We calculate the concentrations of the $\text{H}_2\text{O}/\text{LiBr}$ solution from the estimated pressure levels and the estimated t_1 and t_4 .
7. We calculate the guess values for the enthalpies in each stream using the property functions with guessed temperatures, concentrations and pressures as inputs.
8. Initial guess of the refrigerant mass flow rate is calculated from an internal energy balance in the evaporator

$$m_{ref} = \frac{Q_e}{(h_{10} - h_9)} \quad 4-6$$

4.3 Data Validation for Absorption Refrigeration Systems

9. If the diluted solution mass flow rate is given as a parameter, we estimate the concentrated solution mass flow from a global mass balance

$$m_{conc} = m_{dil} - m_{ref} \quad 4-7$$

otherwise m_{dil} can be estimated through a mass balance in the absorber using the guessed flow rate of the refrigerant and the guessed concentrations.

$$m_{dil} = m_{ref} \frac{x_{conc}}{x_{conc} - x_{dil}} \quad 4-8$$

So far we have been able to give estimates of all the thermodynamic states of the absorption cycle using the external circuits' measurements. The final solution will be different but not far from the guess values. This is illustrated in the t - P diagram of Figure 4-4. This guess values generation step is very important in order to reduce convergence problems during the simulation and during the iterative data reconciliation and parameter estimation procedures.

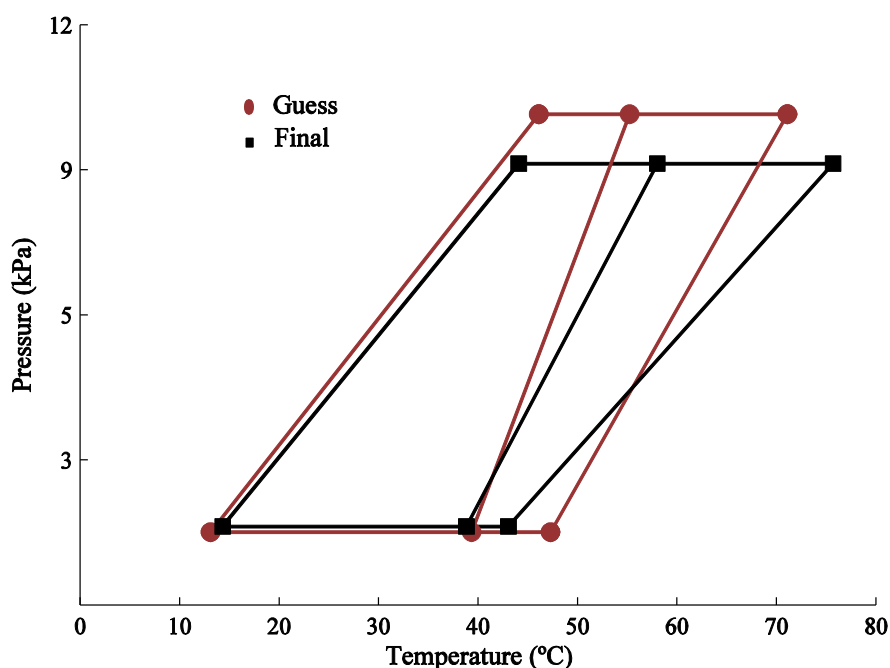


Figure 4-4: Guessed and final state values in a T-P diagram.

4.3.4 Resolution of the DR problem

DR requires a redundant set of measurements in order to be applied. In absorption refrigeration systems, depending on the amount of internal measurements available, two DR cases arise. In *Case 1*, the amount of measurements is enough to obtain the redundancy necessary for the resolution of the DR problem. On the other hand, in *Case 2*, the amount of internal measurements is not enough so there is the need to estimate all or some of the absorption chiller main parameters.

4.3.4.1 Case 1: DR with external and internal measurements

The resolution strategies for the DR problem using NLP are usually adapted to a particular application. Nowadays computers are much powerful than before in terms of calculation capabilities, so complex problems that were difficult to solve in the past can now be handled without much difficulty.

The Engineering Equation Solver (EES) is a convenient tool for rigorous modelling and simulation of absorption refrigeration cycles, because it provides built-in property libraries for the working fluids commonly used in absorption refrigeration cycles. Besides, it allows setting limits and guess values to the variables, and its solving capabilities are remarkable. However, the optimisation algorithms included are limited for performing DR. On the other hand, other modelling and simulation tools such as Matlab and GAMS have strong optimisation algorithms suitable for DR, but it is required to code the absorption system model, including the thermodynamic properties correlations.

Two-Stage Sequential Approach for DR

Faber et al. [202] developed a sequential methodology for parameter estimation and DR of large-scale systems. The main idea behind this approach is to divide the whole problem into three stages, all of which use NLP algorithms. In the upper stage, the parameters are estimated; in the middle stage, the measurements are adjusted; and in the lower stage, the simulation is carried out. Following this idea, Case 1 can be solved applying DR to absorption refrigeration systems, but considering the middle and lower stages only. This approach involves defining which variables are model inputs and which are model outputs. The degrees of freedom analysis is useful for distinguishing between model inputs and outputs. In this case the DR problem is formulated as:

4.3 Data Validation for Absorption Refrigeration Systems

$$J = \min \left[\left(\frac{y - y^*}{\sigma_y} \right)^2 + \left(\frac{u - u^*}{\sigma_u} \right)^2 \right]$$

Subjected to

$$f(x, y, u) = 0 \quad 4-9$$

$$u_{\min} \leq u \leq u_{\max}$$

$$x_{\min} \leq x \leq x_{\max}$$

$$y_{\min} \leq y \leq y_{\max}$$

where J is the scalar value of the objective function, y^* is a vector of measured values of the dependent variables (outputs), y is a vector of dependent variables, u^* is the measured values of the independent variables (inputs), u is a vector of independent variables, x is the unmeasured state variables, f is the vector of model equations, and σ_y and σ_u are the standard deviations of the measurements of the dependent and independent variables, respectively.

Figure 4-5 shows a schematic of the two-stage DR framework used in this study. In the DR stage only the measured independent variables, u , are treated as optimisation variables in Equation 4-9. The measurements belonging to u are adjusted in Matlab using the *fmincon* function. In the simulation stage the values of the dependent variables, y , and state variables, x , are calculated. The simulation is carried out in Engineering Equation Solver (EES) where the model equations are written. Matlab and EES communicate through the dynamic data exchange functions available in Matlab.

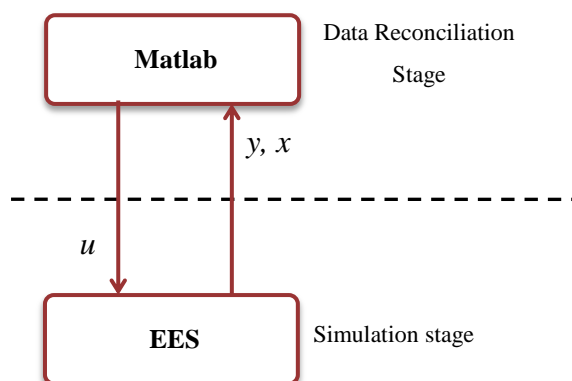


Figure 4-5: Schematic of the two-stage approach for DR.

The DR procedure can be summarized as follows: A Matlab script reads a set of measurements with their corresponding standard deviations. Then the values of vector u are written in a *.txt* file that is read by EES. With these inputs, EES solves the absorption system model and saves the values that belong to vector y in a *.csv* file. Matlab reads this *.csv* file and evaluates the objective function. The *fmincon* function searches for new values of u in order to minimize the objective function. This process is repeated until the solver stops. This DR methodology is rigorous because it uses NLP algorithms (from Matlab and EES); however, it is time consuming (from 5 to 10 minutes) and care has to be taken with the guess values and bounds of variables in EES to prevent from EES warning messages being displayed.

The General Algebraic Modeling System (GAMS) as a DR Tool

GAMS is a software designed for mathematical programming and optimization. It contains solvers which are robust, reliable and can deal with complex NLP problems. The DR is an optimisation problem and for this reason GAMS is a suitable alternative for its resolution.

In this case it is necessary to write within GAMS all the corresponding restrictions: mass and energy balances, thermodynamic properties correlations, minimum and maximum values for the variables, etc.

Some simple examples taken from the DR literature have been solved using EES, Matlab and GAMS. These examples are useful for comparing and assessing the DR capabilities of these tools.

- ***Example 1: Linear DR***

This linear DR example is taken from the book by Narasimhan and Jordache [21]. Figure 4-6 shows a simple process with a bypass where flow rates of the six streams are measured.

The flow balance equations for each component can be written as:

$$x_1 - x_2 - x_3 = 0 \quad 4-10$$

$$x_2 - x_4 = 0 \quad 4-11$$

4.3 Data Validation for Absorption Refrigeration Systems

$$x_3 - x_5 = 0 \quad 4-12$$

$$x_4 - x_5 - x_6 = 0 \quad 4-13$$

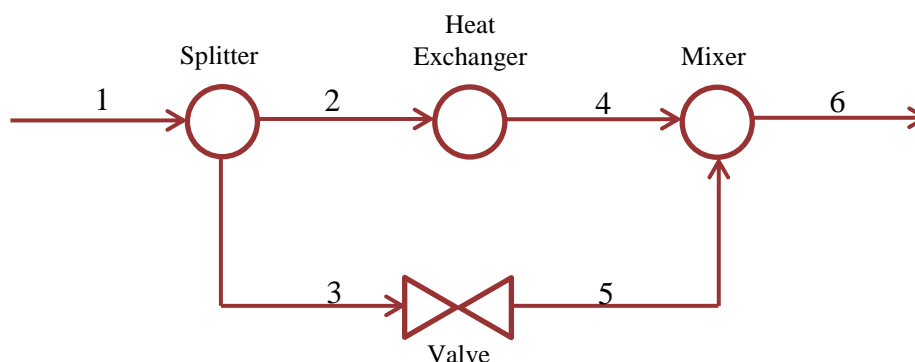


Figure 4-6: Heat exchanger system with bypass.

Table 4-2 shows the measured values (which don't satisfy the balance equations) as well DR results for this example. It can be seen that the same results are obtained using either of the tools.

Table 4-2: Flow reconciliation for the linear example.

Stream	True Value	Measured	Reconciled [21]	Reconciled EES	Reconciled Matlab	Reconciled GAMS
1	100	101.91	100.22	100.20	100.22	100.22
2	64	64.45	64.5	64.50	64.5	64.5
3	36	34.65	35.72	35.72	35.72	35.72
4	64	64.2	64.5	64.50	64.5	64.5
5	36	36.44	35.72	35.72	35.72	35.72
6	100	98.88	100.22	100.2	100.22	100.22
J (Final Value)	-	-	-	6.41	6.41	6.41

- *Example 2: Nonlinear DR*

The nonlinear DR taken from the book by Romagnoli and Sánchez [20] consists on a heat exchanger network where streams A receive heat from streams B, C, and D (see Figure 4-7).

Chapter 4. A framework for the Data Validation of Absorption Refrigeration Systems

The model consist of 16 measured variables, 14 unmeasured variables, and 17 equations including total mass and energy balances applied to each of the components.

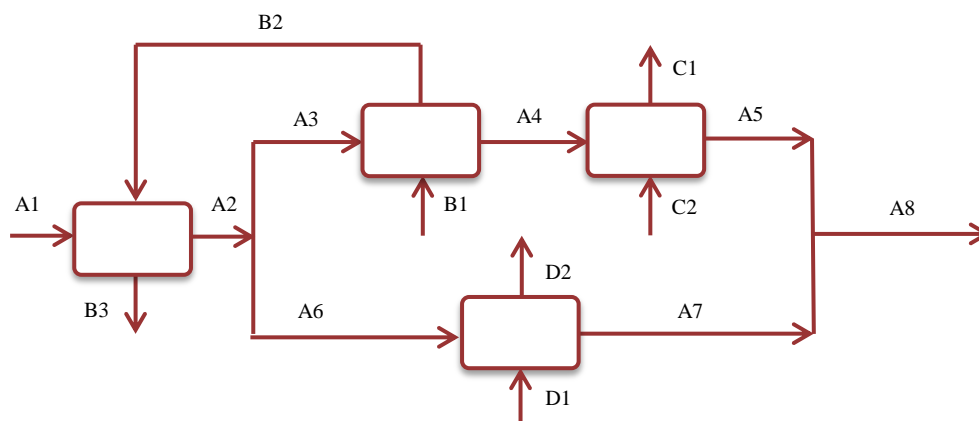


Figure 4-7: Flow diagram for nonlinear example.

Table 4-3: Measured and reconciled values for the nonlinear example.

Variable	Measurement	Reconciled [20]	Reconciled EES	Reconciled Matlab	Reconciled Matlab-EES	Reconciled GAMS
f_{A1}	1000	963.63	963.60	963.63	964.10	963.63
t_{A1}	466.33	466.33	466.30	466.33	466.30	466.33
f_{A2}	-	963.63	963.60	963.63	964.10	963.63
t_{A2}	-	481.91	481.90	481.91	481.90	481.91
f_{A3}	401.7	407.85	407.90	407.86	407.70	407.86
t_{A3}	481.78	481.91	481.90	481.91	481.90	481.91
f_{A4}	-	407.85	407.90	407.86	407.70	407.86
t_{A4}	530.09	530.09	530.10	530.09	530.10	530.09
f_{A5}	-	407.85	407.90	407.86	407.70	407.86
t_{A5}	616.31	615.51	615.50	615.51	615.60	615.51
f_{A6}	552.7	555.77	555.80	555.77	556.30	555.77
t_{A6}	-	481.91	481.90	481.91	481.90	481.91
f_{A7}	-	555.77	555.80	555.77	556.30	555.77
t_{A7}	619	617.77	617.80	617.76	617.80	617.76
f_{A8}	-	963.63	963.60	963.63	964.10	963.63
t_{A8}	614.92	616.81	616.80	616.81	616.90	616.81
f_{B1}	253.2	253.2	253.20	253.2	253.20	253.2
t_{B1}	618.11	618.11	618.10	618.11	618.10	618.11
f_{B2}	-	253.2	253.2	253.2	253.2	253.2
t_{B2}	-	543.9	543.9	543.9	543.9	543.9
f_{B3}	-	253.2	253.2	253.2	253.2	253.2
t_{B3}	-	486.51	486.5	486.5	486.6	486.51
f_{C1}	308.1	308.1	308.1	308.1	308.1	308.1
t_{C1}	694.99	694.99	695	694.99	695	694.99
f_{C2}	-	308.1	308.1	308.1	308.1	308.1
t_{C2}	-	594.8	594.8	594.8	594.7	594.8
f_{D1}	-	689.41	689.4	689.41	690.9	689.42
t_{D1}	667.84	668.02	668	668.02	668	668.02
f_{D2}	680.1	689.41	689.4	689.41	690.9	689.42
t_{D2}	558.34	558.17	558.2	558.17	558.2	558.17
J (Final Value)		14.80	14.80	14.80	14.83	14.80

4.3 Data Validation for Absorption Refrigeration Systems

Table 4-3 shows the measured values and DR results for the nonlinear example. It can be seen that the obtained results are practically the same using either tool, except when using the combined Matlab-EES approach. Nevertheless, for this example, the differences are minimal. For this example, a resolution time of 18 and 8 seconds was reported in [20] (depending on the method used), while the resolution time using gams is just a fraction of second.

4.3.4.2 Case 2: Simultaneous Data Reconciliation and Parameter Estimation

A single-effect H₂O/LiBr absorption chiller (Figure 4-2) can be described in terms of six main parameters: the four UA (product of the overall heat transfer coefficient, U , and the heat exchanger area, A) values of the main heat exchangers of the absorption chiller, the effectiveness of the solution heat exchanger, η_{shx} , and the flow rate of the solution pump m_{dil} . The first five parameters are related to the performance of the heat and mass transfer processes in the cycle, and the flow rate is an indicative of the cooling capacity of the machine.

In order to identify the main parameters of a single-effect H₂O/LiBr absorption chiller Marc et al. [122] and Heintz et al. [203] used an optimisation procedure. They select three sets of measurements at different operating conditions. The objective function to be minimized computes the difference between the simulated and experimental heat input and cooling capacity for the three sets of measurements:

$$J = \min \left[\sum_{i=1}^3 \left(\frac{Q_{g,\text{exp}} - Q_{g,\text{calc}}}{Q_{g,\text{exp}}} \right)^2 + \sum_{i=1}^3 \left(\frac{Q_{e,\text{exp}} - Q_{e,\text{calc}}}{Q_{e,\text{exp}}} \right)^2 \right] \quad 4-14$$

Nevertheless, the random and or systematic errors can bias this estimation procedure. In this study we substitute the previous objective function by another one including the measurements weighted by the standard deviation.

$$J = \min \left[\sum_{i=1}^3 \left(\frac{t - t^*}{\sigma_t} \right)^2 + \sum_{i=1}^3 \left(\frac{G - G^*}{\sigma_G} \right)^2 \right] \quad 4-15$$

Chapter 4. A framework for the Data Validation of Absorption Refrigeration Systems

where t are the external circuits temperatures, G the external circuits flow rates, and σ the corresponding standard deviation.

In the parameter identification procedure we also need a guess value for the parameters in order to reduce the convergence problem during the iterations. These guess values for the parameters are obtained from the nominal conditions of the absorption system.

1. The initial guess of the UA values is obtained from the heat loads at nominal conditions, and the approximation of the logarithmic mean temperature difference calculated using the corresponding guessed temperatures.

$$UA_x = \frac{Q_x}{\Delta t_x} \quad 4-16$$

2. From the experimental cooling capacity we calculate the refrigerant flow rate using Equation 4-6. The diluted solution flow rate is obtained through a mass balance in the absorber using the guessed flow rate of the refrigerant, and the guessed concentrations (Equation 4-8).

3. The guess value of the effectiveness of the heat exchanger is set to 0.6.

4.3.5 Gross Error Detection

Systematic or gross errors occur because of malfunctioning instruments or process leaks. Gross errors differ from random error because their expected mean value is different from zero. The presence of gross errors invalidates the DR results. They have to be identified and eliminated or corrected before or during the DR

The Modified Iterative Measurement Test (MIMT) was initially proposed by Serth and Heenan [36] and further developed by Serth et al. [204] and Kim et al. [205]. In this method a statistical test is applied to the least-squares residuals (the difference between the raw and reconciled value of the measurements). It is assumed that random errors in the data are normally distributed. After solving the DR problem, we obtain an error vector (residuals) defined as

$$e = [u - u^*, y - y^*] \quad 4-17$$

Then, for each measurement we calculate the statistical z

$$z_i = \frac{e_i}{\sigma_i} \quad 4-18$$

In this study the MIMT is used as follows. First, DR is performed for all the available data sets. Second, statistical z is calculated and compared with z_{crit} (2.326 for a 98% confidence level) for all the sets of residuals. Third, the measurement that is flagged as a gross error in the most of the tests is removed. The process is repeated until there are no more gross errors in any of the data sets. This method was selected because it is simple and effective. The drawback is that we may lose redundancy, or even the minimum amount of inputs for the model, if there are too many measurements containing gross errors.

4.4 Case Studies

4.4.1 Data reconciliation of a single-effect NH₃/H₂O absorption chiller (Case 1)

In this case study we analysed a single-effect NH₃/H₂O absorption chiller with a nominal cooling capacity of 12kW, the chillii® PSC12, from SolarNext. This chiller was tested in a test bench at the CREVER-URV facilities. The test bench makes it possible to study and characterize the performance of small capacity absorption systems working in controlled operating conditions, and allows the inlet hot-water temperature, the inlet cooling-water temperature, and the outlet chilled-water temperature of the absorption chiller to be set. Figure 4-8 shows a simplified diagram of the chiller. Water is used as the heat transfer fluid in the external circuits of the absorber, condenser and generator. An ethylene glycol-water mixture is used for the external circuit of the evaporator. The absorber and condenser are connected in series, with the absorber being first.

4.4.1.1 Measurements and operating conditions

Seventeen process variables were measured at different locations in the absorption chiller in the test bench (see Table 4-4). The external circuit temperatures (t_{11} , t_{12} , t_{13} , t_{15} , t_{16} and t_{17}) were measured using PT-100 sensors in direct contact with the fluid. The internal circuit temperatures (t_1 , t_4 , t_7 , t_8) and t_{14} were measured using type-J thermocouples attached to the surface of the tubes. The machine has two pressure gauges to measure the high and low pressure levels. Also, the low pressure gauge indicates t_9 . The measured data consist of a total of 32 tests in different operating conditions.

Chapter 4. A framework for the Data Validation of Absorption Refrigeration Systems

Table 4-4: Process variables measured for the NH₃/H₂O absorption chiller.

Variable	Stream
Temperature (°C)	1, 4, 7, 8, 9, 11, 12, 13, 14, 15, 16, 17
Flow rate (m ³ /h)	11, 13, 16
Pressure (bar)	8, 9

The data acquisition system sampled data every minute. Figure 4-9 shows how the steady-state indicator performs during one day of tests. It can be seen that the steady-state flag (dashed line) agrees visually with the steady regions of all temperature trends.

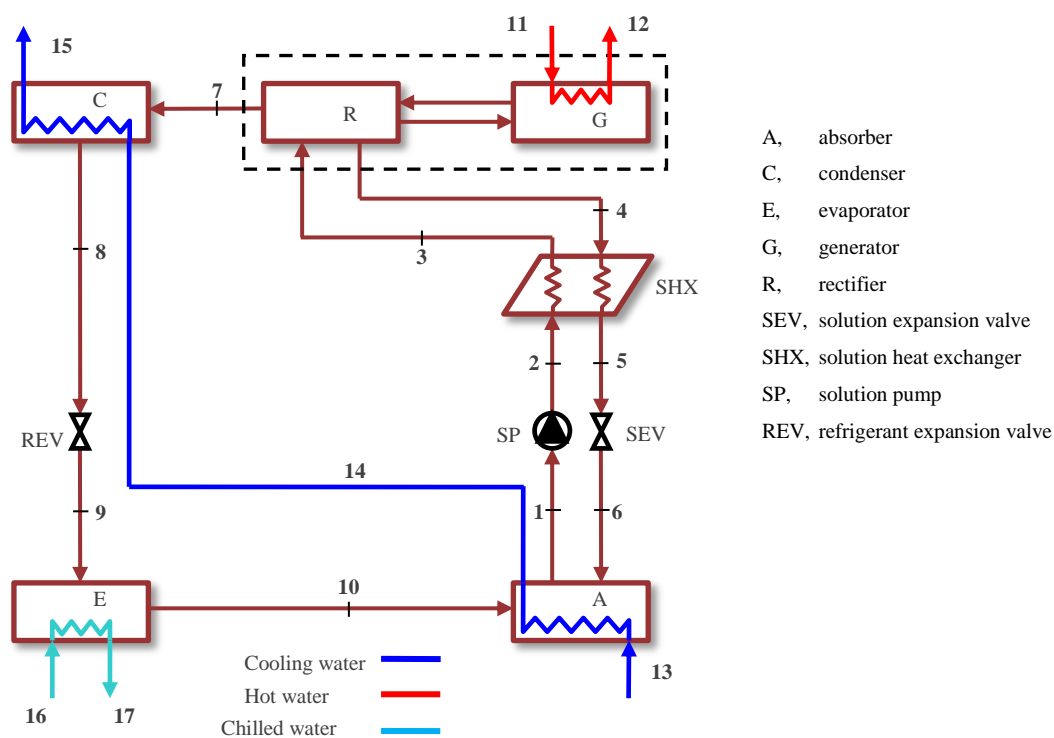


Figure 4-8: Simplified schematic of the single-effect ammonia-water absorption cycle.

4.4.1.2 Degrees of freedom analysis

According to [83], the number of degrees of freedom for a complete single-effect absorption cycle is given by:

$$N_d = (N_{vt} + C) - [N_{rn} + n_c(C + 2) + N_{ih}] \quad 4-19$$

where N_d is the number of degrees of freedom of the absorption cycle, C is the number of components in the working fluid mixture, N_{vt} is the total number of variables, N_{rt} is the total number of independent equations, n_c is the number of single-phase interconnecting streams in the cycle, and N_{ih} is the number of internal heat couplings for multi-effect cycles. Table 4-5 shows the number of variables in each component (N_v), number of independent equations in each component (N_r), together with N_{vt} , N_{rt} , n_c , and N_{ih} , for a single-effect absorption cycle (considering generator and rectifier to be one unit). For an ammonia-water chiller $C = 2$, and Equation 4-19 becomes:

$$N_d = [26C + 82 + C] - [(12C + 44) + 13(C + 2)] = 16 \quad 4-20$$

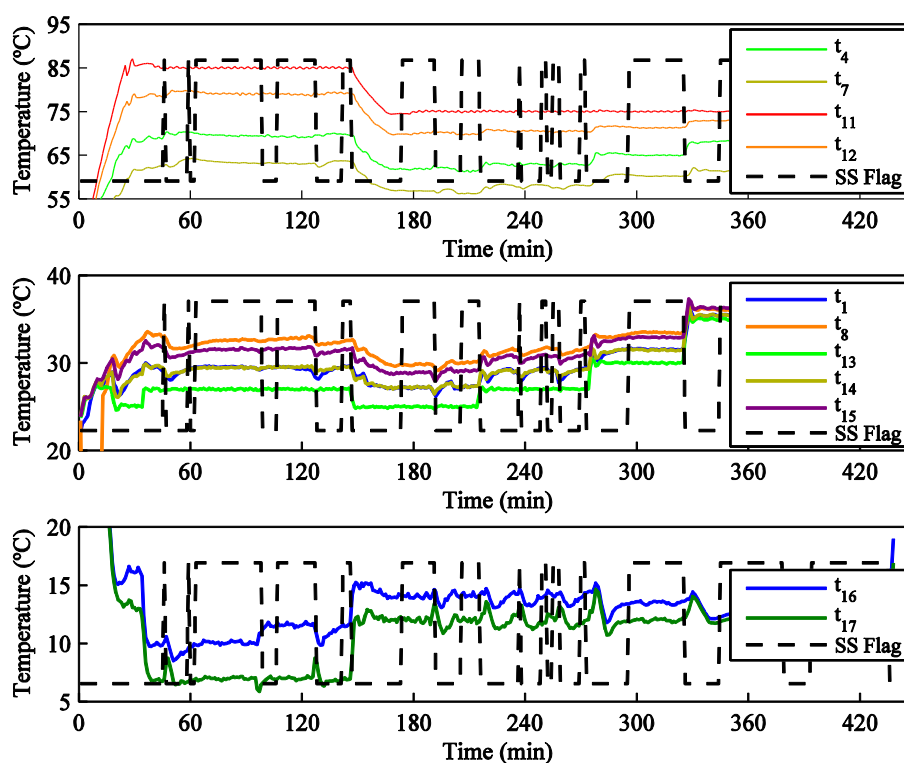


Figure 4-9: Steady-state detector and temperature trends during one day of operation.

Chapter 4. A framework for the Data Validation of Absorption Refrigeration Systems

Table 4-5: Calculation of degrees of freedom for single-effect absorption systems.

Components	Number of variables (N_v)	Number of independent equations (N_r)
A	$5C+17$	$C+8$
C	$2C+11$	$C+7$
E	$4C+15$	$2C+8$
G	$3C+13$	$C+9$
SP	$2C+5$	$C+2$
SHX	$4C+9$	$2C+4$
SEV	$3C+6$	$2C+3$
REV	$3C+6$	$2C+3$

$$N_{vt} = \sum(N_v) = 26C + 82$$

$$N_{rt} = \sum(N_r) = 12C + 44$$

$$n_c = 13$$

$$n_{ih} = 0$$

So we have 16 degrees of freedom for this particular case. However, the cooling water of the absorber and condenser are connected in series. This means that two degrees of freedom which are associated with the external heat transfer circuits are lost. Another degree of freedom is lost because we assume that t_7 is equal to the saturation temperature in the conditions of stream 3. So the number of degrees of freedom for our case study is 13. A detailed account of degrees of freedom for this chiller can be found in [83].

From the seventeen measurements, we selected a set of inputs ($t_1, t_4, t_7, t_8, t_9, t_{11}, t_{12}, t_{13}, t_{15}, t_{14}, t_{16}, t_{17}, P_h, P_b, G_{11}, G_{13}, G_{16}$) that reduces the degrees of freedom to zero. Since there are more measured variables ($N_{MV}=17$) than calculated degrees of freedom ($N_d=13$) some measurements are redundant and DR can be performed.

Since t_7, t_9, t_{12} , and P_h belong to the set of model outputs, they are redundant. We checked that any of the measurements that belong to the model inputs set can also be estimated from the model and other measurements. As a result, all the measurements are redundant for this case.

4.4.1.3 Data reconciliation and gross error detection

DR and GED procedure was executed three times:

1st DR and GED: After the 1st DR and GED we detected that t_9 (refrigerant temperature at the evaporator outlet) was the measurement that was most likely to contain gross error. Figure 4-10a shows that t_9 was flagged as gross error in 7 of the 32 tests. Therefore, t_9 was removed and the methodology was applied again. After repeating the degrees of freedom analysis the set of model inputs remained the same and the set of model outputs lost t_9 . Since the number of measured variables ($N_{MV}=16$) was still greater than the number of calculated degrees of freedom ($N_d=13$), some measurements were redundant and DR was performed. In this case all 16 measurements were still redundant and all the state points and heat duties could be determined.

The reason t_9 contains a gross error is not because the gauge is defective. The measurement was biased because of the way the measurement was taken (the values of t_9 were read visually in a 10-minute interval) and because the temperature scale depicted in the gauge is fixed (and probably assumes that the refrigerant is 100% ammonia, neglecting the influence of the refrigerant composition on the temperature).

2nd DR and GED: Figure 4-10b shows that, after removing t_9 and performing DR and GED for a second time, the number and frequency of measurements suspected of containing gross errors decreases. However, some measurements are still flagged as containing gross errors. In this case t_1 , t_7 , and t_8 were the most suspect measurements. We decided to remove t_7 because its z value is greater than the z value of t_1 and t_8 . When the degrees of freedom analysis was repeated, the set of model inputs was found to remain the same and the set of model outputs lost t_7 . The number of measured variables ($N_{MV}=15$) was also greater than the number of calculated degrees of freedom ($N_d=13$). Some measurements, then, were redundant and DR was performed again.

3rd DR and GED: After the 3rd DR and GED no measurements were flagged as containing gross errors.

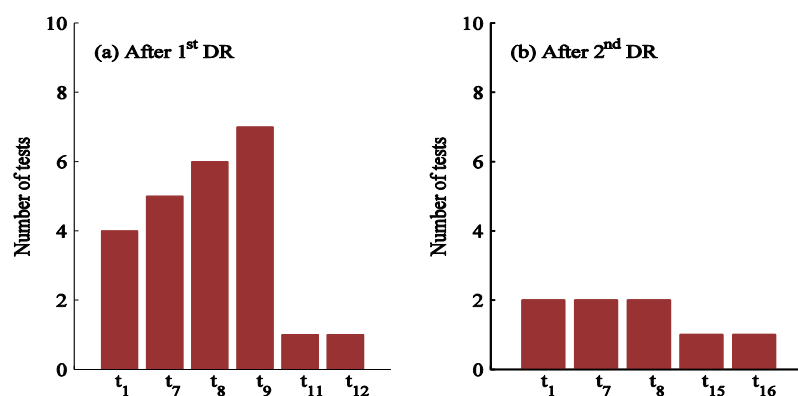


Figure 4-10: Number of tests with measurements containing gross errors after the 1st DR (a) and the 2nd DR (b).

Chapter 4. A framework for the Data Validation of Absorption Refrigeration Systems

Figure 4-10 shows that the weighted least squares estimator tends to spread the gross error over all the measurements. This is why in Figure 4-10a and Figure 4-10b measurements other than t_7 and t_9 are also flagged as gross errors. However, after t_7 and t_9 were removed the remaining measurements were no longer suspected of containing gross errors.

Figure 4-11a, b, and c show the scalar value of the objective function before and after DR. These figures highlight two things: first, the significant reductions in the objective function because of DR; and second, the reductions in the initial value of the objective function due the removal of the measurements with gross errors.

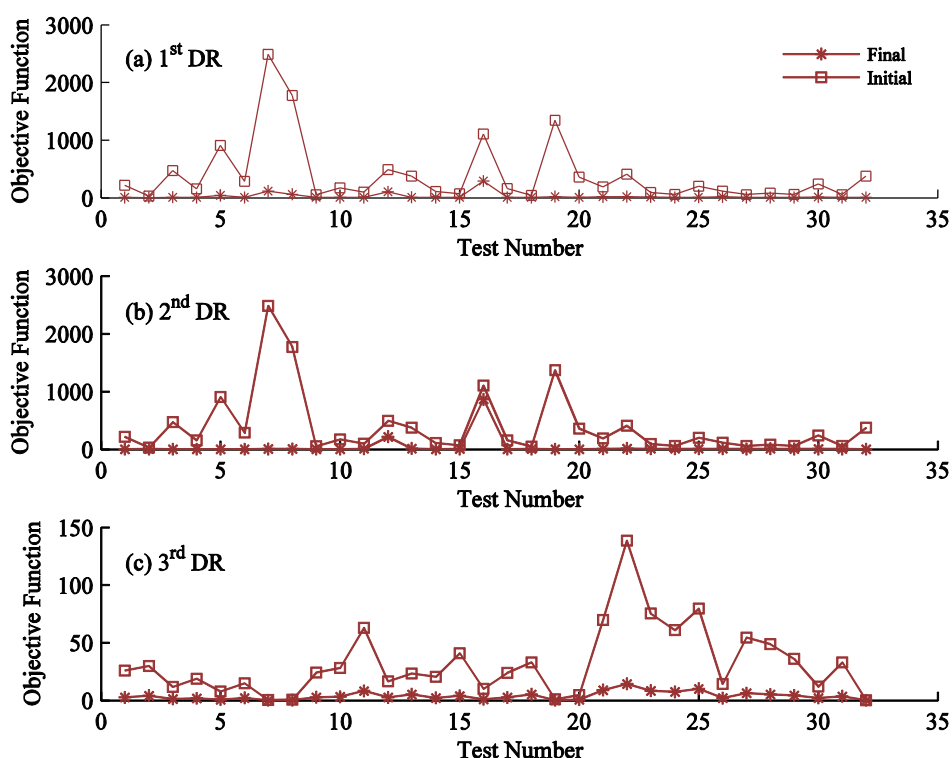


Figure 4-11: Value of the objective function before and after DR

Figure 4-12 shows Q_e and COP calculated using raw and reconciled data for the 32 tests at different operating conditions. In this figure, Q_e and COP are plotted against the chilled-water outlet temperature (t_{17}), for different values of the hot-water inlet temperature (t_{11}) and cooling-water inlet temperature (t_{13}). It can be seen that there is a small difference between the calculations using raw (filled markers) and reconciled (blank markers) data. According to this figure, it seems that the Q_e and COP were slightly underestimated in some of the tests when raw data was used, particularly when the chiller was working at a driving temperature of 95 °C.

Figure 4-13 shows the calculation of the heat input into the evaporator (Q_e), the heat rejected by the absorber and condenser ($Q_a + Q_c$), the heat input into the generator (Q_g), and the heat balance ($Q_a + Q_c - Q_g - Q_e$) using raw and reconciled data. This figure shows how the mismatch in the energy balance is eliminated through data reconciliation. For example, at $t_{17} = -3$ °C, the cooling capacity is 2.4 kW, the heat input into the generator is 8.3 kW, and the heat rejected through the cooling water circuit is 11.9 kW. The corresponding heat balance has a mismatch of 1.19 kW. The power consumption of the chiller is 0.30 kW, and only part of this power is used in the solution pump (the rest is used for the internal control of the chiller), so the mismatch in the energy balance at these conditions is around 1kW. After DR, mismatch in the heat balance is 0.14 kW, which corresponds roughly to the estimated work input into the solution pump. Therefore, the energy balance is satisfied.

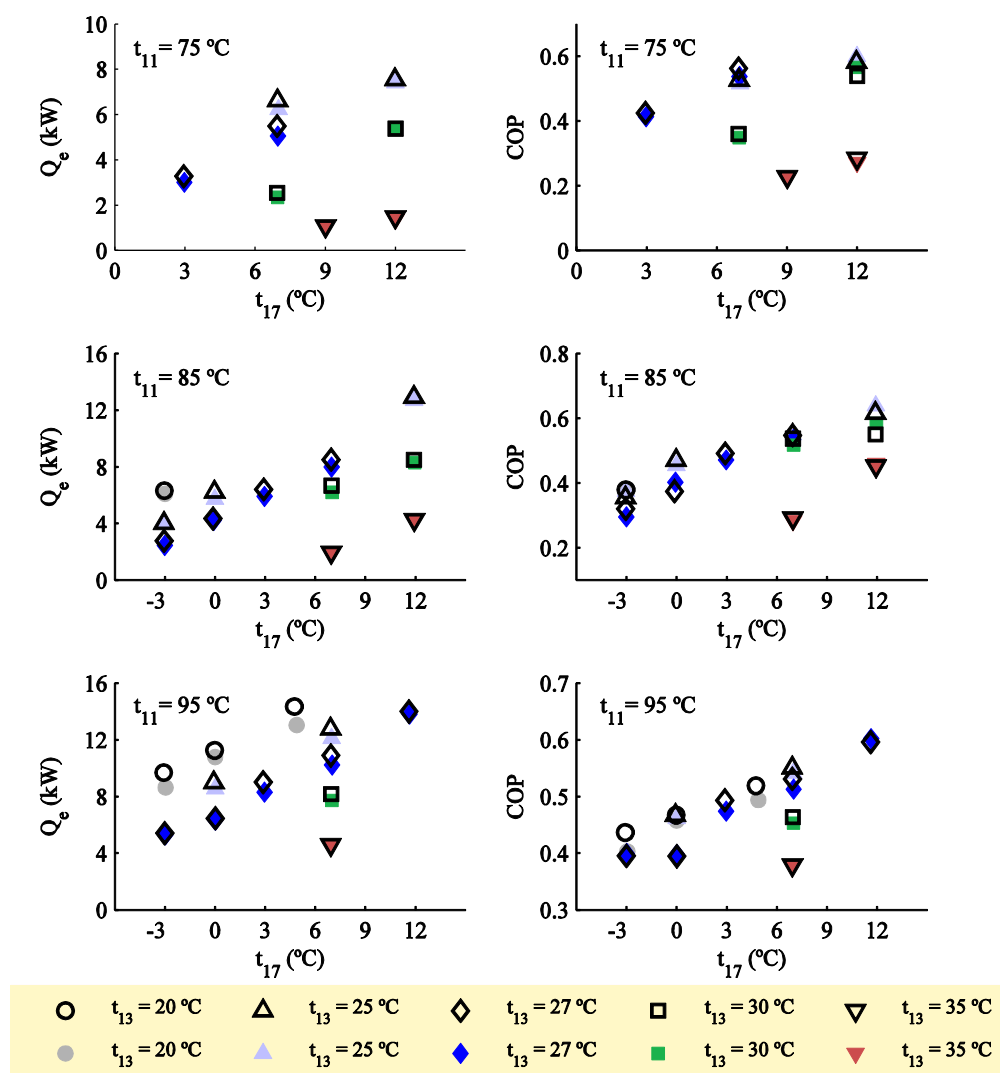


Figure 4-12: Q_e and COP calculation using raw and reconciled measurements (filled markers correspond to raw data and blank markers correspond to reconciled data).

Chapter 4. A framework for the Data Validation of Absorption Refrigeration Systems

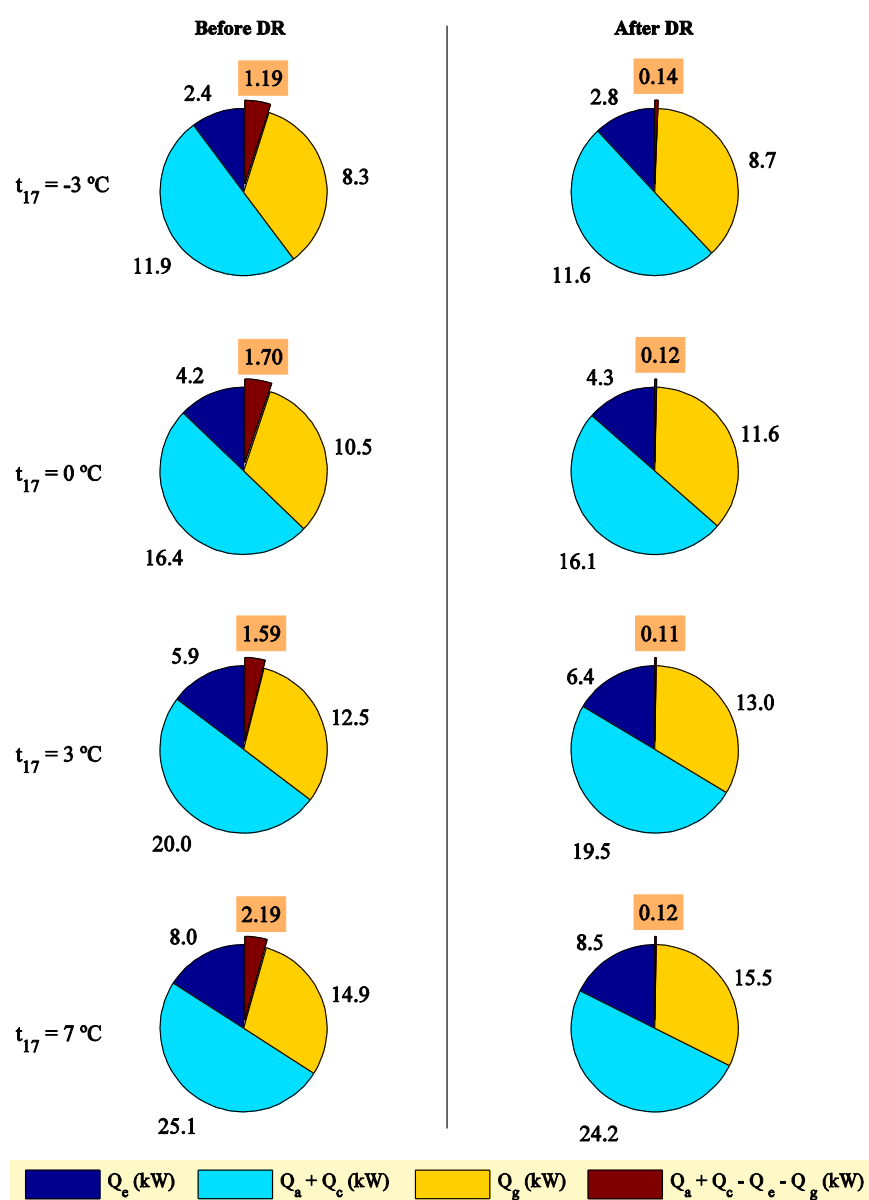


Figure 4-13: Energy balances before and after DR for hot-water inlet temperature (T_{11}) at 85 °C and cooling-water inlet temperature (T_{13}) at 27°.

Table 4-6 presents the values of the raw measurements, their corresponding standard deviations, reconciled measurements, residuals after DR, and the calculated z values for one of the 32 tests. It can be seen that in order to satisfy the mass and energy balances small adjustments were made to all the measurements. In general the residuals and z values are very low, except in the case of t_7 . As stated above, t_7 and t_9 were considered to be unmeasured and did not take part in the final DR since they were flagged as containing gross errors.

Table 4-6: Raw and reconciled measurements for hot-water inlet temperature (t_{11}) at 85 °C, cooling-water inlet temperature (t_{13}) at 27, and chilled -water outlet temperature (t_{17}) at 7 °C.

Measurement	Standard deviation	Original value	Reconciled value	Residual	z
t_1 (°C)	0.08	29.6	29.6	2.90E-04	0.00
t_4 (°C)	0.12	70.5	70.5	3.13E-04	0.00
t_7 (°C)	0.13	64.1	65.0	8.86E-01	6.81
t_7 (°C)	0.09	32.7	32.7	1.33E-04	0.00
t_9 (°C)	1.00	1.9	1.9	3.55E-02	0.04
t_{11} (°C)	0.19	85.0	85.1	1.48E-01	0.78
t_{12} (°C)	0.13	79.0	78.9	9.21E-02	0.71
t_{13} (°C)	0.08	27.0	27.1	7.22E-02	0.90
t_{14} (°C)	0.09	29.5	29.5	8.28E-04	0.01
t_{15} (°C)	0.09	31.5	31.4	9.39E-02	1.04
t_{16} (°C)	0.13	9.2	9.4	1.09E-01	0.84
t_1 (°C)	0.09	7.0	6.9	4.14E-02	0.46
P_h (kPa)	50	1250	1254	4	0.08
P_l (kPa)	50	460	457	3	0.07
G_{11} (m ³ /h)	0.01	2.20	2.20	2.43E-03	0.24
G_{13} (m ³ /h)	0.01	4.79	4.79	1.18E-03	0.12
G_{16} (m ³ /h)	0.01	3.37	3.37	1.26E-03	0.13

Table 4-7: Parameters calculated during the three DR steps (in the same conditions as Table 4-6).

Parameter	Without	After 1 st	After 2 nd	After 3 rd
	DR	DR	DR	DR
Q_e (kW)	7.98	8.55	8.69	8.52
Q_a (kW)	13.85	13.50	13.42	13.45
Q_c (kW)	11.26	10.64	10.91	10.73
Q_g (kW)	17.01	15.49	15.53	15.55
W_p (kW)	0.12	0.10	0.10	0.12
COP	0.47	0.55	0.56	0.54
η_{shx}	0.82	0.83	0.84	0.86

Chapter 4. A framework for the Data Validation of Absorption Refrigeration Systems

Table 4-7 shows the calculated value of important parameters (heat duties, work input, *COP*, etc.) through the different steps of DR. Differences in the calculations can be important when raw or reconciled data are used, as in the case of *COP* or cooling capacity. Also, the presence of gross errors affects the calculations.

4.4.2 Simultaneous Data Reconciliation and Parameter Estimation of a single-effect H₂O/LiBr absorption chiller (Case 2)

As an example we analyse a H₂O/LiBr single-effect absorption chiller working in the polygeneration plant ST4 in Cerdanyola del Vallès (Spain). The ST4 polygeneration plant has been installed in the framework of the PolyCity project. The rated *COP* and chilled water capacity of the single effect chillers is 0.75 and 3 MW, respectively, and is fired directly with the cooling water of the cogeneration engines.

4.4.2.1 Measurements and operating conditions

The chiller operates from 10:00 to around 20:00 at a fixed chilled water set point. It works at partial load. The available measurements for this case are the inlet and outlet temperatures for each of the external circuits, as well as their corresponding volumetric mass flow rate. Measurements are sampled each minute. Table 4-8 summarizes the operating conditions for this particular case.

Table 4-8: Operating conditions for the single effect H₂O/LiBr Absorption Chiller

Variable	Set point
Chilled water temperature (t_{18})	5 °C
Cooling water temperature (t_{13})	27 – 30 °C
Hot water temperature (t_{11})	85 – 90 °C
Chilled water flow rate (G_{ch})	440 m ³ /h
Cooling water flow rate (G_{cw})	870 m ³ /h
Hot water flow rate (G_{hw})	variable

Figure 4-14 shows the operation trends together with the steady state indicator. This is a one day example. It can be seen that the chiller operates at the beginning at 75% of capacity. Afterwards its capacity decreases. In the middle there is an unstable period with a lot of oscillation. The last steady state has slow drifting.

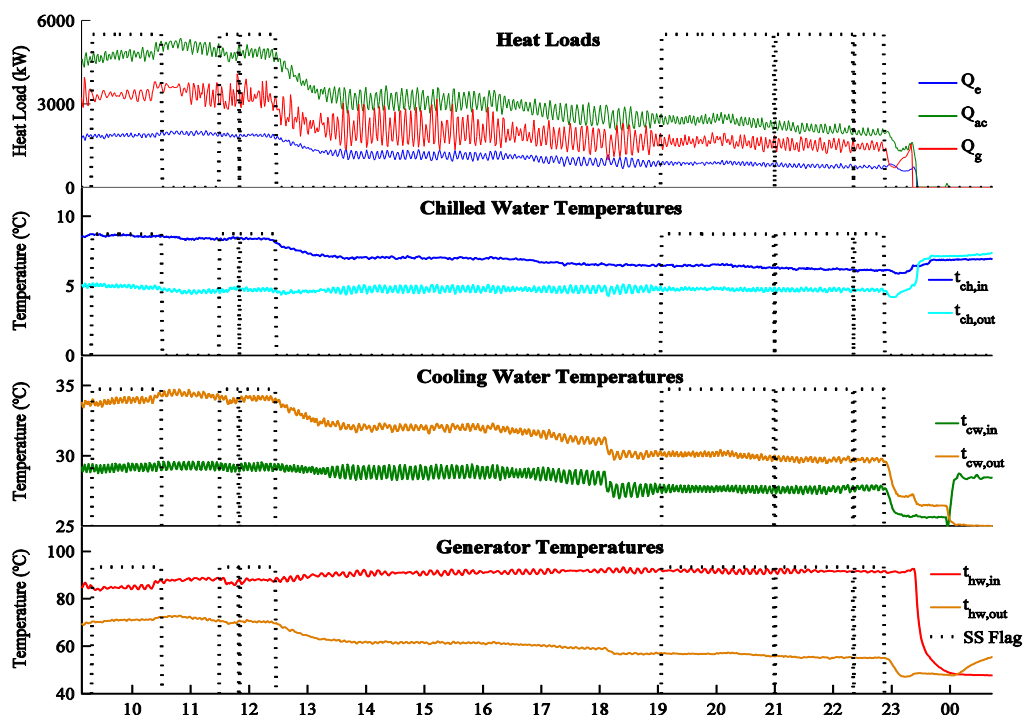


Figure 4-14: Absorption chiller heat loads, temperature trends and steady-state indicator during one day of operation.

Table 4-9 summarises the operating conditions together with the untreated measurements as well as the calculated heat loads for steady-state periods during five days of operation. It can be seen that the chiller operates at fixed chilled water outlet temperature, hot water inlet temperature, cooling water inlet temperature, chilled water flow rate and cooling water flow rate. The hot water flow rate is variable.

4.4.2.2 Degrees of freedom analysis

For this case there are not measurements of the internal circuits of the absorption refrigeration cycle. We are able to calculate the performance of the system in terms of cooling capacity and COP, but we are not able to retrieve any qualitative or quantitative information about the internal conditions of the system.

For this case there are not measurements of the internal circuits of the absorption refrigeration cycle. We are able to calculate the performance of the system in terms of cooling capacity and COP, but we are not able to retrieve any qualitative or quantitative information about the internal conditions of the system.

Table 4-10 shows the number of variables of each component (N_v), number of independent equations of each component (N_r), together with N_{vt} , N_{rt} , n_c , and N_{ih} , for a single-effect absorption cycle (considering generator and rectifier to be one unit). For a H₂O/LiBr chiller $C = 2$, and Equation 4-19 becomes:

Chapter 4. A framework for the Data Validation of Absorption Refrigeration Systems

$$N_d = [26C + 82 + C] - [(12C + 44) + 13(C + 2)] = 16 \quad 4-21$$

So we have 16 degrees of freedom for this particular case. However, the cooling water of the absorber and condenser are connected in series. This means that two degrees of freedom which are associated with the external heat transfer circuits are lost. Another degree of freedom is lost because we assume that t_7 is equal to the saturation temperature in the conditions of stream 3. Since the refrigerant is pure component (water) another degree of freedom is lost. As a result the degrees of freedom for this case study is 12.

Table 4-9: Summary of the operating steady state points during 5 days of operation

	$t_{11} (^{\circ}\text{C})$	$t_{13} (^{\circ}\text{C})$	$t_{18} (^{\circ}\text{C})$	G_{hw} (m^3/h)	G_{cw} (m^3/h)	G_{ch} (m^3/h)	Q_e (kW)	Q_g (kW)	Q_{ac} (kW)
1	81.2	27.8	4.6	127.3	871.0	440.0	1708	2722	3971
2	85.7	27.8	4.6	54.0	866.2	439.7	1107	1804	2757
3	87.1	27.4	4.7	38.4	871.8	439.3	778.7	1485	2018
4	87.3	27.5	4.7	37.3	867.0	441.0	806.3	1426	2107
5	84.1	27.9	4.7	78.6	874.1	439.8	1369	2251	3368
6	84.7	27.8	4.6	63.6	873.8	439.8	1256	1958	3074
7	91.0	26.4	4.7	26.3	863.6	439.7	677	1269	1830
8	85.0	29.2	5.0	206.6	880.9	437.7	1861	3277	4890
9	87.1	29.2	4.7	163.1	878.0	437.7	1867	3149	4883
10	87.8	29.2	4.7	159.2	877.0	437.8	1857	3162	4939
11	91.7	27.6	4.8	40.0	868.4	437.4	856.9	1598	2432
12	91.6	27.6	4.7	36.0	869.2	437.5	770.5	1485	2153
13	91.5	27.7	4.7	34.7	871.9	437.9	725.2	1438	2008
14	85.9	28.2	4.7	159.1	908.0	438.6	1968	3192	5062
15	90.5	28.0	4.8	58.0	901.0	437.8	1194	2049	3355
16	90.7	27.9	4.8	56.1	901.6	438.0	1190	2016	3339
17	91.7	28.1	4.8	56.9	869.2	438.0	1205	2060	3440
18	91.9	28.0	4.8	53.6	869.4	439.0	1154	1985	3290
19	91.9	28.0	4.8	50.8	868.9	437.9	1108	1904	3197
20	92.0	27.9	4.8	46.4	869.3	437.9	1016	1778	2988
21	92.3	27.8	4.8	43.6	869.2	438.0	969.8	1707	2857
22	92.4	27.8	4.8	42.6	869.3	437.8	934.2	1690	2787
23	92.3	27.8	4.8	41.5	867.0	437.7	898.3	1652	2699
24	91.9	28.0	4.8	22.9	868.7	437.4	454.1	1050	1488
25	87.1	27.9	4.7	78.0	897.7	439.0	1387	2252	3542

For this case there are not measurements of the internal circuits of the absorption refrigeration cycle. We are able to calculate the performance of the system in terms of cooling capacity and COP, but we are not able to retrieve any qualitative or quantitative information about the internal conditions of the system.

Table 4-10: Calculation of degrees of freedom for single-effect absorption systems.

Components	Number of variables (N_v)	Number of independent equations (N_r)
A	$5C+17$	$C+8$
C	$2C+11$	$C+7$
E	$4C+15$	$2C+8$
G	$3C+13$	$C+9$
SP	$2C+5$	$C+2$
SHX	$4C+9$	$2C+4$
SEV	$3C+6$	$2C+3$
REV	$3C+6$	$2C+3$

$$N_{vt} = \sum(N_v) = 26C + 82$$

$$N_{rt} = \sum(N_r) = 12C + 44$$

$$n_c = 13$$

$$n_{ih} = 0$$

A parameter identification procedure allows us to determine from experimental data the main parameters of the absorption refrigeration system. With these parameters and the operating conditions all the thermodynamic states of each stream of the absorption refrigeration cycle can be calculated.

4.4.2.3 Joint Parameter Estimation and Data Reconciliation

Table 4-11 shows the initial guess value of the parameters before the parameter estimation procedure, as well as their final value. The initial guess was estimated from the nominal operating conditions given in Table 4-12. The final values of the parameters were obtained through Equation 4-14 using three data sets: nominal conditions, data from steady-state period 14, and data from steady-state period 20. It can be seen that the parameter values are slightly different if they are obtained through just parameter estimation (using equation 4-14 as proposed by Heintz et al. [203] and Marc et al. [122]) or through joint data reconciliation and parameter estimation (using equation 4-15 as

Chapter 4. A framework for the Data Validation of Absorption Refrigeration Systems

proposed in this thesis). These parameters should not be considered as the true values or design values, but as values that are able to represent the behaviour of the absorption refrigeration cycle in a determined operation range.

Table 4-11: Absorption chiller parameters

Parameter	Initial Value	Estimated Value (PE)	Estimated Value (PE + DR)
m_{sol} (l/h)	10	8.2	9.2
η_{shx}	0.6	0.37	0.31
UA_a (kW/K)	563	1661.6	1145.3
UA_c (kW/K)	529	1045.9	1015.3
UA_e (kW/K)	727	458.7	577.4
UA_g (kW/K)	385	335.8	302.6

Table 4-12: Nominal conditions for calculating the initial value of the chiller parameters

Variable	Nominal Value
Chilled water temperature (t_{18})	13 °C
Cooling water temperature (t_{13})	30 °C
Hot water temperature (t_{11})	95 °C
Chilled water flow rate (G_{ch})	433 m ³ /h
Cooling water flow rate (G_{cw})	909 m ³ /h
Hot water flow rate (G_{hw})	234 m ³ /h
Cooling Capacity (Q_e)	3275 kW
COP	0.75

Figure 4-15 shows the experimental capacity and COP versus their corresponding predictions by the model using the three set of parameters of Table 4-11 (initial guess, obtained by parameter estimation only, and obtained through data reconciliation and parameter estimation). It can be seen that the cooling capacity is predicted very well using any of the three parameter sets, while the COP is better predicted by the model using the estimated parameters.

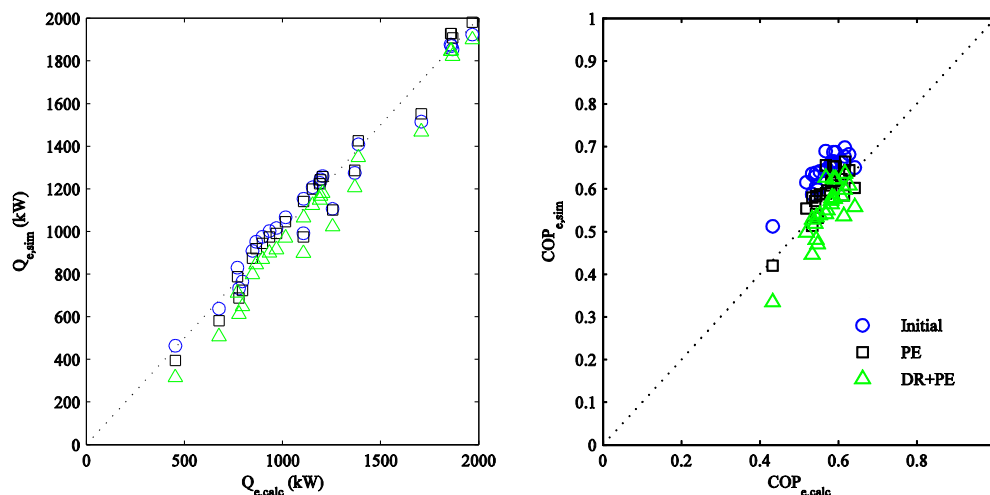


Figure 4-15: Experimental and predicted cooling capacity and COP using the thermodynamic model with three different sets of parameters and raw measurements.

4.4.2.4 Data reconciliation of all the steady-state sets

By means of the thermodynamic model, operating conditions, and the estimated chiller parameters, one is able to calculate the performance of the absorption chiller as well as the internal states values. Since the thermodynamic model is complete DR has been applied to the measurements for the 25 operating steady-state points of Table 4-9. Table 4-13 shows the reconciled values of these measurements.

Figure 4-16 shows the same information as Figure 4-15 but instead of using the raw measurements, the calculations are based on the reconciled measurements of Table 4-13. It can be seen that in this case the model with parameters estimated using data reconciliation gives better results.

The goodness-of-fit of models is usually evaluated in terms of the statistical indicators. One useful indicator is the coefficient of variation of the root-mean-square error (*CV*) which is a normalised measure of dispersion of probability distribution. *CV* is defined as RMSE divided by dependent variable mean, and is expressed as percentage.

$$CV = \frac{RMSE}{\bar{X}} \cdot 100 \quad 4-22$$

where RSME is the root-mean-square error and \bar{X} is the mean value of the variable under study.

Chapter 4. A framework for the Data Validation of Absorption Refrigeration Systems

Table 4-13: Reconciled measurements values

	$t_{11} (^{\circ}\text{C})$	$t_{12} (^{\circ}\text{C})$	$t_{13} (^{\circ}\text{C})$	$t_{16} (^{\circ}\text{C})$	$t_{17} (^{\circ}\text{C})$	$t_{18} (^{\circ}\text{C})$	G_{ch} (m^3/h)	G_{cw} (m^3/h)	G_{hw} (m^3/h)
1	7.9	4.8	26.8	30.9	80.5	63.2	440.0	869.9	126.0
2	6.8	4.8	26.5	29.2	85.5	56.7	439.7	864.5	52.5
3	6.3	5.0	26.3	28.2	86.7	54.2	439.2	870.2	33.4
4	6.3	4.9	26.3	28.3	87.1	54.4	440.4	871.8	34.3
5	7.4	4.8	27.0	30.3	83.5	59.7	439.8	861.4	76.0
6	7.1	4.9	27.1	30.0	84.4	58.4	439.7	876.7	62.2
7	5.9	4.5	24.8	26.8	85.7	51.7	439.7	865.5	33.3
8	8.7	4.7	28.1	33.1	84.6	71.5	437.8	880.9	205.3
9	8.4	4.5	28.1	33.1	86.8	70.4	437.7	871.6	162.1
10	8.5	4.6	28.4	33.3	87.4	70.6	437.8	873.4	157.3
11	6.5	4.8	27.1	29.5	91.8	57.1	437.3	867.3	38.9
12	6.4	4.7	26.8	29.2	91.4	56.7	437.6	869.2	38.9
13	6.3	4.7	26.5	28.7	91.6	55.6	437.5	869.0	34.5
14	8.6	4.6	27.4	32.2	85.6	68.5	438.6	905.8	157.6
15	7.2	4.8	27.6	30.6	90.5	59.8	437.8	899.2	55.5
16	7.1	4.8	27.4	30.4	90.7	59.3	438.0	901.2	54.3
17	7.2	4.8	27.6	30.8	91.6	60.1	438.0	868.4	55.5
18	7.1	4.9	27.6	30.6	91.8	59.6	438.1	868.6	51.7
19	7.0	4.8	27.5	30.4	91.8	59.2	437.9	868.5	49.7
20	6.8	4.8	27.4	30.1	91.9	58.5	437.9	869.0	45.1
21	6.7	4.8	27.4	30.0	92.2	58.1	437.8	868.8	42.5
22	6.7	4.9	27.4	29.9	92.3	57.9	437.8	868.9	40.7
23	6.6	4.9	27.3	29.7	92.2	57.5	437.7	866.8	39.0
24	5.8	4.8	26.7	28.2	81.6	54.2	437.4	870.5	33.6
25	7.4	4.7	27.7	31.2	87.0	61.8	439.0	896.3	77.0

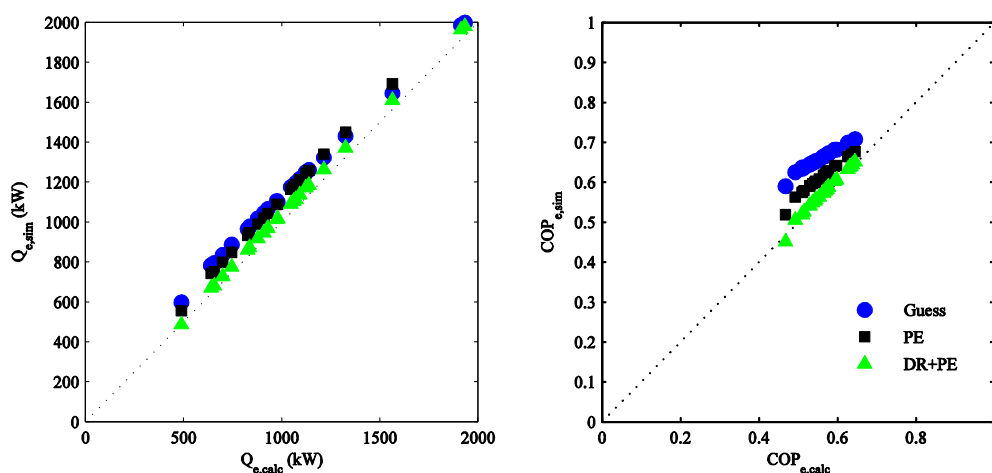


Figure 4-16: Experimental and predicted cooling capacity and COP using the thermodynamic model with three different sets of parameters and reconciled measurements.

Figure 4-17 shows the coefficient of variation for the predicted cooling capacity and COP using the thermodynamic model with three different sets of parameters and raw and reconciled measurements. Here it can be seen more clearly that the model using the parameters calculated by simultaneous data reconciliation and parameter estimation is the most accurate, especially with reconciled data.

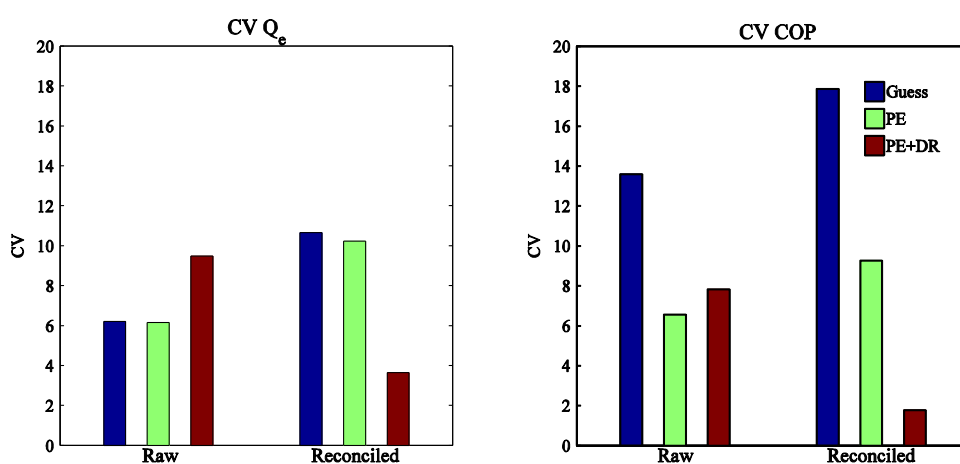


Figure 4-17: Coefficient of variation for the predicted cooling capacity and COP using the thermodynamic model with three different sets of parameters and raw and reconciled measurements.

4.5 Conclusions

This chapter presents a methodology for the steady-state data treatment of absorption chillers. The methodology includes a steady-state detection step, a systematic degrees of freedom analysis, and DR including GED as well as parameter estimation. This methodology enables important parameters, such as COP and cooling capacity, to be reliably calculated and measurements with systematic errors to be identified.

Depending on the amount of available measurements two different cases arise. In Case 1, the amount of measurements is enough to obtain the redundancy necessary for the resolution of the DR problem. The DR can be solved using a sequential or a direct approach. On the other hand, in Case 2, the amount of internal measurements is not enough so there is the need to estimate all or some of the absorption chiller main parameters. In this case a joint DR and parameter estimation procedure is required.

Case 1 is demonstrated by analysing the operational data of a small-capacity single-effect $\text{NH}_3/\text{H}_2\text{O}$ absorption chiller. An intensive data set consisting of several measurements in 32 different operating conditions was treated. DR is performed using a sequential approach in which the reconciled values of the measurements were estimated in

Chapter 4. A framework for the Data Validation of Absorption Refrigeration Systems

Matlab while the simulation that ensures that the process constraints are satisfied was carried out using EES. An approach based on the MIMT method is used for GED, which is a combined DR and GED procedure.

The GED step is fundamental if the DR problem is to be appropriately solved. The least-squares estimator spreads the random or systematic error over all measurements. If systematic errors are present, the residuals of some measurements may be higher than they should be, the calculations will be biased, and the benefit from DR is lost.

According to the results of the case study Q_e and COP were underestimated when raw data was used. After the final DR step, the calculated value of Q_e was, on average, 5% greater than the calculations based on raw measurements. In consequence, the COP calculated with reconciled data was also greater (0.05 in average) than when it was calculated with the raw measurements.

Case 2 is demonstrated by analysing the operational data of a large-capacity single-effect H₂O/LiBr absorption chiller. Since the internal measurements are not available, a combined DR and parameter estimation procedure has been applied using GAMS. The main parameters of the absorption chiller have been estimated using three data sets.

The coefficient of variation shows that the model using the parameters calculated by simultaneous data reconciliation and parameter estimation is the most accurate, especially with reconciled data.

The results in both case studies show that the data validation framework is useful for obtaining performance data that is consistent with the mass and energy balances. These calculations are more reliable than calculations based on raw measurements.

The reconciled data of both examples can be used for the characterisation both absorption chillers. This topic will be treated in the next chapter.

Nomenclature

C_p ,	Specific heat capacity (kJ/kg-K)
CV ,	Coefficient of variation of the root-mean-square error
G ,	Volumetric flow rate (m ³ /h)
J ,	Objective function
Q ,	Heat load (kW)
UA ,	Overall heat transfer coefficient times the heat exchanger area (kW/K)
Δt_{lm}	Logarithmic mean temperature difference
e ,	Residual of the least-squares estimation
h ,	Specific enthalpy (kJ/kg)
m ,	Mass flow rate (kg/s)
n ,	Data window size
t ,	Temperature (°C)
u ,	Set of measured independent variables
x ,	Concentration
y ,	Set of measured dependent variables
z ,	Statistical for the Modified Iterative Measurement Test

Greek letters

η ,	Effectiveness of the solution heat exchanger
σ ,	Standard deviation
χ ,	Unmeasured dependent variables

Subscripts

a ,	Absorber
ac ,	Absorber and condenser
c ,	Condenser
$calc$,	Calculated or simulated data
ch ,	Chilled water circuit
$cold$,	Cold stream

Chapter 4. A framework for the Data Validation of Absorption Refrigeration Systems

<i>conc,</i>	Concentrated solution
<i>crit</i>	Critical value for the t-test
<i>cw,</i>	Cooling water circuit
<i>dil,</i>	Diluted solution
<i>e,</i>	Evaporator
<i>exp,</i>	Experimental data
<i>g,</i>	Generator
<i>hot,</i>	Hot stream
<i>hw,</i>	Hot water circuit
<i>in,</i>	Inlet
<i>out,</i>	Outlet
<i>ref,</i>	Refrigerant
<i>shx,</i>	Solution heat exchanger

Superscripts

*	Measured
---	----------

Chapter 5

Characterisation of Absorption Refrigeration Systems through Data Validation

Abstract

The Characteristic Equation Method, mentioned in Chapter 2, offers a good compromise between simplicity and accuracy in order to predict the performance of an absorption system. This method requires experimental data in order to fit some parameters. It is important, therefore, that the data used for the fitting to be reliable. These methods benefit from the data validation procedure since the data used for their construction have lower noise and are consistent with the laws of conservation. Thus it is interesting to characterise a determined absorption refrigeration system by the Characteristic Equation Method using validated or reconciled data.

The objective of this chapter is to demonstrate the usefulness of the data validation framework proposed in Chapter 4 for the development of characteristic equations for absorption refrigeration systems.

5.1 Introduction

Current tools for modelling and simulation offer an adequate framework for studying the integration of absorption cycles into advanced energy generation systems. However, often the models of absorption cycles used for this task are too simple, sometimes only making use of tabulated data; or, on the other hand, are so complex that detailed design specifications are needed to solve the model. In many cases these design data is not available.

In this sense, experimental data of absorption refrigeration systems are a good basis of knowledge in order to develop simple, yet robust, models for their integration into larger systems such as trigeneration systems, thermal desalination systems, solar cooling, etc.

The characteristic equation method, mentioned in Chapter 2, offers a good compromise between simplicity and thermodynamic fundamentals in order to predict the performance of an absorption chiller. This modelling approach requires experimental data for fitting the characteristic parameters of the absorption system. Nevertheless, measured data tend to be contaminated by random and/or gross errors. The use of data validation procedures allows obtaining reliable data. The objective of this chapter is to demonstrate the usefulness of the data validation framework proposed in Chapter 4 for the development of characteristic equations for absorption refrigeration systems. A case study using a single-effect $\text{NH}_3/\text{LiNO}_3$ absorption chiller is presented in this chapter.

5.2 The Characteristic Equation Method

The characteristic equation describes the performance of an absorption chiller through simple algebraic equations. These equations are based on thermodynamic fundamentals. The characteristic equation can predict the part load behaviour of absorption chillers, avoiding the use of more complex numerical simulations of the thermodynamic cycle.

According to Puig-Arnavat et al. [118] two approaches are available in order to obtain the characteristic equation for a single-effect $\text{H}_2\text{O}/\text{LiBr}$ absorption chiller. The first approach [114] requires solving the following equation system:

$$Q_e = s_e(\Delta t_{ace}) \cdot \Delta \Delta t - s_e(\Delta t_{ace}) \cdot \Delta \Delta t_{\min,e}(\Delta t_{ace}) \quad 5-1$$

$$Q_g = s_g(\Delta t_{ace}) \cdot \Delta \Delta t - s_g(\Delta t_{ace}) \cdot \Delta \Delta t_{\min,g}(\Delta t_{ace}) \quad 5-2$$

5.2 The Characteristic Equation Method

$$Q_{ac} = s_{ac}(\Delta t_{ace}) \cdot \Delta \Delta t - s_{ac}(\Delta t_{ace}) \cdot \Delta \Delta t_{\min ac}(\Delta t_{ace}) \quad 5-3$$

$$s_x(\Delta t_{ace}) = s_{x1} \cdot \Delta t_{ace} + s_{x2} \quad 5-4$$

$$\Delta \Delta t_{\min, x}(\Delta t_{ace}) = r_{x1} \cdot \Delta t_{ace} + r_{x2} \quad 5-5$$

where $\Delta t_{ace} = T_{ac} - T_e$, $\Delta \Delta t$ is the characteristic temperature difference (equation 2-45), the subscript x corresponds to the different heat exchanger units (evaporator, generator, absorber and condenser). To find values s_{x1} , s_{x2} , r_{x1} , r_{x2} to determine the characteristic parameters (s_x and $\Delta \Delta t_{\min, x}$), four reference operation points must be evaluated either from manufacturer or experimental data.

The second approach [116] requires a numerical fit to obtain the characteristic parameters of an arbitrary characteristic temperature function $\Delta \Delta t'$

$$\Delta \Delta t' = T_g - A \cdot T_{ac} + E \cdot T_e \quad 5-6$$

and the linear characteristic equation for the cooling load

$$Q_e = s' \cdot \Delta \Delta t' + r \quad 5-7$$

Combining equations 5-6 and 5-7 and we obtain

$$Q_e = s'_e \cdot T_g - s'_e \cdot A \cdot T_{ac} + s'_e \cdot E \cdot T_e + r_e \quad 5-8$$

and similarly for the heat input in the generator

$$Q_g = s'_g \cdot T_g - s'_g \cdot A \cdot T_{ac} + s'_g \cdot E \cdot T_e + r_g \quad 5-9$$

The characteristic parameters of each equation (s' , A , E and r) are obtained through data fitting.

The study of Puig-Arnavat et al. [118] concluded that the second approach is the simplest and that it provides similar or better accuracy than the first approach. Since experimental data is required, it could be interesting to apply data validation procedures to ensure the quality of the experimental data through data validation procedures.

5.3 Case study

As an application example it is analysed an $\text{NH}_3/\text{LiNO}_3$ single-effect absorption chiller with a nominal cooling capacity of 10 kW [206]. Figure 5-1 shows a simplified schematic of this chiller and Table 5-1 summarizes the operating conditions used for the tests. The cooling water circuit rejecting heat in absorber and condenser is set in parallel.

The available measurements are the inlet and outlet temperatures and the flow rate of the three external circuits: t_{13} , t_{14} , t_{15} , t_{18} , t_{19} , t_{20} , G_{ch} , G_{cw} and G_{hw} .

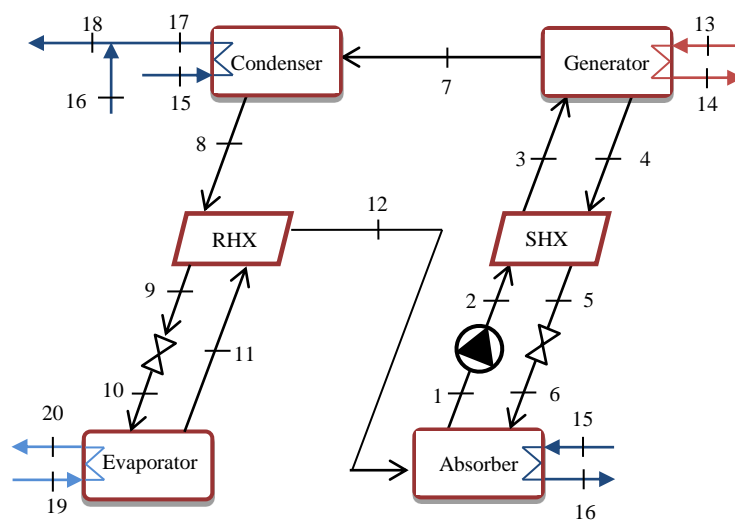


Figure 5-1: Schematic of the single-effect $\text{NH}_3/\text{LiNO}_3$ absorption chiller.

5.3.1 Data Validation

A total of 32 steady-state points at different operating conditions were obtained during the testing. From this set, three representative points were selected for the data reconciliation and parameter estimation procedure. These points correspond to the nominal capacity, low capacity, and above the nominal capacity conditions of the absorption chiller.

Table 5-1: Summary of the operating conditions.

Variable	Set point
Chilled water outlet temperature (t_{20})	7, 15 (°C)
Cooling water inlet temperature (t_{15})	30, 35, 40 (°C)
Hot water inlet temperature (t_{13})	80, 85, 90, 95, 100 (°C)
Chilled water flow rate (G_{ch})	3 (m ³ /h)
Cooling water flow rate (G_{cw})	6 (m ³ /h)
Hot water flow rate (G_{hw})	3 (m ³ /h)

The joint data reconciliation and parameter estimation problem was solved using the General Algebraic Modeling System (GAMS) with the CONOPT solver. Table 5-2 shows the values of the parameters after both the parameter estimation procedure (*PE*, using equation 4-14 as proposed by Heintz et al. [203] and Marc et al. [122]) and the joint parameter estimation and data reconciliation procedure (*DR+PE*, using equation 4-15 as proposed in this thesis). It can be seen that their values are different. These parameters should not be considered as the true values or design values, but as values that are able to represent the behaviour of the absorption refrigeration cycle within a determined operation range.

Table 5-2: Estimated parameters using Parameter Estimation (PE) and Data Reconciliation and Parameter Estimation (DR+PE).

Parameter	PE	DR + PE
m_{sol} (l/s)	0.12	0.18
η_{shx}	0.69	0.80
η_{rhx}	0.54	0.52
UA_a (kW/K)	7.44	5.27
UA_c (kW/K)	3.15	3.32
UA_e (kW/K)	3.05	3.21
UA_g (kW/K)	1.10	1.06

Figure 5-2 shows the comparison between the predicted and experimental cooling capacity and COP when using the model with the estimated parameters through just parameter estimation (*PE*, triangular markers) and joint parameter estimation and data reconciliation (*PE+DR*, circular markers). Both sets of parameters give very similar results and good agreement. Despite the fact that the parameters for each case have different values, the performance calculations given for each set are very similar.

Chapter 5. Characterisation of Absorption Systems through Data Validation

The coefficient of variation of the root-mean-square error (CV) is used to compare the models in terms of predicting capabilities. CV is defined as the root-mean-square error divided by the dependent variable average. A lower CV means better prediction. After obtaining the main parameters of the absorption chiller we reconcile the data of the 32 steady-state points using the thermodynamic model with the estimated parameters with DR. The DR procedure was carried out in GAMS with the CONOPT solver. Afterwards, the reconciled set of data is used for finding the adapted characteristic equation of this chiller.

Table 5-3 shows the CV values for both parameter sets. The parameters estimated through joint data reconciliation and parameter estimation show better prediction capabilities. In the case of the cooling capacity prediction, the CV value is 12.42 when data reconciliation is used and 13.19 without DR. In the case of the COP, the CV value is 5.23 when data reconciliation is used and 6.16 without DR. The differences in the CV are not large but the parameters found using DR have better prediction capabilities.

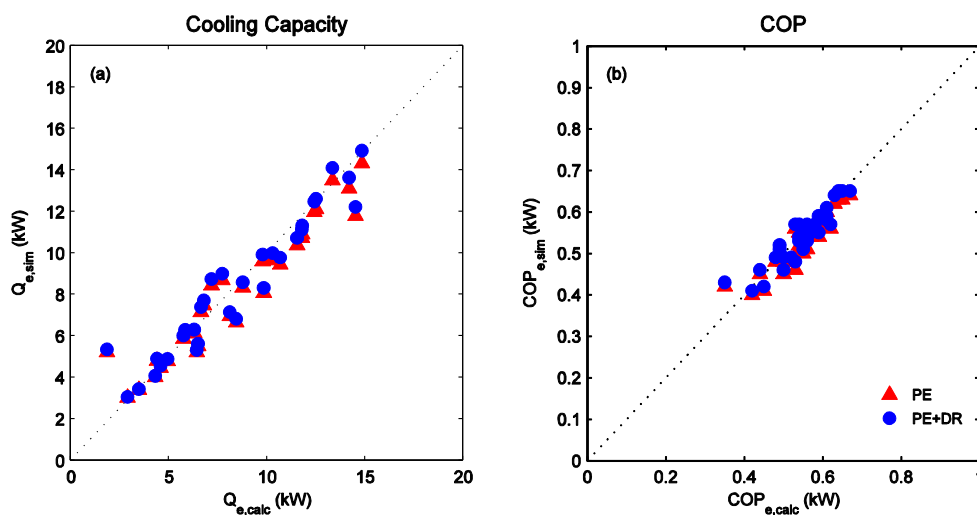


Figure 5-2: Experimental cooling capacity (Q_e) and COP vs simulated predicted by the thermodynamic model with the estimated parameters.

After obtaining the main parameters of the absorption chiller we reconcile the data of the 32 steady-state points using the thermodynamic model with the estimated parameters with DR. The DR procedure was carried out in (GAMS) with the CONOPT solver. Afterwards, the reconciled set of data is used for finding the adapted characteristic equation of this chiller.

Table 5-3: Coefficient of variation (CV) for the thermodynamic model with estimated parameters.

Parameter	<i>PE</i>	<i>DR + PE</i>
Q_e	13.19	12.42
COP	6.16	5.23

5.3.2 Adapted Characteristic Equation

From the 32 steady-state points we have used a set of for fitting the parameters of equations 5-8 and 5-9. These parameters have been fit using the raw (untreated) and reconciled (treated) data. Table 5-4 shows the values of the fitted parameters. In the case of parameters s' , A and E they have a similar value when obtained from raw or reconciled data. However, in the case of parameter r the difference is significant: 13.71 versus 2.47 for Q_e and 14.99 versus 6.03 for Q_g .

Table 5-4: Fitted parameters of the adapted characteristic equation for this case study.

Parameter	Q_e		Q_g	
	Value (raw)	Value (rec)	Value (raw)	Value (rec)
s'	0.31	0.32	0.57	0.54
A	3.54	2.43	2.81	2.23
E	1.95	1.49	1.19	0.92
r	13.71	2.47	14.99	6.03

Figure 5-3 shows a comparison of the predicted cooling capacity and COP using the characteristic equations from raw and reconciled data. In Figure 5-3 (a) and (b) the characteristic equations use the untreated data for calculating the cooling capacity and COP. It can be seen that the prediction is similar using either characteristic equation. Nevertheless, predictions using the characteristic equation from reconciled values seem to be less scattered, especially for the COP. In Figure 5-3 (c) and (d) the characteristic equations use the reconciled data for calculating the cooling capacity and COP. As expected, very good agreement is obtained with the characteristic equations from reconciled values.

Chapter 5. Characterisation of Absorption Systems through Data Validation

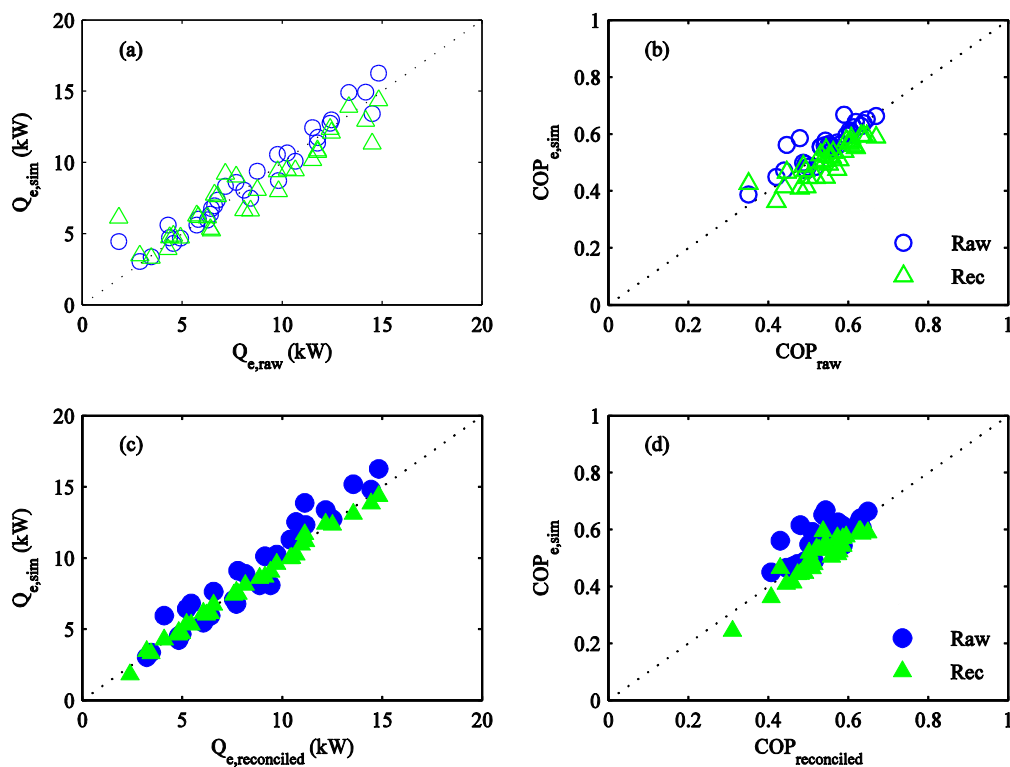


Figure 5-3: Comparison of the predicted cooling capacity and COP using the Characteristic Equation from raw data (circular markers) and reconciled data (triangular markers).

Figure 5-4 shows the coefficient of variation of the root-mean-square error for the predictions using both data sets (untreated and reconciled) and both derived characteristic equations (from raw data and from reconciled data). In the case of the cooling capacity (Figure 5-4a), the prediction using the raw data set is slightly better using the characteristic equation from the reconciled data, while the prediction using the raw data set is obviously much better using the characteristic equation from reconciled data. In the case of the COP (Figure 5-4b), using the raw data set the prediction is better when using the characteristic equation from raw data, but when the reconciled data set is used, the prediction is much better using the characteristic equation from reconciled data, as expected.

Summarising, the above study shows that the adapted characteristic equation obtained from reconciled data is able to predict the performance of an absorption chiller with similar accuracy than an adapted characteristic equation obtained from raw data. However, the prediction using reconciled data is far better with the adapted characteristic equation from reconciled data.

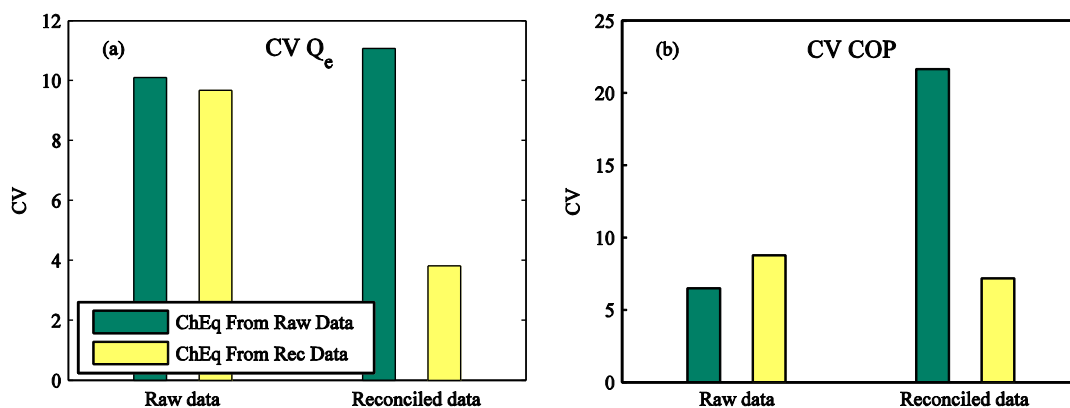


Figure 5-4: Coefficient of variation for the predicted cooling capacity and COP using the Characteristic Equation from raw data (green bars) and the Characteristic Equation from reconciled data (yellow bars).

5.4 Conclusion

In this chapter data from data validation has been used to obtain the parameters of an adapted characteristic equation of a single-effect $\text{NH}_3/\text{LiNO}_3$ absorption chiller. First, the main parameters of this chiller were obtained by means of a joint data reconciliation and parameter estimation procedure. The thermodynamic model using the parameters estimated using DR is more accurate than the model using the parameters estimated without DR.

Afterwards, the measurements of all the steady state points were reconciled using the thermodynamic model. The parameters for characteristic equations have been found using just five steady-state points from both sets of untreated and reconciled data. Two pairs of adapted characteristic equations for Q_e and Q_g are obtained: one from the raw data, and another from the reconciled data.

The prediction of Q_e and COP using adapted characteristic equation with reconciled data is similar in terms of accuracy when compared with the adapted characteristic equation obtained from raw data. However, the prediction using reconciled data is much better with the adapted characteristic equation from reconciled data. The predictions using the characteristic equation from reconciled values seem to be less scattered, especially for the COP.

Nomenclature

A ,	Adapted characteristic equation parameter
CV ,	Coefficient of variation of the root-mean-square error
E ,	Adapted characteristic equation parameter
G ,	Volumetric flow rate (m^3/h)
J ,	Objective function
Q ,	Heat load (kW)
T ,	Arithmetic mean temperature
UA ,	Overall heat transfer coefficient times the heat exchanger area (kW/K)

m ,	Mass flow rate (kg/s)
r ,	Adapted characteristic equation parameter
s' ,	Adapted characteristic equation parameter
t ,	Temperature ($^{\circ}\text{C}$)
$\Delta\Delta t$	Characteristic temperature function
$\Delta\Delta t'$	Adapted characteristic temperature function

Greek letters

η ,	Effectiveness of the solution heat exchanger
σ ,	Standard deviation

Subscripts

a ,	Absorber
ac ,	Absorber and condenser
c ,	Condenser
ch ,	Chilled water circuit
cw ,	Cooling water circuit
e ,	Evaporator
g ,	Generator

Chapter 6

Conclusions and further work

6.1 Conclusions

Absorption refrigeration systems have been proved to be important within an energy efficiency framework. Nevertheless, it is still necessary to continue the research on absorption systems to overcome some barriers related to cost and performance. Not less important is the development of robust methodologies for the adequate monitoring and characterisation of these systems. The focus of this thesis is the application of a data validation procedure for obtaining reliable performance data of absorption refrigeration systems.

Data validation has been proved to be a valuable methodology for the energy analysis of absorption refrigeration systems. The methodology includes a steady-state detection step, a systematic degrees of freedom analysis, and data reconciliation including the detection of gross and systematic errors. This methodology enables important parameters, such as COP and cooling capacity, to be reliably calculated and measurements with systematic errors to be identified.

This thesis has presented an overview about the existing approaches for the steady-state modelling and simulation of absorption chillers. In order to use thermodynamic models for data reconciliation it is necessary to take into account important modelling aspects that are usually overlooked: setting adequate variables limits and guess values, performing adequate degrees of freedom analysis, selecting adequate properties correlations, etc. The use of simultaneous data reconciliation and parameter estimation techniques seems promising for its application with semi-empirical modelling of absorption refrigeration systems.

Chapter 6. Conclusions and Further Work

A combined test to detect steady-state in absorption systems has been developed. This test takes into account the possible slow drifts that occur in this kind of systems. The combined test consists in two different tests that are applied sequentially. The first test compares the standard deviation calculated in a data window with a predefined threshold. If the first test indicates steady operation, the second test is applied. In the second test a Student t-test to the difference of the means is applied following an extended period strategy. If the second test detects a change in operating conditions, then a new steady-state period with different operating conditions is defined. The effectiveness of this test is demonstrated using real absorption chiller operational data. It can be seen that the estimated uncertainties of the performance parameters (Q_e and COP) are much smaller using the combined test than using a traditional SSD method. This is very important for the data validation framework, since the measurements that will be treated in the DR step will carry a smaller standard deviation, needing smaller adjustments.

Depending on the amount of available measurements two different DR cases arise. In Case 1, the amount of measurements is enough to obtain the redundancy necessary for the resolution of the DR problem. The DR can be solved using a sequential or a direct approach. On the other hand, in Case 2, the amount of internal measurements is not enough so there is the need to estimate all or some of the absorption chiller main parameters. In this case a joint DR and parameter estimation procedure is required.

Case 1 is demonstrated by analysing the operational data of a small-capacity single-effect $\text{NH}_3/\text{H}_2\text{O}$ absorption chiller. For this example the DR problem has been solved using a sequential approach in which the reconciled values of the measurements were estimated in Matlab while the simulation that ensures that the process constraints are satisfied was carried out using EES. According to the results of this case study Q_e and COP were underestimated when raw data was used. After the final DR step, the calculated value of Q_e was, on average, 5% greater than the calculations based on raw measurements. In consequence, the COP calculated with reconciled data was also greater (0.05 in average) than when it was calculated with the raw measurements.

Case 2 is demonstrated by analysing the operational data of a large-capacity single-effect $\text{H}_2\text{O}/\text{LiBr}$ absorption chiller. Since the internal measurements are not available, a combined DR and parameter estimation procedure has been applied using GAMS. The main parameters of the absorption chiller have been estimated using three data sets. The coefficient of variation shows that model using the parameters calculated by simultaneous

data reconciliation and parameter estimation is the most accurate, especially with reconciled data.

Reconciled data can be used to characterize the performance of the absorption chiller. If the data is not reliable, the empirical models obtained as a result of this characterization are also not reliable. The DR and GED methodology presented in this study can be used to improve the reliability of the data by identifying and removing the sources of gross errors, and by obtaining calculations that are consistent with the laws of conservations.

Validated data, using the methodology proposed in this thesis, has been used to obtain the parameters of an adapted characteristic equation of a single-effect $\text{NH}_3/\text{LiNO}_3$ absorption chiller. The prediction of Q_e and COP using adapted characteristic equation with reconciled data is similar in terms of accuracy when compared with the adapted characteristic equation obtained from raw data. However, the prediction using reconciled data is much better with the adapted characteristic equation from reconciled data. The predictions using the characteristic equation from reconciled values seem to be less scattered, especially for the COP

6.2 Further work

Several aspects developed in the present thesis encourage future research topics:

- Fault detection and diagnosis techniques are very important when monitoring a system, since it allows identifying when a malfunction has occurred, which type of malfunction as well as its location. Model based fault detection can benefit from reconciled data since the measurements are used check if there is discrepancy between the read data and the expected data.
- The modelling and simulation of absorption refrigeration systems under dynamic regime is not extensively studied. Transient behaviour is important for the energy analysis of these systems because, especially in large scale systems, they present thermal inertia that can have a significant effect on the rest of components interacting with the absorption system. Adequate characterization of these inertias would be useful for the development of control strategies.
- As a consequence of dynamic modelling, dynamic data reconciliation can be an interesting and valuable tool for on-line monitoring of absorption refrigeration systems. Dynamic data reconciliation makes use, besides of the topological redundancy, of the temporal redundancy obtained of the successive measurements being analysed.

Chapter 6. Conclusions and Further Work

- The UA values are parameters which are commonly considered to be constant, but in the practice they vary with the operating conditions. It is difficult, nevertheless, to account for this variation. An interesting approach would be the use of a hybrid model consisting on the mass and energy balances, thermodynamic properties correlations, and an ANN able to learn the variation of the UA values with the operating conditions. The training of the AAN would be indirect.

Appendix A

Uncertainty Calculation

A.1 Introduction

Generally speaking, a measurement is an approximation or estimation of the real value of a determined quantity. The uncertainty of a measurement is an associated parameter that defines the range of the values that could reasonably be attributed to the measured quantity.

The uncertainty is the result random effects and is expressed as a quantity in the form of an interval about the result. It is evaluated by combining a number of uncertainty components which are quantified by evaluation several repeated measurements results, or by estimation based on historical data, knowledge about the measurement devices and experience of the measurement.

Measurements can be direct or indirect. A measurement, whose value can be obtained directly from the experimental results by means of a specific measurement device, is a direct measurement. On the other hand, a measurement whose value is obtained from direct measurements of other quantities is an indirect measurement.

A measurement can be mathematically described by:

$$y = f(x_1, x_2, \dots, x_n) \quad \text{A-1}$$

where a set of observations (x_1, x_2, \dots, x_n) are related to the resulting value of the measurement (y) .

Appendix A. Uncertainty Calculation

The combined standard uncertainty is calculated using the law of propagation of uncertainty as follows:

$$u_c(y) = \sqrt{\sum_{i=1}^n \left(\frac{\delta f}{\delta x_i} \right)^2 u^2(x_i)} = \sqrt{\sum_{i=1}^n c_i^2 u^2(x_i)} \quad \text{A-2}$$

where $u(x_i)$ is the standard uncertainty of each component and c_i is the sensitivity coefficient associated with each input estimate x_i . It is the partial derivative of the model function f with respect to x_i .

Finally, the expanded uncertainty, U , is calculated using the recommended coverage factor of $k = 2$. This value will give a coverage probability of approximately 95%, assuming a normal distribution.

$$U = k \cdot u_c(y) \quad \text{A-3}$$

A.2 Uncertainty calculation for the performance parameters of an absorption refrigeration system

The performance of absorption refrigeration systems is usually reported in terms of the cooling capacity (Q_e) and the corresponding thermal COP. These quantities are indirectly estimated from the direct measurements of temperature and flow rate.

The estimation of uncertainty was done by constructing the uncertainty budgets for each of the derived variables.

The cooling capacity is a function of the chilled water inlet and outlet temperatures ($t_{ch,in}$ and $t_{ch,out}$), the chilled water flow rate (G_{ch}), as well as the chilled water density (ρ_{ch}) and specific heat capacity (Cp_{ch}) as shown in Equation A-4. The thermodynamic properties ρ_{ch} and Cp_{ch} depend on the temperature and they have been calculated at a mean value between $t_{ch,in}$ and $t_{ch,out}$. Table A-1 shows the contribution of the different uncertainty sources to Q_e .

$$Q_e = G_{ch} \rho_{ch} Cp_{ch} (t_{ch,in} - t_{ch,out}) \quad \text{A-4}$$

Appendix A. Uncertainty Calculation

Table A-1: Uncertainty budget for Q_e

Quantity X_i	Estimate x_i	Repeatability $u_1(x_i)$	Probability distribution p_1	Accuracy $u_2(x_i)$	Probability distribution p_2	Resolution $u_3(x_i)$	Probability distribution p_3	Reference data $u_4(x_i)$	Probability distribution p_4	Sensitivity coefficient c_i	Uncertainty contribution $u_i(y_i)$
$t_{ch,in}$	Value	Std. Dev.	1	0.1	$\frac{1}{\sqrt{3}}$	0.01	$\frac{1}{2\sqrt{3}}$			$\frac{\delta Q_e}{\delta t_{ch,in}}$	$\sqrt{\sum_{i=1}^n p_i^2 u_i^2(x_i)}$
$t_{ch,out}$	Value	Std. Dev.	1	0.1	$\frac{1}{\sqrt{3}}$	0.01	$\frac{1}{2\sqrt{3}}$			$\frac{\delta Q_e}{\delta t_{ch,out}}$	$\sqrt{\sum_{i=1}^n p_i^2 u_i^2(x_i)}$
G_{ch}	Value	Std. Dev.	1	0.5% G_{ch}	$\frac{1}{\sqrt{3}}$	0.01	$\frac{1}{2\sqrt{3}}$			$\frac{\delta Q_e}{\delta G_{ch}}$	$\sqrt{\sum_{i=1}^n p_i^2 u_i^2(x_i)}$
ρ_{ch}	Value							0.001 % ρ_{ch}	$\frac{1}{\sqrt{3}}$	$\frac{\delta Q_e}{\delta \rho_{ch}}$	$\sqrt{\sum_{i=1}^n p_i^2 u_i^2(x_i)}$
Cp_{ch}	Value							0.1% Cp_{ch}	$\frac{1}{\sqrt{3}}$	$\frac{\delta Q_e}{\delta Cp_{ch}}$	$\sqrt{\sum_{i=1}^n p_i^2 u_i^2(x_i)}$
Combined Uncertainty										$u_c(y) = \sqrt{\sum_{i=1}^n c_i^2 u_i^2(y)}$	
Expanded Uncertainty										$U = k \cdot u_c(y)$	

The thermal COP is the ratio of the cooling capacity and the heat input to the generator (Q_g). Therefore, besides being function of the same quantities as Q_e , it is also function of hot water inlet and outlet temperatures ($t_{hw,in}$ and $t_{hw,out}$), the hot water flow rate (G_{hw}), as well as the hot water density (ρ_{hw}) and specific heat capacity (Cp_{hw}) as shown in Equation A-5. The thermodynamic properties ρ_{hw} and Cp_{hw} depend on the temperature and they have been calculated at a mean value between $t_{hw,in}$ and $t_{hw,out}$. Table A-2 shows the contribution of the different uncertainty sources to Q_e .

$$COP = \frac{Q_e}{Q_g} = \frac{G_{ch} \rho_{ch} Cp_{ch} (t_{ch,in} - t_{ch,out})}{G_{hw} \rho_{hw} Cp_{hw} (t_{hw,in} - t_{hw,out})} \quad A-5$$

Appendix A. Uncertainty Calculation

Table A-2: Uncertainty budget for COP

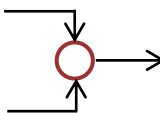
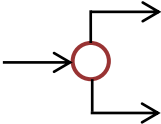

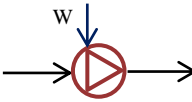
Quantity X_i	Estimate x_i	Repeatability $u_1(x_i)$	Probability distribution p_1	Accuracy $u_2(x_i)$	Probability distribution p_2	Resolution $u_3(x_i)$	Probability distribution p_3	Reference data $u_4(x_i)$	Probability distribution p_4	Sensitivity coefficient c_i	Uncertainty contribution $u_i(y_i)$
$t_{ch,in}$	Value	Std. Dev.	1	0.1	$\frac{1}{\sqrt{3}}$	0.01	$\frac{1}{2\sqrt{3}}$			$\frac{\delta COP}{\delta t_{ch,in}}$	$\sqrt{\sum_{i=1}^n p_i^2 u_i^2(x_i)}$
$t_{ch,out}$	Value	Std. Dev.	1	0.1	$\frac{1}{\sqrt{3}}$	0.01	$\frac{1}{2\sqrt{3}}$			$\frac{\delta COP}{\delta t_{ch,out}}$	$\sqrt{\sum_{i=1}^n p_i^2 u_i^2(x_i)}$
G_{ch}	Value	Std. Dev.	1	0.5% G_{ch}	$\frac{1}{\sqrt{3}}$	0.01	$\frac{1}{2\sqrt{3}}$			$\frac{\delta COP}{\delta G_{ch}}$	$\sqrt{\sum_{i=1}^n p_i^2 u_i^2(x_i)}$
ρ_{ch}	Value							0.001 % ρ_{ch}	$\frac{1}{\sqrt{3}}$	$\frac{\delta COP}{\delta \rho_{ch}}$	$\sqrt{\sum_{i=1}^n p_i^2 u_i^2(x_i)}$
Cp_{ch}	Value							0.1% Cp_{ch}	$\frac{1}{\sqrt{3}}$	$\frac{\delta COP}{\delta Cp_{ch}}$	$\sqrt{\sum_{i=1}^n p_i^2 u_i^2(x_i)}$
$t_{hw,in}$	Value	Std. Dev.	1	0.1	$\frac{1}{\sqrt{3}}$	0.01	$\frac{1}{2\sqrt{3}}$			$\frac{\delta COP}{\delta t_{hw,in}}$	$\sqrt{\sum_{i=1}^n p_i^2 u_i^2(x_i)}$
$t_{hw,out}$	Value	Std. Dev.	1	0.1	$\frac{1}{\sqrt{3}}$	0.01	$\frac{1}{2\sqrt{3}}$			$\frac{\delta COP}{\delta t_{hw,out}}$	$\sqrt{\sum_{i=1}^n p_i^2 u_i^2(x_i)}$
G_{hw}	Value	Std. Dev.	1	0.5% G_{hw}	$\frac{1}{\sqrt{3}}$	0.01	$\frac{1}{2\sqrt{3}}$			$\frac{\delta COP}{\delta G_{hw}}$	$\sqrt{\sum_{i=1}^n p_i^2 u_i^2(x_i)}$
ρ_{hw}	Value							0.001 % ρ_{hw}	$\frac{1}{\sqrt{3}}$	$\frac{\delta COP}{\delta \rho_{hw}}$	$\sqrt{\sum_{i=1}^n p_i^2 u_i^2(x_i)}$
Cp_{hw}	Value							0.1% Cp_{hw}	$\frac{1}{\sqrt{3}}$	$\frac{\delta COP}{\delta Cp_{hw}}$	$\sqrt{\sum_{i=1}^n p_i^2 u_i^2(x_i)}$
Combined Uncertainty										$u_c(y) = \sqrt{\sum_{i=1}^n c_i^2 u_i^2(y_i)}$	
Expanded Uncertainty										$U = k \cdot u_c(y)$	

Appendix B

Degrees of freedom catalogue

Ayou et al. [83] presented a systematic methodology for finding the number of degrees of freedom of absorption chillers and heat pumps. This methodology also allows identifying a set of variables appropriate to reduce the available degrees of freedom to zero. This methodology is based on summing the degrees of freedom corresponding to each of the components present in the absorption cycle under study. The tables below summarize the number of variables, relationships and degrees of freedom of the typical components found in absorption chillers and heat pumps.

Table B-1: Elements catalogue of vapour absorption cycles

Element	Streams	N_v^e	N_r^e	N_d^e
Adiabatic stream mixer		$3C + 6$	$C + 3$	$2C + 3$
Adiabatic stream splitter		$3C + 6$	$2C + 3$	$C + 3$
Expansion valve (EV)		$3C + 6$	$2C + 3$	$C + 3$
Solution pump (SP)		$2C + 5$	$C + 2$	$C + 3$

Appendix B. Degrees of Freedom Catalogue

Table B-2: Component catalogue of vapour absorption cycles

Unit	Streams	N_v^u	N_r^u	N_d^u
Absorber (A)		$5C + 17$	$C + 8$	$4C + 9$
Condenser without external (C_0)		$2C + 5$	$C + 3$	$C + 2$
Condenser with one inlet (C_1)		$2C + 11$	$C + 7$	$C + 4$
Condenser with two inputs (C_2)		$4C + 15$	$C + 8$	$3C + 7$
Condenser without external and with two inputs (C_{02})		$4C + 9$	$C + 4$	$3C + 5$
Evaporator (E)		$4C + 15$	$2C + 8$	$2C + 7$
Generator without reflux (G)		$3C + 13$	$C + 9$	$2C + 4$
Generator without external and reflux (G_0)		$3C + 7$	$C + 5$	$2(C + 1)$
Generator with reflux (G_R)		$4C + 15$	$C + 11$	$3C + 4$
Generator for parallel flow (G_p)		$6C + 13$	$3C + 6$	$3C + 7$
Solution heat exchanger (SHX)		$4C + 9$	$2C + 4$	$2C + 5$
Rectifier (R)		$3C + 13$	$2C + 8$	$C + 5$

Appendix B. Degrees of Freedom Catalogue

Table B-3: Stream legend for Tables B-1 and B2

	—————>	Liquid stream
>	Vapour stream
Stream description:	- · - · - · >	Vapour-liquid mixture stream
	—————>	Energy (heat) stream
	—————>	Energy (work) stream

The degrees of freedom are then determined using the catalogue. To use this method only the schematic of the cycle configuration and the number of components in the working fluid mixture are required. The number of degrees of freedom of a complete absorption cycle is calculated as:

$$N_d = (N_{vt} + C) - [N_{rt} + n_c(C + 2) + N_{ih}] \quad \text{B-1}$$

where the total number of variables N_{vt} is:

$$N_{vt} = \sum (N_v^e + N_v^u) \quad \text{B-2}$$

the total number of independent restrictions N_{rt} is:

$$N_{rt} = \sum (N_r^e + N_r^u) \quad \text{B-3}$$

n_c is the number of single-phase interconnecting mass streams in the cycle; N_{ih} is the number of internal heat coupling (for multi-effect cycles); and C is the number of components in the working fluid mixture.

References

1. *BP Statistical Review of World Energy 2013*.
2. Coulomb D., *Refrigeration Main Challenges*. Industria & Formazione, International Special Issue 2012-2013. p. 4-7.
3. Herold K., Radermacher R., Klein S.A. *Absorption Chillers and Heat Pumps*. 1996. CRC Press.
4. Brown C.M., Nuorti P.J., Breiman R.F., Hathcock A.L., Fields B.S., Lipman H.B., Llewellyn G.C., Hofmann J., Cetron M. *A community outbreak of Legionnaires' disease linked to hospital cooling towers: An epidemiological method to calculate dose of exposure*. International Journal of Epidemiology, 1999. **28**(2): p. 353-359.
5. Balamuru V.G., Ibrahim O.M., Barnett S.M., *Simulation of ternary ammonia-water-salt absorption refrigeration cycles*. International Journal of Refrigeration, 2000. **23**(1): p. 31-42.
6. Steiu S., Martínez-Maradiaga D., Salavera D., Bruno J.C, Coronas A. *Effect of alkaline hydroxides on the vapor-liquid equilibrium of ammonia/water and the performance of absorption chillers*. Industrial and Engineering Chemistry Research, 2011. **50**(23): p. 13037-13044.
7. Steiu S., Salavera D., Bruno J.C, Coronas A, *A basis for the development of new ammonia-water-sodium hydroxide absorption chillers*. International Journal of Refrigeration, 2009. **32**(4): p. 577-587.
8. Sun J., Fu L., Zhang S., *A review of working fluids of absorption cycles*. Renewable and Sustainable Energy Reviews, 2012. **16**(4): p. 1899-1906.
9. Balaras C.A., Grossman G., Henning H.-M., Infante Ferreira C.A., Podesser E., Wang L., Wiemken E. *Solar air conditioning in Europe-an overview*. Renewable and Sustainable Energy Reviews, 2007. **11**(2): p. 299-314.
10. Srihirin P., Aphornratana S., Chungpaibulpatana S. *A review of absorption refrigeration technologies*. Renewable and Sustainable Energy Reviews, 2001. **5**(4): p. 343-372.
11. Ortiga J., Bruno J.C., Coronas A. *Operational optimisation of a complex trigeneration system connected to a district heating and cooling network*. Applied Thermal Engineering, 2013. **50**(2): p. 1536-1542.

12. PolicCity, <http://www.polycity.net/en/index.html>.
13. Bruno J.C., Martínez-Maradiaga D., Rodríguez J., Coronas A. *Refrigeration using recovered waste heat in fishing vessels: Potential application and case study*, in 2nd European Conference on Polygeneration 2011 Tarragona, Spain
14. Ullah K.R., Saidur R., Ping H.W., Akikur R.K., Shuvo N.H. *A review of solar thermal refrigeration and cooling methods*. Renewable and Sustainable Energy Reviews, 2013. **24**: p. 499-513.
15. Mazloumi M., Naghashzadegan M., Javaherdeh K. *Simulation of solar lithium bromide-water absorption cooling system with parabolic trough collector*. Energy Conversion and Management, 2008. **49**(10): p. 2820-2832.
16. Infante-Ferreira C., *Advancement in solar cooling*, in International Sorption Heat Pump Conference (ISHPC11). 2011: Padua, Italy. p. 23-46.
17. Kalinowski P, Hwang Y., Radermacher R., Al Hashimi S., Rodgers, P. *Application of waste heat powered absorption refrigeration system to the LNG recovery process*. International Journal of Refrigeration, 2009. **32**(4): p. 687-694.
18. Costa A., Bakhtiari B., Schuster S., Paris J. *Integration of absorption heat pumps in a Kraft pulp process for enhanced energy efficiency*. Energy, 2009. **34**(3): p. 254-260.
19. Crowe C.M. *Data reconciliation - Progress and challenges*. Journal of Process Control, 1996. **6**(2-3): p. 89-98.
20. Romagnoli J.A., Sánchez M.C. *Data Processing and Reconciliation for Chemical Process Operations*. 2000, Academic Press Inc., San Diego, California, USA.
21. Narasimhan S., Jordache C. *Data Reconciliation & Gross Error Detection*. 2000, Gulf Publishing Company, Houston, Texas.
22. Meyer M., Koehret B., Enjalbert M. *Data reconciliation on multicomponent network process*. Computers & Chemical Engineering, 1993. **17**(8): p. 807-817.
23. Stanley G.M., Mah R.S.H. *Observability and redundancy classification in process networks – Theorems and algorithms*. Chemical Engineering Science, 1981. **36**(12): p. 1941-1954.
24. Stanley G.M., Mah R.S.H. *Observability and redundancy in process data estimation*. Chemical Engineering Science, 1981. **36**(2): p. 259-272.
25. Kretsovalis A., Mah R.S.H. *Observability and redundancy classification in multicomponent process networks*. Aiche Journal, 1987. **33**(1): p. 70-82.
26. Kretsovalis A., Mah R.S.H. *Observability and redundancy classification in generalized process networks. 1. Theorems*. Computers & Chemical Engineering, 1988. **12**(7): p. 671-687.
27. Kretsovalis A., Mah R.S.H. *Observability and redundancy classification in generalized process networks. 2. Algorithms*. Computers & Chemical Engineering, 1988. **12**(7): p. 689-703.
28. Ponzoni I., Vazquez G.E., Sanchez M.C. Brignole M.B. *Parallel observability analysis on networks of workstations*. Computers & Chemical Engineering, 2001. **25**(7-8): p. 997-1002.

29. Crowe C.M. *Observability and redundancy of process data for steady-state reconciliation*. Chemical Engineering Science, 1989. **44**(12): p. 2909-2917.
30. Albuquerque J.S., Biegler L.T. *Data reconciliation and gross-error detection for dynamic systems*. Aiche Journal, 1996. **42**(10): p. 2841-2856.
31. Kelly J.D. *On finding the matrix projection in the data reconciliation solution*. Computers & Chemical Engineering, 1998. **22**(11): p. 1553-1557.
32. Sanchez M., Bandoni A., Romagnoli, J. *PLADAT - A package for process variable classification and plant-data reconciliation*. Computers & Chemical Engineering, 1992. **16**: p. S499-S506.
33. Ponzoni I., Sanchez M.C., Brignole N.B. *A new structural algorithm for observability classification*. Industrial & Engineering Chemistry Research, 1999. **38**(8): p. 3027-3035.
34. Ponzoni I., Sanchez M.C., Brignole N.B. *Direct method for structural observability analysis*. Industrial & Engineering Chemistry Research, 2004. **43**(2): p. 577-588.
35. Heenan W.A., Serth R.W. *Detectin errors in process data*. Chemical Engineering 1986. **93**(21): p. 99-103.
36. Serth R.W., Heenan W.A. *Gross-error detection and data reconciliation in steam-metering systems*. Aiche Journal, 1986. **32**(5): p. 733-742.
37. Martinez-Prata D., Schwaab M., Luis Lima E., Carlos Pinto J. *Simultaneous robust data reconciliation and gross error detection through particle swarm optimization for an industrial polypropylene reactor*. Chemical Engineering Science, 2010. **65**(17): p. 4943-4954.
38. Tjoa I.B., Biegler L.T. *Simultaneous strategies for data reconciliation and gorss-error detection of nonlinear-systems*. Computers & Chemical Engineering, 1991. **15**(10): p. 679-690.
39. Wang D., Romagnoli J.A. *A framework for robust data reconciliation based on a generalized objective function*. Industrial & Engineering Chemistry Research, 2003. **42**(13): p. 3075-3084.
40. Zhang Z., Shao Z., Chen X., Wang K., Qian J. *Quasi-weighted least squares estimator for data reconciliation*. Computers and Chemical Engineering, 2010. **34**(2): p. 154-162.
41. Ozyurt D.B., Pike R.W. *Theory and practice of simultaneous data reconciliation and gross error detection for chemical processes*. Computers & Chemical Engineering, 2004. **28**(3): p. 381-402.
42. Bruno J.C., Romera S., Figueredo G., Coronas A. *Hybrid solar/gas single/double effect absorption chiller: operational results using data reconciliation*. in 2nd International Conference on Solar Air-Conditioning. 2007. Tarragona, Spain.
43. Ngouateu Wouagfack P.A., Tchinda R. *Finite-time thermodynamics optimization of absorption refrigeration systems: A review*. Renewable and Sustainable Energy Reviews, 2013. **21**: p. 524-536.
44. Feidt, M. *Evolution of thermodynamic modelling for three and four heat reservoirs reverse cycle machines: A review and new trends*. International Journal of Refrigeration, 2013. **36**(1): p. 8-23.

45. Anand S., Gupta A., Tyagi S.K. *Simulation studies of refrigeration cycles: A review*. Renewable and Sustainable Energy Reviews, 2013. **17**: p. 260-277.
46. Mohanraj M., Jayaraj S., Muraleedharan C. *Applications of artificial neural networks for refrigeration, air-conditioning and heat pump systems - A review*. Renewable and Sustainable Energy Reviews, 2012. **16**(2): p. 1340-1358.
47. Le Lostec B., Millette J., Galanis, N. *Finite time thermodynamics study and exergetic analysis of ammonia-water absorption systems*. International Journal of Thermal Sciences, 2010. **49**(7): p. 1264-1276.
48. Ng K.C., Chua H.T., Han Q.A., Kashiwagi T., Akisawa A., Tsurusawa T. *Thermodynamic modeling of absorption chiller and comparison with experiments*. Heat Transfer Engineering, 1999. **20**(2): p. 42-51.
49. Chen J., Yan Z. *Equivalent combined systems of three-heat-source heat pumps*. The Journal of Chemical Physics, 1989. **90**(9): p. 4951-4955.
50. Wijesundera N.E., *Analysis of the ideal absorption cycle with external heat-transfer irreversibilities*. Energy, 1995. **20**(2): p. 123-130.
51. Wijesundera N.E., *Performance limits of absorption cycles with external heat-transfer irreversibilities*. Applied Thermal Engineering, 1996. **16**(2): p. 175-181.
52. Hellmann H.M., *Carnot-COP for sorption heat pumps working between four temperature levels*. International Journal of Refrigeration, 2002. **25**(1): p. 66-74.
53. Chen L., Zheng T., Sun F., Wu C. *Optimal cooling load and COP relationship of a four-heat-reservoir endoreversible absorption refrigeration cycle*. Entropy, 2004. **6**(3): p. 316-326.
54. Zheng T., Chen L., Sun F., Wu C. *The influence of heat resistance and heat leak on the performance of a four-heat-reservoir absorption refrigerator with heat transfer law of $Q \propto \Delta(T-I)$* . International Journal of Thermal Sciences, 2004. **43**(12): p. 1187-1195.
55. Qin X., Chen L., Sun F., Wu C. *Performance of an endoreversible four-heat-reservoir absorption heat pump with a generalized heat transfer law*. International Journal of Thermal Sciences, 2006. **45**(6): p. 627-633.
56. Qin X., Chen L., Sun F., Wu C. *Thermo-economic optimization of an endoreversible four-heat-reservoir absorption-refrigerator*. Applied Energy, 2005. **81**(4): p. 420-433.
57. Ng K.C., Chua H.T., Han Q., *On the modeling of absorption chillers with external and internal irreversibilities*. Applied Thermal Engineering, 1997. **17**(5): p. 413-425.
58. Zheng T., Chen L., Sun F., Wu C. *Performance optimization of an irreversible four-heat-reservoir absorption refrigerator*. Applied Energy, 2003. **76**(4): p. 391-414.
59. Chen L., Zheng T., Sun F., Wu C. *Irreversible four-temperature-level absorption refrigerator*. Solar Energy, 2006. **80**(3): p. 347-360.
60. Huang Y., Sun D., Kang Y. *Performance optimization for an irreversible four-temperature-level absorption heat pump*. International Journal of Thermal Sciences, 2008. **47**(4): p. 479-485.

61. Wijesundera N.E., *Performance of three-heat-reservoir absorption cycles with external and internal irreversibilities*. Applied Thermal Engineering, 1997. **17**(12): p. 1151-1161.
62. Ng K.C., Tu K. Chua H.T., Gordon J.M., Kashiwagi T., Akisawa A., Saha B.B. *Thermodynamic analysis of absorption chillers: Internal dissipation and process average temperature*. Applied Thermal Engineering, 1998. **18**(8): p. 671-682.
63. Chua H.T., Toh H.K., Malek A., Ng K.C. *A general thermodynamic framework for understanding the behaviour of absorption chillers*. International Journal of Refrigeration-Revue Internationale Du Froid, 2000. **23**(7): p. 491-507.
64. Chua H.T., Toh H.K., Ng K.C. *Thermodynamic modeling of an ammonia-water absorption chiller*. International Journal of Refrigeration-Revue Internationale Du Froid, 2002. **25**(7): p. 896-906.
65. McNeely L.A., *Thermodynamic properties of aqueous solutions of lithium bromide*. ASHRAE Trans, 1979. **85**(pt 1): p. 413-434.
66. Herold K.E., Moran M.J. *Thermodynamic properties of lithium bromide/water solutions*. ASHRAE Trans, 1987. **93**(pt 1): p. 35-48
67. Chua H.T., Toh H.K., Malek A., Ng K.C, Srinivasan K. *Improved thermodynamic property fields of LiBr-H₂O solution*. International Journal of Refrigeration-Revue Internationale Du Froid, 2000. **23**(6): p. 412-429.
68. Kaita Y. *Thermodynamic properties of lithium bromide-water solutions at high temperatures*. International Journal of Refrigeration, 2001. **24**(5): p. 374-390.
69. Kim D.S., Infante-Ferreira C.A. *A Gibbs energy equation for LiBr aqueous solutions*. International Journal of Refrigeration, 2006. **29**(1): p. 36-46.
70. Patek J., Klomfar J. *A computationally effective formulation of the thermodynamic properties of LiBr-H₂O solutions from 273 to 500 K over full composition range*. International Journal of Refrigeration-Revue Internationale Du Froid, 2006. **29**(4): p. 566-578.
71. Ziegler B., Trepp C. *Equation of state for ammonia-water mixtures*. International Journal of Refrigeration, 1984. **7**(2): p. 101-106.
72. Stecco S.S., Desideri U. *A thermodynamic analysis of the Kalina cycles: comparisons, problems and perspectives.*, in 34th ASME International Gas Turbine and Aeroengine Congress and Exposition. 1989: Toronto, Canada.
73. Pátek J., Klomfar J. *Simple functions for fast calculations of selected thermodynamic properties of the ammonia-water system*. International Journal of Refrigeration, 1995. **18**(4): p. 228-234.
74. Tillner-Roth R., Friend D.G. *A Helmholtz free energy formulation of the thermodynamic properties of the mixture {water + ammonia}*. Journal of Physical and Chemical Reference Data, 1998. **27**(1): p. 63-77.
75. Tillner-Roth R., Friend D.G. *Survey and assessment of available measurements on thermodynamic properties of the mixture {water+ammonia}*. Journal of Physical and Chemical Reference Data, 1998. **27**(1): p. 45-61.
76. Ayou D.S., Bruno J.C., Coronas A. *An overview of combined absorption power and cooling cycles*. Renewable and Sustainable Energy Reviews, 2013. **21**: p. 728-748.

77. El-Sayed Y.M., Tribus M.. *Thermodynamic properties of water-ammonia mixtures. Theoretical implementation for use in power cycles analysis*. Winter Annual Meeting of the American Society of Mechanical Engineers 1985. Miami, Florida, USA.
78. Smolen T.M., Manley D.B., Poling B.E. *Vapor-liquid equilibrium data for the NH₃-H₂O system and its description with a modified cubic equation of state*. Journal of Chemical and Engineering Data, 1991. **36**(2): p. 202-208.
79. Moshfeghian M., Shariat A., Maddox R.N. *Prediction of refrigerant thermodynamic properties by equations of state: vapor liquid equilibrium behavior of binary mixtures*. Fluid Phase Equilibria, 1992. **80**(C): p. 33-44.
80. Ibrahim O.M., Klein S.A. *Thermodynamic properties of ammonia-water mixtures*. 1993.
81. Xu F., Goswami D.Y. *Thermodynamic properties of ammonia-water mixtures for power-cycle applications*. Energy, 1999. **24**(6): p. 525-536.
82. Thorin E., *Comparison of correlations for predicting thermodynamic properties of ammonia-water mixtures*. International Journal of Thermophysics, 2000. **21**(4): p. 853-870.
83. Ayoub D.S., Bruno J.C., Coronas, A. *Steady-state operational degrees of freedom in absorption chillers and heat pumps: Methodology and case study*. International Journal of Refrigeration, 2012. **35**(6): p. 1570-1582.
84. Sathyabhama A., Babu T.P.A. *Thermodynamic simulation of ammonia-water absorption refrigeration system*. Thermal Science, 2008. **12**(3): p. 45-53.
85. Gomri R., Hakimi R., *Second law analysis of double effect vapour absorption cooler system*. Energy Conversion and Management, 2008. **49**(11): p. 3343-3348.
86. Bakhtiari B., Fradette L., Legros R., Paris J. *A model for analysis and design of H₂O-LiBr absorption heat pumps*. Energy Conversion and Management, 2011. **52**(2): p. 1439-1448.
87. Ahmed M.S.A.M.S., Gilani S.I.U. *Steady state simulation of a double-effect steam absorption chiller*. Journal of Applied Sciences, 2011. **11**(11): p. 2018-2023.
88. Wang L., Chen G.M., Wang Q., Zhong M. *Thermodynamic performance analysis of gas-fired air-cooled adiabatic absorption refrigeration systems*. Applied Thermal Engineering, 2007. **27**(8-9): p. 1642-1652.
89. *EES, Engineering Equation Solver*. F-Chart Software, <http://www.fchart.com/ees/>
90. Adewusi S.A., Zubair S.M. *Second law based thermodynamic analysis of ammonia-water absorption systems*. Energy Conversion and Management, 2004. **45**(15-16): p. 2355-2369.
91. Yin H., Qu M., Archer D.H. *Model based experimental performance analysis of a microscale LiBr-H₂O steam-driven double-effect absorption Chiller*. Applied Thermal Engineering, 2010. **30**(13): p. 1741-1750.
92. Arora A., Kaushik S.C. *Theoretical analysis of LiBr/H₂O absorption refrigeration systems*. International Journal of Energy Research, 2009. **33**(15): p. 1321-1340.

93. Garousi Farshi L., Seyed Mahmoudi S.M., Rosen M.A., Yari M. *A comparative study of the performance characteristics of double-effect absorption refrigeration systems*. International Journal of Energy Research, 2012. **36**(2): p. 182-192.
94. Iranmanesh A., Mehrabian M.A., *Thermodynamic modelling of a double-effect LiBr-H₂O absorption refrigeration cycle*. Heat and Mass Transfer/Waerme- und Stoffuebertragung, 2012. **48**(12): p. 2113-2123.
95. Grossman G., Zaltash A., *ABSIM - modular simulation of advanced absorption systems*. International Journal of Refrigeration-Revue Internationale Du Froid, 2001. **24**(6): p. 531-543.
96. Park C.W., Jeong J.H., Kang Y.T., *Energy consumption characteristics of an absorption chiller during the partial load operation*. International Journal of Refrigeration, 2004. **27**(8): p. 948-954.
97. Darwish N.A., Al-Hashimi S.H., Al-Mansoori A.S. *Performance analysis and evaluation of a commercial absorption-refrigeration water-ammonia (ARWA) system*. International Journal of Refrigeration-Revue Internationale Du Froid, 2008. **31**(7): p. 1214-1223.
98. Somers C., Mortazavi A., Hwang Y., Radermacher R., Rodgers P., Al-Hashimi S. *Modeling water/lithium bromide absorption chillers in ASPEN Plus*. Applied Energy, 2011. **88**(11): p. 4197-4205.
99. Brunet R., Reyes-Labarta J.A., Guillén-Gosálbez G., Jiménez L., Boer D. *Combined simulation-optimization methodology for the design of environmental conscious absorption systems*. Computers and Chemical Engineering, 2012. **46**: p. 205-216.
100. Martins L.N., Fábrega F.M., d'Angelo J.V.H. *Thermodynamic Performance Investigation of a Trigeration Cycle Considering the Influence of Operational Variables*. Procedia Engineering, 2012. **42**(0): p. 1879-1888.
101. Manohar H.J., Saravanan R., Renganarayanan S. *Modelling of steam fired double effect vapour absorption chiller using neural network*. Energy Conversion and Management, 2006. **47**(15-16): p. 2202-2210.
102. Şencan A. *Performance of ammonia-water refrigeration systems using artificial neural networks*. Renewable Energy, 2007. **32**(2): p. 314-328.
103. Rosiek S., Batlles F.J. *Modelling a solar-assisted air-conditioning system installed in CIESOL building using an artificial neural network*. Renewable Energy, 2010. **35**(12): p. 2894-2901.
104. Sözen A., Arcaklioğlu E. *Exergy analysis of an ejector-absorption heat transformer using artificial neural network approach*. Applied Thermal Engineering, 2007. **27**(2-3): p. 481-491.
105. Chow T.T., Zhang G.Q., Lin Z., Song C. L. *Global optimization of absorption chiller system by genetic algorithm and neural network*. Energy and Buildings, 2002. **34**(1): p. 103-109.
106. Labus J., Hernández, J.A. Bruno, J.C., Coronas A. *Inverse neural network based control strategy for absorption chillers*. Renewable Energy, 2012. **39**(1): p. 471-482.

107. Kim M., Yoon S.H., Payne W.V., Domanski P.A. *Development of the reference model for a residential heat pump system for cooling mode fault detection and diagnosis*. Journal of Mechanical Science and Technology, 2010. **24**(7): p. 1481-1489.
108. Martínez P.J., Pinazo J.M. *A method for design analysis of absorption machines*. International Journal of Refrigeration, 2002. **25**(5): p. 634-639.
109. Martínez P.J., Pinazo J.M. *A method for obtaining performance correlations of absorption machines*. International Journal of Thermal Sciences, 2003. **42**(4): p. 379-384.
110. Şencan A. *Artificial intelligent methods for thermodynamic evaluation of ammonia-water refrigeration systems*. Energy Conversion and Management, 2006. **47**(18-19): p. 3319-3332.
111. Şencan A., Kızılkın O., Bezir N.Ç., Kalogirou S.A. *Different methods for modeling absorption heat transformer powered by solar pond*. Energy Conversion and Management, 2007. **48**(3): p. 724-735.
112. Gordon J.M., Ng K.C. *A general thermodynamic model for absorption chiller – Theory and experiment*. Heat Recovery Systems & Chp, 1995. **15**(1): p. 73-83.
113. Gordon J.M., Ng K.C. *Predictive and diagnostic aspects of a universal thermodynamic model for chillers*. International Journal of Heat and Mass Transfer, 1995. **38**(5): p. 807-818.
114. Hellmann H.-M., Schweigler C., Ziegler F. *The characteristic equations of absorption chillers*. in Proceedings of the International Sorption Heat Pump Conference. 1999. Munich, Germany.
115. Ziegler F., Hellmann H.-M., Schweigler C. *An approximative method for modelling the operating characteristics of advanced absorption chillers*. in 20th International Congress of Refrigeration. IIR/IIF 1999. Sidney, Australia.
116. Kühn A., Ziegler F. *Operational results of a 10 kW absorption chiller and adaptation of the characteristic equation*. in International Conference Solar Air Conditioning, 2005. Bad-Staffelstein, Germany.
117. Lecuona, A., Ventas, R., Venegas, M., Zacarías, A., Salgado, R. *Optimum hot water temperature for absorption solar cooling*. Solar Energy, 2009. **83**(10): p. 1806-1814.
118. Puig-Arnabat M., López-Villada J., Bruno J.C., Coronas A., *Analysis and parameter identification for characteristic equations of single- and double-effect absorption chillers by means of multivariable regression*. International Journal of Refrigeration, 2010. **33**(1): p. 70-78.
119. Gutiérrez-Urueta G., Rodríguez P., Ziegler F., Lecuona A., Rodríguez-Hidalgo M.C. *Extension of the characteristic equation to absorption chillers with adiabatic absorbers*. International Journal of Refrigeration, 2012. **35**(3): p. 709-718.
120. Jakob U., Eicker U., Schneider D., Taki A.H., Cook M.J. *Simulation and experimental investigation into diffusion absorption cooling machines for air-conditioning applications*. Applied Thermal Engineering, 2008. **28**(10): p. 1138-1150.

121. Kim D.S., Infante-Ferreira C.A., *Analytic modelling of steady state single-effect absorption cycles*. International Journal of Refrigeration-Revue Internationale Du Froid, 2008. **31**(6): p. 1012-1020.
122. Marc O., Anies G., Lucas F., Castaing-Lasvignottes J. *Assessing performance and controlling operating conditions of a solar driven absorption chiller using simplified numerical models*. Solar Energy, 2012. **86**(9): p. 2231-2239.
123. Sözen A., Arcaklioğlu E., Özalp M. *A new approach to thermodynamic analysis of ejector-absorption cycle: Artificial neural networks*. Applied Thermal Engineering, 2003. **23**(8): p. 937-952.
124. Sözen A., Arcaklioglu E., Özalp M. *Performance analysis of ejector absorption heat pump using ozone safe fluid couple through artificial neural networks*. Energy Conversion and Management, 2004. **45**(13-14): p. 2233-2253.
125. Sözen A., Özalp M., Arcaklioğlu E. *Investigation of thermodynamic properties of refrigerant/absorbent couples using artificial neural networks*. Chemical Engineering and Processing: Process Intensification, 2004. **43**(10): p. 1253-1264.
126. Sözen A., Arcaklioğlu E., Özalp M. *Formulation based on artificial neural network of thermodynamic properties of ozone friendly refrigerant/absorbent couples*. Applied Thermal Engineering, 2005. **25**(11-12): p. 1808-1820.
127. Sencan A., Yakut K.A., Kalogirou S.A. *Thermodynamic analysis of absorption systems using artificial neural network*. Renewable Energy, 2006. **31**(1): p. 29-43.
128. Singh D.V., Maheshwari G. *Energy analysis of single-stage LiBr-water vapour absorption refrigeration system using artificial neural network approach*. International Journal of Ambient Energy, 2011. **32**(4): p. 194-202.
129. Labus J., Bruno J.C., Coronas A. *Performance analysis of small capacity absorption chillers by using different modeling methods*. Applied Thermal Engineering, 2013. **58**(1-2): p. 305-313.
130. Lazzarin R.M., Gasparella A., Longo G.A. *Ammonia-water absorption machines for refrigeration: Theoretical and real performances*. International Journal of Refrigeration-Revue Internationale Du Froid, 1996. **19**(4): p. 239-246.
131. Xu G.P., Dai Y.Q., Tou K.W., Tso C.P. *Theoretical analysis and optimization of a double-effect series-flow-type absorption chiller*. Applied Thermal Engineering, 1996. **16**(12): p. 975-987.
132. Kaynakli O., Kilic M. *Theoretical study on the effect of operating conditions on performance of absorption refrigeration system*. Energy Conversion and Management, 2007. **48**(2): p. 599-607.
133. Fernández-Seara J., Sieres J. *The importance of the ammonia purification process in ammonia-water absorption systems*. Energy Conversion and Management, 2006. **47**(13-14): p. 1975-1987.
134. Gomri R. *Second law comparison of single effect and double effect vapour absorption refrigeration systems*. Energy Conversion and Management, 2009. **50**(5): p. 1279-1287.
135. Kaushik S.C. Arora A. *Energy and exergy analysis of single effect and series flow double effect water-lithium bromide absorption refrigeration systems*. International Journal of Refrigeration, 2009. **32**(6): p. 1247-1258.

136. Gebreslassie B.H., Medrano M., Boer D. *Exergy analysis of multi-effect water-LiBr absorption systems: From half to triple effect*. Renewable Energy, 2010. **35**(8): p. 1773-1782.
137. Ahmed M.S.A.M.S., Ul-Haq Gilani S.I. *Exergy analysis of a double-effect parallel-flow commercial steam absorption chiller*. Journal of Applied Sciences, 2012. **12**(24): p. 2580-2585.
138. Garousi Farshi L., Mahmoudi S.M.S, Rosen M.A., Yari M, Amidpour M. *Exergoeconomic analysis of double effect absorption refrigeration systems*. Energy Conversion and Management, 2013. **65**: p. 13-25.
139. Garousi Farshi L., Mahmoudi S.M.S., Rosen M.A. *Exergoeconomic comparison of double effect and combined ejector-double effect absorption refrigeration systems*. Applied Energy, 2013. **103**: p. 700-711.
140. Sözen A. *Effect of heat exchangers on performance of absorption refrigeration systems*. Energy Conversion and Management, 2001. **42**(14): p. 1699-1716.
141. Ezzine N.B., Barhoumi M., Mejbri Kh., Chemkhi S., Bellagi A. *Solar cooling with the absorption principle: First and Second Law analysis of an ammonia - Water double-generator absorption chiller*. Desalination, 2004. **168**(1-3): p. 137-144.
142. Lin P., Wang R.Z., Xia Z.Z. *Numerical investigation of a two-stage air-cooled absorption refrigeration system for solar cooling: Cycle analysis and absorption cooling performances*. Renewable Energy, 2011. **36**(5): p. 1401-1412.
143. Garousi Farshi L., Seyed Mahmoudi S.M., Rosen M.A. *Analysis of crystallization risk in double effect absorption refrigeration systems*. Applied Thermal Engineering, 2011. **31**(10): p. 1712-1717.
144. Mehr A.S., Yari M., Mahmoudi S.M.S, Soroureddin A. *A comparative study on the GAX based absorption refrigeration systems: SGAX, GAXH and GAX-E*. Applied Thermal Engineering, 2012. **44**: p. 29-38.
145. Figueredo G.R., Bourouis M., Coronas A. *Thermodynamic modelling of a two-stage absorption chiller driven at two-temperature levels*. Applied Thermal Engineering, 2008. **28**(2-3): p. 211-217.
146. Rameshkumar A., Udayakumar M., Saravanan R. *Heat transfer studies on a GAXAC (generator-absorber-exchange absorption compression) cooler*. Applied Energy, 2009. **86**(10): p. 2056-2064.
147. Ventas R., Lecuona A., Zacarías A., Venegas M. *Ammonia-lithium nitrate absorption chiller with an integrated low-pressure compression booster cycle for low driving temperatures*. Applied Thermal Engineering, 2010. **30**(11-12): p. 1351-1359.
148. Vereda C., Ventas R., Lecuona A., Venegas M. *Study of an ejector-absorption refrigeration cycle with an adaptable ejector nozzle for different working conditions*. Applied Energy, 2012. **97**: p. 305-312.
149. Yari M., Zarin A., Mahmoudi S.M.S. *Energy and exergy analyses of GAX and GAX hybrid absorption refrigeration cycles*. Renewable Energy, 2011. **36**(7): p. 2011-2020.

150. Bruno J.C., Miquel J., Castells F. *Modeling of ammonia absorption chillers integration in energy systems of process plants*. Applied Thermal Engineering, 1999. **19**(12): p. 1297-1328.
151. Gomri R. *Simulation study on the performance of solar/natural gas absorption cooling chillers*. Energy Conversion and Management, 2013. **65**: p. 675-681.
152. Atmaca I., Yigit A. *Simulation of solar-powered absorption cooling system*. Renewable Energy, 2003. **28**(8): p. 1277-1293.
153. Karno A., Ajib S. *Thermodynamic analysis of an absorption refrigeration machine with new working fluid for solar applications*. Heat and Mass Transfer/Waerme- und Stoffuebertragung, 2008. **45**(1): p. 71-81.
154. Zhang X., Hu D. *Performance simulation of the absorption chiller using water and ionic liquid 1-ethyl-3-methylimidazolium dimethylphosphate as the working pair*. Applied Thermal Engineering, 2011. **31**(16): p. 3316-3321.
155. Dong L., Zheng D., Nie N., Li Y. *Performance prediction of absorption refrigeration cycle based on the measurements of vapor pressure and heat capacity of H₂O+[DMIM]DMP system*. Applied Energy, 2012. **98**: p. 326-332.
156. Chekir N., Bellagi A. *Performance improvement of a butane/octane absorption chiller*. Energy, 2011. **36**(10): p. 6278-6284.
157. Bulgan A.T. *Optimization of the thermodynamic model of aqua-ammonia absorption refrigeration systems*. Energy Conversion and Management, 1995. **36**(2): p. 135-143.
158. Fernandez-Seara J., Vazquez M. *Study and control of the optimal generation temperature in NH₃-H₂O absorption refrigeration systems*. Applied Thermal Engineering, 2001. **21**(3): p. 343-357.
159. Chávez-Islands L.M., Heard C.L. *Design and analysis of an ammonia/water absorption refrigeration cycle by means of an equation-oriented method*. Industrial and Engineering Chemistry Research, 2009. **48**(4): p. 1944-1956.
160. Chávez-Islands L.M., Heard C.L. *Optimization of a simple ammonia-water absorption refrigeration cycle by application of mixed-integer nonlinear programming*. Industrial and Engineering Chemistry Research, 2009. **48**(4): p. 1957-1962.
161. Gebreslassie B.H., Guillén-Gosálbez G, Jiménez L., Boer, D. *Design of environmentally conscious absorption cooling systems via multi-objective optimization and life cycle assessment*. Applied Energy, 2009. **86**(9): p. 1712-1722.
162. Gebreslassie B.H., Guillén-Gosálbez G, Jiménez L., Boer, D. *A systematic tool for the minimization of the life cycle impact of solar assisted absorption cooling systems*. Energy, 2010. **35**(9): p. 3849-3862.
163. Gebreslassie B.H., Guillén-Gosálbez G, Jiménez L., Boer, D. *Solar assisted absorption cooling cycles for reduction of global warming: A multi-objective optimization approach*. Solar Energy, 2012. **86**(7): p. 2083-2094.
164. Marcos J.D., Izquierdo M., Palacios E. *New method for COP optimization in water- and air-cooled single and double effect LiBr-water absorption machines*. International Journal of Refrigeration, 2011. **34**(6): p. 1348-1359.

165. Rubio-Maya C., Pacheco-Ibarra J.J., Belman-Flores J.M., Galván-González S.R., Mendoza-Covarrubias C. *NLP model of a LiBr-H₂O absorption refrigeration system for the minimization of the annual operating cost*. Applied Thermal Engineering, 2012. **37**: p. 10-18.
166. Pettersson F. *Heat exchanger network design using geometric mean temperature difference*. Computers and Chemical Engineering, 2008. **32**(8): p. 1726-1734.
167. Chen J.J.J. *Comments on improvements on a replacement for the logarithmic mean*. Chemical Engineering Science, 1987. **42**(10): p. 2488-2489.
168. Poulin É., Hodouin D., Lachance L. *Impact of plant dynamics on the performance of steady-state data reconciliation*. Computers & Chemical Engineering, 2010. **34**(3): p. 354-360.
169. Almassy G.A., Mah R.S.H. *Estimation of measurement error variances from process data*. Industrial & Engineering Chemistry Process Design and Development, 1984. **23**(4): p. 779-784.
170. Narasimhan S., Mah R.S.H., Tamhane A.C., Woodward J.W., Hale J.C. *A Composite Statistical Test for Detecting Changes of Steady States*. AIChE Journal, 1986. **32** (9): p. 1409-1418
171. Narasimhan S., Kao C.S., Mah R.S.H. *Detecting chances of steady states using the mathematical theory of evidence*. AIChE Journal, 1987. **33**(11): p. 1930-1932.
172. Cao S., Rhinehart R.R. *An efficient method for on-line identification of steady state*. Journal of Process Control, 1995. **5**(6): p. 363-374.
173. Siyi J., Chuanguang Z., Wen Z., Chaohe Y., *Detecting changes of process steady states using the period extending strategy*. Computer Aided Chemical Engineering, 2003. **15**: p. 858-863.
174. Önöz B., Bayazit M. *The power of statistical tests for trend detection*. Turkish Journal of Engineering and Environmental Sciences, 2003. **27**(4): p. 247-251.
175. Bendat J.S., Piersol A.G. *Random Data: Analysis and Measurement Procedures*, Wiley John and Sons. 2000.
176. Jiang T., Chen B., He X., Stuart P. *Application of steady-state detection method based on wavelet transform*. Computers & Chemical Engineering, 2003. **27**(4): p. 569-578.
177. Kim M., Yoon S.H., Domanski P.A., Vance Payne W. *Design of a steady-state detector for fault detection and diagnosis of a residential air conditioner*. International Journal of Refrigeration, 2008. **31**(5): p. 790-799.
178. Kim M., Vance Payne W., Domanski P.A., Yoon S.H., Hermes C.J.L. *Performance of a residential heat pump operating in the cooling mode with single faults imposed*. Applied Thermal Engineering, 2009. **29**(4): p. 770-778.
179. Han H., Gu B., Kang J., Li Z.R. *Study on a hybrid SVM model for chiller FDD applications*. Applied Thermal Engineering, 2011. **31**(4): p. 582-592.
180. Le Roux G.A.C., Santoro B.F., Sotelo F.F., Teissier M., Joulia X., *Improving steady-state identification*. Computer Aided Chemical Engineering, 2008. **25**: p. 459-464.

181. *M3003, The Expression of Uncertainty and Confidence in Measurement*. 2012. http://www.ukas.com/library/Technical-Information/Pubs-Technical-Articles/Pubs-List/M3003_Ed3_final.pdf
182. Hodouin D., Everell M.D. *A hierarchical procedure for adjustment and material balancing of mineral processes data*. International Journal of Mineral Processing, 1980. **7**(2): p. 91-116.
183. Pierucci S., Brandani P., Ranzi E., Sogaro A. *An industrial application of an on-line data reconciliation and optimization problem*. in European Symposium on Computer Aided Process Engineering - 6 (ESCAPE-6). 1996. Rhodes, Greece.
184. Schladt M. *Soft sensors based on nonlinear steady-state data reconciliation in the process industry*. Chemical Engineering and Processing, 2007. **46**(11): p. 1107-1115.
185. Weiss G.H., Romagnoli J.A., Islam K.A. *Data reconciliation - An industrial case study*. Computers & Chemical Engineering, 1996. **20**(12): p. 1441-1449.
186. Placido J., Loureiro L.V. *Industrial application of data reconciliation*. in European Symposium on Computer Aided Process Engineering (ESCAPE 8). 1998. Brugge, Belgium.
187. Bagajewicz M.J., Cabrera E. *Data reconciliation in gas pipeline systems*. Industrial & Engineering Chemistry Research, 2003. **42**(22): p. 5596-5606.
188. Lid T., Skogestad S. *Data reconciliation and optimal operation of a catalytic naphtha reformer*. Journal of Process Control, 2008. **18**(3-4): p. 320-331.
189. *Matlab 2011a*, The MathWorks Inc., <http://www.mathworks.es/products/matlab/>
190. *General Algebraic Modeling System (GAMS)*, www.gams.com
191. Kuehn D.R., Davidson H. *Computer control II: Mathematics of control*. Chemical Engineering Progress, 1961. **57**(6): p. 1653-1672.
192. Crowe C.M., Campos Y.A.G., Hrymak A. *Reconciliation of process flow-rates by matrix projection. 1. Linear case..* Aiche Journal, 1983. **29**(6): p. 881-888.
193. Crowe C.M. *Formulation of linear data reconciliation using information theory*. Chemical Engineering Science, 1996. **51**(12): p. 3359-3366.
194. Wu Q.F., Litrico X., Bayen A.M. *Data reconciliation of an open channel flow network using modal decomposition*. Advances in Water Resources, 2009. **32**(2): p. 193-204.
195. Mitsas C.L. *Data reconciliation and variable classification by null space methods*. Measurement: Journal of the International Measurement Confederation, 2010. **43**(5): p. 702-707.
196. Václavek V., Loučka M. *Selection of measurements necessary to achieve multicomponent mass balances in chemical plant*. Chemical Engineering Science, 1976. **31**(12): p. 1199-1205.
197. Romagnoli J.A., Stephanopoulos G. *On the rectification of measurement errors for complex chemical plants – steady state analysis..* Chemical Engineering Science, 1980. **35**(5): p. 1067-1081.
198. Crowe C.M. *Reconciliation of process flow-rates by matrix projection. 2. The nonlinear case*. Aiche Journal, 1986. **32**(4): p. 616-623.

199. Sanchez M. Romagnoli J. *Use of orthogonal transformations in data classification-reconciliation*. Computers & Chemical Engineering, 1996. **20**(5): p. 483-493.
200. Kelly J.D. *Reconciliation of process data using other projection matrices*. Computers & Chemical Engineering, 1999. **23**(6): p. 785-789.
201. Kim I.-W., Liebman J., Edgar T.F. *Robust error-in-variables estimation using nonlinear programming techniques*. AIChE Journal, 1990. **36**(7): p. 985-993.
202. Faber R., Li P., Wozny G. *Sequential parameter estimation for large-scale systems with multiple data sets. 1. Computational framework*. Industrial & Engineering Chemistry Research, 2003. **42**(23): p. 5850-5860.
203. Heintz J., Benabdelmoumene N., Aines G., Gibout S., Franquet E., Castaign-Lasvignottes J. *Modeling and main parameter identification of an absorption chiller, experimental validation*, in *International Conference on Solar Heating, Cooling and Buildings. Eurosun 2010*. 2010: Graz, Austria.
204. Serth R.W., Valero C.M., Heenan W.A. *Detection of gross errors in nonlinearly constrained data – A case study*. Chemical Engineering Communications, 1987(21): p. 775-782.
205. Kim I.W., Kang M. S., Park S. W. Edgar, T. F., *Robust data reconciliation and gross error detection: The modified MIMT using NLP*. Computers & Chemical Engineering, 1997. **21**(7): p. 775-782.
206. Zamora M., Bourouis M., Valles M., Coronas A. *Development of a small capacity air-cooled ammonia/lithium nitrate absorption chiller -first coolingcapacity and COP measurements*. in *International Sorption Heat Pump Conference (ISHPC'11)*. 2011. Padua, Italy.